1971

Hydroisomerization and Hydrocracking of Cyclohexane Over a Faujasite Catalyst.

Mamerto Goar Luzarraga
Louisiana State University and Agricultural & Mechanical College

HYDROISOMERIZATION AND HYDROCRACKING OF CYCLOHEXANE OVER A FAUJASITE CATALYST

A Dissertation

Submitted to the Graduate Faculty of the
Louisiana State University and
Agricultural and Mechanical College
in partial fulfillment of the
requirements for the degree of
Doctor of Philosophy

in

The Department of Chemical Engineering

by
Mamerto Goar Luzarraga
B.S. in Chem. Engr., University of Florida, 1967
M.S. in Chem. Engr., University of Florida, 1968
May, 1971

ACKNOWLEDGEMENT

The author is obliged to Dr. Alexis Voorhies, Jr. for providing the opportunity to participate in this research project. His guidance and encouragement during the course of this work are deeply appreciated.

Gratitude is expressed to the Esso Research and Engineering Company for sponsoring this project and to the staff of the Esso Research Laboratories at Baton Rouge for furnishing the experimental equipment, the chemicals, and the catalysts.

The consultation and advice received from Dr. P. A. Bryant are highly prized. Also, the author is indebted to Mr. D. M. Selman for the suggestions offered upon reading several parts of the manuscript.

To Mrs. Arlene D. Smith for her diligence, cooperation, and skill in typing this manuscript, the author acknowledges his indebtedness.

The cheerfulness, patience, and general support of my wife, Vilma Rosa, are specially regarded. Without her many sacrifices, this work would not have been possible.

Dedicated to my wife, Vilma Rosa, and to my sons, Mamerto Luis, and Jose Manuel.

TABLE OF CONTENTS

LIST OF TABLES

LIST OF FIGURES

ABSTRACT

A kinetic investigation was conducted of the simultaneous hydroisomerization and hydrocracking of cyclohexane in the presence of a particular zeolite, namely, a Pd-H-faujasite of low sodium content.

The catalyst was prepared, by steaming and ammonium exchanging a Na-faujasite material (SK-40) obtained from the Union Carbide Company, Linde Division. Presumably, the effect of steaming is to dislodge the sodium from the faujasite structure. Ammonium exchanging replaces the dislodged sodium cations with ammonium cations. Hydrogenation-dehydrogenation functionality is imparted to the catalyst by impregnating with ~0.6 wt.% of palladium. Upon calcination, ammonia and physically sorbed water are driven off resulting in the desired Pd-H-faujasite catalyst.

An integral tubular reactor was utilized to study the simultaneous hydroisomerization and hydrocracking of cyclohexane. The reactor was immersed in a fluidized bed of silica-alumina particles in order to insure isothermal conditions. Electrolytic hydrogen, deoxygenated and dried, was employed as a diluent to keep the catalytic surface free of carbonaceous materials commonly referred to as "coke."

The cyclohexane feed was metered and introduced into the reacting system with the aid of a Ruska pump. Liquid flow rates could be accurately adjusted by varying the gear ratios of the pump. Hydrogen

flow rates were measured by means of a Foxboro jewel orifice. A control valve was used to regulate the hydrogen flow. The reactor products were analyzed in a dual-column F&M Model 810R chromatograph.

A kinetic model was developed for the simultaneous hydroisomerization and hydrocracking of cyclohexane. The model involved a first order reversible hydroisomerization of cyclohexane to methylcyclopentane accompanied by first order irreversible hydrocracking of cyclohexane and methylcyclopentane. It was found that the hydrocracking rate constants for cyclohexane and methylcyclopentane, in the presence of the Pd-H-faujasite catalyst used in this work, were essentially the same. The kinetic model was extensively tested and it was found to be in close agreement with the experimental data.

The Pd-H-faujasite catalyst employed in this study was found to be very effective for hydroisomerizing cyclohexane in the temperature range 490-550^{o}F. It was demonstrated that as the severity of operations was increased, by increasing either temperature or contact time,the hydrocracking reactions became more pronounced.

Mass transfer from the bulk gas stream t the surface of the catalyst particles had no effect on the hydroisomerization and hydrocracking rate constants. This was demonstrated by varying the superficial velocity of the reacting stream at otherwise constant operating conditions.

Intraparticle diffusion was investigated in the range 14-200 mesh. It was concluded that the hydroisomerization and hydrocracking reactions were not diffusion limited.

Activation energies were obtained for the cyclohexane hydroisomerization and hydrocracking reactions in the presence of the

Pd-H-faujasite catalyst employed for this work. Values of 24($\pm$1) Kcal/gmole and 33($\pm$3) Kcal/gmole were computed for the hydroisomerization and hydrocracking reactions respectively. These results were shown to be in good agreement with those reported in the literature.

The hydroisomerization rate constants were found to be compatible with a dual site adsorption mechanism. The dual site model was formulated in terms of the hydrogen partial pressure and the hydrocarbons partial pressure. Temperature dependencies were tied up with the adsorption parameters.

The hydrocracking rate constant was also compatible with a dual site adsorption mechanism. At temperatures below 520^{o}F, it was found that the hydrocracking rate constant depended on both the hydrogen partial pressure and the hydrocarbons partial pressures. However, at temperatures in excess of 520^{o}F, the hydrocracking rate constant appeared to be mainly determined by the total pressure of the system.

CHAPTER I

INTRODUCTION

Research work on cyclohexane isomerization catalysis has been extensive. Chronologically, the acidic halide catalysts (e.g., $AlCl_3$ + HCl) entered the cyclohexane isomerization arena in the nineteen thirties. They were followed by the acidic chalcides (e.g., WS_2) in the forties, by the dual function metal on amorphous supports (e.g., $Ni-SiO_2-Al_2O_3$) in the fifties, and by the dual-function metal on zeolites (crystalline aluminosilicates) in the sixties.

In general, the same catalyst-types employed for hydroisomerizing cyclohexane have been utilized to study the hydrocracking or ring-opening reactions.

The acidic halide catalysts are effective at temperatures below 350°F. On the other hand, the acidic chalcides and the dual function metal on amorphous support catalysts operate at temperatures in excess of 600°F. Intermediate temperatures, in the range 400-600°F, are required for the zeolite catalysts.

Little attention has been given to the competitive kinetics involved in the simultaneous hydroisomerization and hydrocracking of cyclohexane.

The objective of this work is to study the simultaneous hydroisomerization and hydrocracking of cyclohexane in the presence of a specific zeolite; namely, a Pd-H-faujasite of low % Na (0.32) prepared and furnished by the Esso Research Laboratories at Baton Rouge.

CHAPTER II

LITERATURE REVIEW

A. Introduction

The first part of this chapter contains a compilation of the equilibrium measurements obtained by several investigators for the cyclohexane-methylcyclopentane system. Subsequently, a schematic review of the cyclohexane hydroisomerization or hydrocracking reactions conducted in the presence of non-zeolite and zeolite catalysts is presented. Some time is also spent emphasizing the importance of zeolites as catalysts.

The chapter is concluded with a discussion of the proposed mechanisms for the hydroisomerization or hydrocracking of cyclohexane.

B. Cyclohexane-Methylcyclopentane Equilibrium

The equilibrium measurements obtained by several investigators for the cyclohexane-methylcyclopentane system are summarized in Figure 1.

The indicated temperature levels give a good indication of the differences in operating conditions among the most frequently employed cyclohexane isomerization catalysts. As noted from Figure 1, the acidic halide catalysts ($AlCl_3$) operate below 340°F. On the other hand, the acidic chalcide catalyst ($Ni-SiO_2-Al_2O_3$) is effective at temperatures in excess of 650°F. Intermediate temperatures are required for the zeolite catalyst (Pd-H-mordenite).

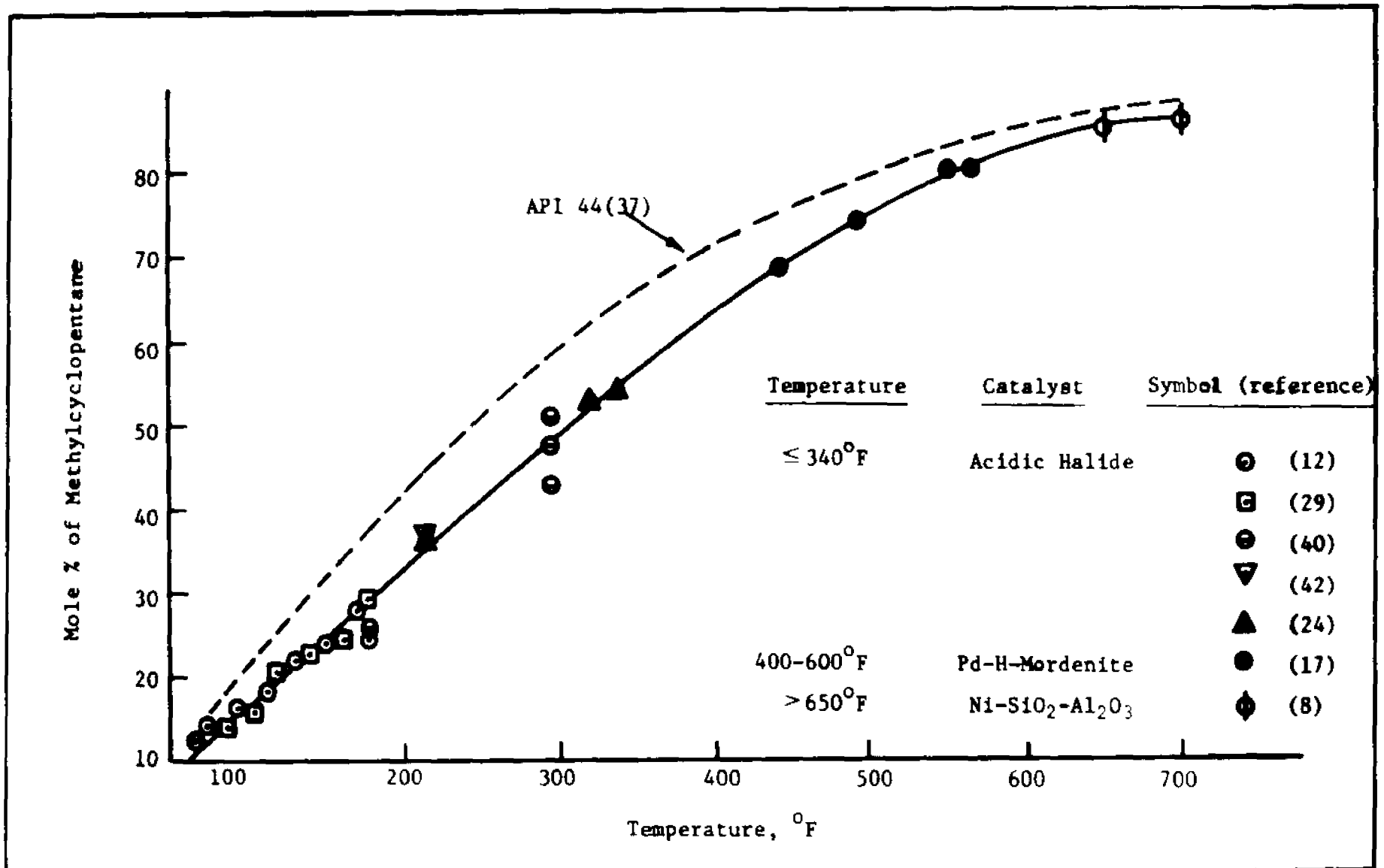

Figure 1: Summary of Equilibrium Measurements for the Cyclohexane - Methylcyclopentane System.

The dotted line in Figure 1 corresponds to the equilibrium compositions of cyclohexane and methylcyclopentane as computed from the free energy data available in the API Project 44 (37). There is considerable disagreement between the equilibrium compositions obtained experimentally and those calculated by means of the free energies of formation. Since the changes in free energy involved for the cyclohexane-methylcyclopentane system are small, erroneous results could occur by taking the difference between two large numbers. Consequently, the equilibrium constant employed in the present study was based on the experimentally determined equilibrium compositions.

C. Non-Zeolite Catalysts

1. Isomerization of Cyclohexane

a. In the Presence of Acidic Halide Catalysts

Aluminum chloride and aluminum bromide have been extensively employed (9,42,24,34,35,46) for isomerizing cyclohexane and methylcyclopentane. In order for these catalysts to be active, a promoter must be introduced into the reacting system. Water, hydrogen halides (42,30,11), cyclohexene (32), and oxygen (33) have been successfully used as promoters or initiators.

The nature of the catalytic action involves a push-pull (43) strain on the hydrocarbon molecule. Consider for example an aluminum chloride-hydrogen chloride catalytic system in which trace amounts of water have been introduced. It is postulated (24) that a complex is formed according to the following reaction:

$$HCl + AlCl_3 \underset{H_2O}{\rightleftharpoons} H^+ AlCl_4^-$$

Catalytic action can be visualized as a proton (H^+) - anion ($AlCl_4^-$) attack on the hydrocarbon molecule forcing it to rearrange.

In order to avoid aluminum chloride sludges, a hydrogen atmosphere (~600 psig) was employed by Lien and co-workers (24) to study the rate of isomerization of cyclohexane in the presence of an $AlCl_3$-HCl-H_2O (traces) catalytic system. A 30% decrease in the reaction rate was observed as the hydrogen partial pressure was increased from 0-1000 psig.

Other acidic halide catalysts employed to isomerize cyclohexane include: $GaCl_3$ (38), $FeCl_3$ (47,4), $SnCl_4$ (47,4), $ZnCl_2$ (47,4), $TiCl_3$(26), and $TiCl_4$ (26).

Acidic halide catalysts are not attractive for isomerizing cyclohexane to methylcyclopentane since they operate at low temperatures (~220°F.) where the isomer equilibrium yield is unfavorable. Moreover, they are corrosive and very susceptible to deactivation (32).

b. In the Presence of other Catalysts

Acidic chalcides (9) derive their name from the "chalcogens" employed to prepare them; namely, oxygen, sulfur, selenium, and tellurium. They comprise a wide variety of oxides, sulfides, and amorphous silica-alumina mixtures.

An extensive study of the cyclohexane hydroisomerization kinetics over a tungsten sulfide catalyst was conducted by Gonikberg and Levistskii (14,22,13,21). Some of their most important findings are summarized as follows:

- In the temperature range (610-710°F.) the isomerization reaction proceeded without diffusion limitations. Above 710°F. the isomerization rate was

diffusion limited.

- An activation energy of 30 Kcal/gmole was obtained in the temperature region (610-710°F.) where diffusion was not limiting the reaction rate.
- At 610°F. and 645°F. an increase in total pressure led to a decrease in the extent of isomerization. At 695°F, the isomerization rate remained constant as pressure was increased. At 750°F. and 800°F, the isomerization rate increased with total pressure.
- The presence of oxygen and water lowered the hydrogenation activity of the catalyst but increased its isomerization functionality.

Maslyanskii (25) investigated the cyclohexane hydroisomerization kinetics in the presence of a molybdenum sulfide catalyst. He concluded that the isomerization rate decreased with an increase in the partial pressure of cyclohexane and was independent of the hydrogen partial pressure. An activation energy of 35.4 Kcal/gmole was reported.

An improvement in chalcide catalysts results when hydrogenation functionality, via a transition metal or metal oxide, is combined with the acidic activity of silica alumina mixtures. Dual function chalcide catalysts employed to isomerize cyclohexane include: $Ni-SiO_2-Al_2O_3$ (8), $Cr_2O_3-Al_2O_3$ (23), $NiMoO_4-SiO_2-Al_2O_3$ (51).

The main asset of the dual function chalcide catalysts for isomerizing cyclohexane is that they operate at a higher temperature level (600-700°F.) where the isomer equilibrium yield is more favorable. They are also less corrosive, easier to handle, and more rugged. However, at the higher temperature levels, the hydrocracking reactions become more pronounced and the yields of methylcyclopentane are considerably reduced, as pointed out in the next section.

2. Hydrocracking of Cyclohexane

Cawley and Hall (7) investigated the hydrocracking of cyclohexane over a molybdenum sulfide catalyst. A summary of the experimental conditions and product distribution is presented in Table 1.

As observed from Table 1, Run A corresponds to the mildest conditions at 710°F. and 1 hourly space velocity. As the temperature is increased to 750°F. at the same space velocity, Run B, isomerization increases at a faster rate than hydrocracking. However, the hydrocracking reactions predominate as the severity of operations is further augmented either by increasing temperature, Run C, or by decreasing space velocity, Run D.

A MoS_2-Al_2O_3 catalyst proved to be less active than the pure pelleted MoS_2 catalyst shown in Table 1. It was proposed that cyclohexane disappeared according to the following scheme:

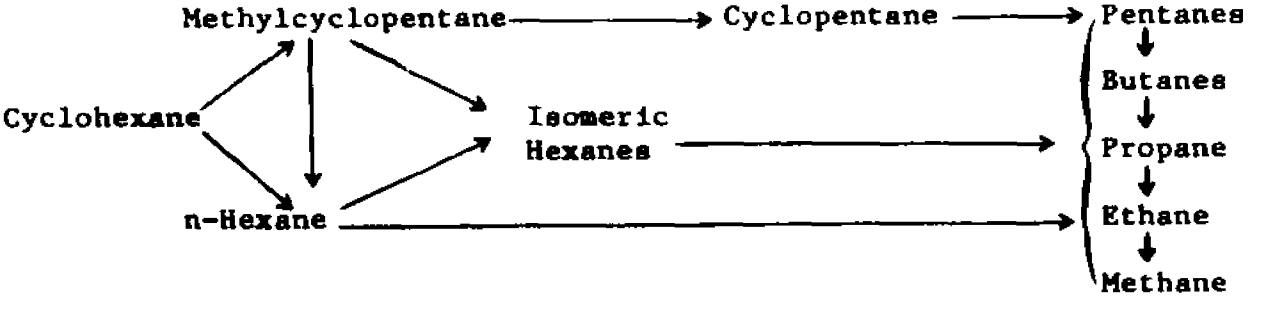

Table 1: Product Distribution from Hydrocracking Cyclohexane in the Presence of a Molybdenum Disulfide Catalyst (7).

Run	A	B	C	D
Catalyst	----------	MoS_2	----------	
H_2 Pressure, psig	----------	3000	----------	
Throughput, vol. liq./vol. cat./hr.	1.0	1.0	1.0	0.5
Temperature, °F.	710	750	880	880
Yields of Product (wt.%)				
Pentanes	2.6	3.3	23.3	59.2
Pentanes	0.0	trace	9.4	7.1
Isomeric hexanes	0.0	5.8	27.3	19.8
n-Hexane	0.0			
Methylcyclopentane	14.5	81.0	36.6	12.4
Cyclohexane	82.9	9.9	3.4	1.5

An activation energy of 30-35 Kcal/gmole has been reported (18) for the cyclohexane hydrocracking reaction over a platinum-alumina catalyst. Cyclohexane hydrocracking reactions have also been conducted in the presence of a cobalt-molybdenum-alumina catalyst (19,31).

The hydrocracking of alkylcyclohexanes was studied by Egan and co-workers (10) over a nickel sulfide on silica-alumina, and a silica-alumina catalyst. The experimental data appeared consistent with a first order irreversible kinetic model.

The splitting of cyclohexane to lower molecular weight hydrocarbons has also been observed over an acidic halide catalyst; namely, $AlCl_3$-HCl (20). It was concluded that the ring splitting to isohexanes predominated. Only small concentrations of isobutane were detected.

D. Zeolite Catalysts

1. General

Zeolites are crystalline aluminosilicates consisting of SiO_4 and AlO_4 tetrahedral structures arranged in a variety of geometrical forms. The growth in zeolite research can be demonstrated by the number of publications that have appeared in recent years. From 1909 until 1969, 4500 papers have appeared in the open literature, and 1000 patents have been issued in the United States alone (6).

Zeolites, natural or synthetic, may be represented (5) by the general formula where M is a metal cation of valence n, and x, y, and a

$$M_{x/n}\,[(AlO_2)_x\,(SiO_2)_y] \bullet aH_2O$$

are the moles of alumina, silica, and water associated with a unit cell size.

The fundamental crystalline structure of zeolites consists of Si or Al atoms in the center of a tetrahedron with oxygen in the corners being shared by adjacent tetrahedral configurations. The SiO_4 tetrahedron is electrically neutral since four negatively charged oxygen ions are exactly paired by Si^{+4}. However, the alumina tetrahedron containing Al^{+3} is negatively charged. In order to maintain electrical neutrality, the alumina tetrahedron can take up a monovalent metal cation such as Na^+ or K^+. Also, two alumina tetrahedra can share a divalent metal cation such as Ca^{2+} or Ba^{2+}.

A recent structural classification of zeolites has been proposed by Breck (6). An abridged summary of the classification is presented in Table 2. Within each group, the zeolites have a common substructure.

The catalyst employed in the present investigation was prepared by the Esso Research Laboratories at Baton Rouge, from a faujasite base material. Further description of the catalyst and its preparation are given in Chapter III.

The catalytic applications of zeolites have been numerous. There are several bibliographic reviews (28,44,45) pertaining to catalysis with zeolites and on zeolites in general (2,5) covering the literature up to 1966. Rabo (36) has presented a selective review up to 1970.

2. Cyclohexane Hydroisomerization over Zeolite Catalysts

Hopper (17) studied the cyclohexane hydroisomerization kinetics over structurally modified Pd-H-mordenites having silica to alumina mole ratios of 9/1, 10/1, 26/1, and 52/1. The following results were obtained:

Table 2: Structural Classification of Zeolites (6)

Name	Unit Cell Size Formula	Void Fraction	Main Channel Aperture Å
Group 1			
Analcime	$(Na)_{16}[(AlO_2)_{16}(SiO_2)_{32}] \bullet 16\ H_2O$	0.18	2.6
Phillipsite	$(K,Na)_{10}[(AlO_2)_{10}(SiO_2)_{22}] \bullet 20\ H_2O$	0.31	4.2-4.4
Paulingite	$(K)_{68}(Na)_{13}(Ca)_{3.6}(Ba)_{1.5}[(AlO_2)_{152}(SiO_2)_{520}] \bullet 700\ H_2O$	0.49	3.9
Yugawaralite	$(Ca)_2[(AlO_2)_4(SiO_2)_{12}] \bullet 8\ H_2O$	0.27	3.5
Group 2			
Erionite	$(Ca, Mg, K_2, Na_2)_{4.5}[(AlO_2)_9(SiO_2)_{27}] \bullet 27\ H_2O$	0.35	3.6-4.8
Offretite	$(K_2, Ca)_{2.7}[(AlO_2)_{5.4}(SiO_2)_{12.6}] \bullet 15\ H_2O$	0.40	3.6-6.3
Omega	$(Na)_{6.8}(TMA)_{1.6}[(AlO_2)_8(SiO_2)_{28}] \bullet 21\ H_2O$	0.38	7.5
T	$(Na)_{1.2}(K)_{2.8}[(AlO_2)_4(SiO_2)_{14}] \bullet 14\ H_2O$	0.40	3.6-4.8
Group 3			
A	$(Na)_{12}[(AlO_2)_{12}(SiO_2)_{12}] \bullet 27\ H_2O$	0.47	4.2
P	$(Na)_6[(AlO_2)_6(SiO_2)_{10}] \bullet 15\ H_2O$	0.41	3.5
Group 4			
Faujasite	$(Na_2, K_2, Ca, Mg)_{29.5}[(AlO_2)_{59}(SiO_2)_{133}] \bullet 235\ H_2O$	0.47	7.4
X	$(Na)_{86}[(AlO_2)_{86}(SiO_2)_{106}] \bullet 264\ H_2O$	0.50	7.4
Chabazite	$(Ca)_2[(AlO_2)_4(SiO_2)_8] \bullet 18\ H_2O$	0.47	3.7-4.2
Gmelinite	$(Na)_8[(AlO_2)_8(SiO_2)_{16}] \bullet 24\ H_2O$	0.44	3.4-4.1
ZK-5	$(R_2, Na_2)_{30}[(AlO_2)_{30}(SiO_2)_{66}] \bullet 98\ H_2O$	0.44	3.9
L	$(K)_9[(AlO_2)_9(SiO_2)_{27}] \bullet 22\ H_2O$	0.32	7.5
Group 5			
Natrolite	$(Na)_{16}[(Al_2O_3)_{16}(SiO_2)_{24}] \bullet 16\ H_2O$	0.23	2.6-3.9
Thomsonite	$(Na)_4(Ca)_8[(AlO_2)_{20}(SiO_2)_{20}] \bullet 24\ H_2O$	0.32	2.6-3.9
Edingtonite	$(Ba)_2[(AlO_2)_4(SiO_2)_6] \bullet 8\ H_2O$	0.36	3.5-3.9

Table 2 Cont'd: Structural Classification of Zeolites (6)

Name	Unit Cell Size Formula	Void Fraction	Main Channel Aperture Å
Group 6			
Mordenite	$(Na)_8[(AlO_2)_8(SiO_2)_{40}] \bullet 24\ H_2O$	0.28	2.9-7.0
Dachiardite	$(Na)_5[(AlO_2)_5(SiO_2)_{19}] \bullet 12\ H_2O$	0.32	3.7-6.7
Epistilbite	$(Ca)_3[(AlO_2)_6(SiO_2)_{18}] \bullet 18\ H_2O$	0.25	3.6-6.3
Group 7			
Heulandite	$(Ca)_4[(AlO_2)_8(SiO_2)_{28}] \bullet 24\ H_2O$	0.39	3.9-7.1
Stilbite	$(Ca)_4[(AlO_2)_8(SiO_2)_{28}] \bullet 28\ H_2O$	0.39	2.7-6.2

- The hydroisomerization of cyclohexane was compatible with a first order reversible reaction rate model.
- Activation energies of 23-35 Kcal/gmole were obtained.
- The hydroisomerization rate decreased with an increase in hydrocarbon partial pressure, at constant hydrogen partial pressure, for all Pd-H-mordenites investigated.
- The hydroisomerization rate decreased with an increase in hydrogen partial pressure, at constant hydrocarbon partial pressure, for the 9/1 and 10/1 silica to alumina mole ratio catalysts.
- The hydroisomerization rate was independent of hydrogen partial pressure, at constant hydrocarbon partial pressure, for the 52/1 silica to alumina mole ratio catalyst.
- The rate constants were correlated with the hydrogen and hydrocarbons partial pressure by means of a dual site adsorption mechanism.

The simultaneous hydroisomerization and dehydrogenation of cyclohexane at reforming conditions over a Pt-alumina-mordenite catalyst was investigated by Allan (1). An activation energy of 12.5 Kcal/gmole was obtained for the hydroisomerization reaction. The low value of the activation energy was explained in terms of diffusion limitations within the zeolite "micropores." The hydroisomerization

data was consistent with a first order reversible reaction model and was compatible with either a single or dual site adsorption mechanism.

The hydroisomerization of cyclohexane has also been conducted (27) over zeolites A, X, and Y in their cationic forms impregnated with 0.5% Pt, Pd, Rh or Ir. The silica to alumina mole ratios were varied from 2 to 6. It was found that zeolites in the Na-form were inactive. The catalytic activity was improved when the Na^{+} cations were replaced by Ca^{2+}. By increasing the silica to alumina mole ratios, the hydroisomerization activity was augmented.

The optimal preactivation treatment of zeolite catalysts for hydroisomerizing cyclohexane has been the subject of several patents (50,52,48,49).

3. Cyclohexane Hydrocracking over Zeolite Catalysts

A comparative study of the cyclohexane hydrocracking reactions over a Pd-H-mordenite and a Pd-H-faujasite catalyst was conducted by Hatcher (15). The experimental data was consistent with a first order irreversible kinetic model. An activation energy of 31 Kcal/gmole was reported for the cyclohexane hydrocracking reaction. Pressure effects were accounted for by means of a dual site adsorption mechanism. It was found that the Pd-H-mordenite catalyst was more active than the Pd-H-faujasite for hydrocracking cyclohexane.

The rate of coke deposition on Ca-X zeolites (as a function temperature and time), has been investigated (39) for different feeds, namely; cyclohexane, n-hexadecane, decalin, and benzene. The coking tendencies of these compounds increased in the order shown, which is also the order of increasing adsorption coefficients.

E. Mechanisms for the Hydroisomerization or Hydrocracking of Cyclohexane

A widely accepted (32,34,33) mechanism for the isomerization of cyclohexane in the presence of acidic halide catalysts involves three steps: carbonium ion formation, carbonium ion rearrangement, and carbonium ion propagation. The carbonium ion formation step requires the presence of a promoter as discussed in Section C. A schematic representation of the chemical reactions is as follows:

- Carbonium ion formation

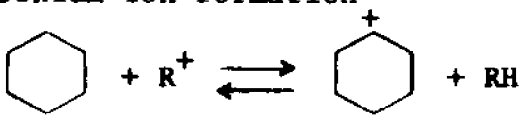

- Carbonium ion rearrangement

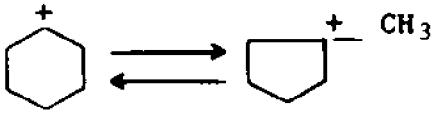

- Carbonium ion propagation

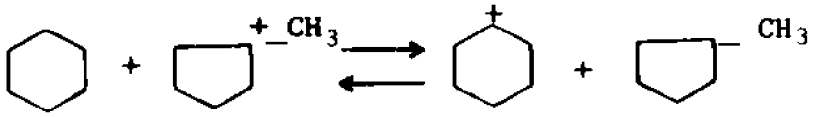

For the dual function catalysts, chalcides (16) or zeolites (17), the overall cyclohexane hydroisomerization process results from the combined action of the metallic and acidic sites. Dehydrogenation-hydrogenation occurs at the metallic sites while carbonium ion rearrangements take place at the acidic sites. A stepwise formulation of the whole process can be visualized as:

- Dehydrogenation to form an olefin (metallic sites)

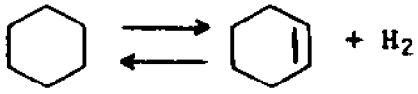

- Olefin hydroisomerization by carbonium ion rearrangement (acidic sites).

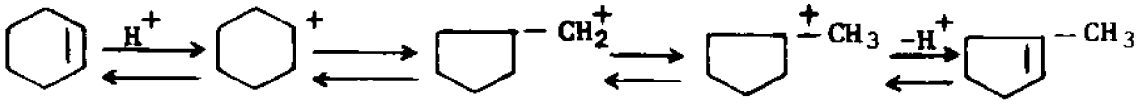

- Hydrogenation of iso-olefin (metallic sites)

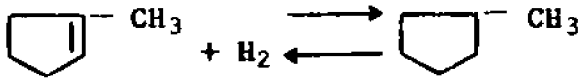

The hydrocracking mechanism (3,10,15) is very similar to that for hydroisomerization over dual function chalcide or zeolite catalysts. The only difference is that once the carbonium ion is formed, it can be either cracked or isomerized or both.

LIST OF REFERENCES - CHAPTER II

1. Allan, D. E., "The Dehydrogenation and Isomerization of Cyclohexane Over a Pt Alumina Mordenite Catalyst," Ph.D. dissertation, Department of Chemical Engineering, Louisiana State University, 1970.

2. Barrer, R. M., "Molecular Sieves [as Zeolites]," Endeavour, 23, 122 (1964).

3. Beuther, H. and Larson, O. A., "Role of Catalytic Metals in Hydrocracking," Industrial and Engineering Chemistry Process Design and Development, 4, 177 (1965).

4. Bonnot, L. and Jenny, R., "Isomerization Reactions Catalyzed by Metallic Chlorides in Aqueous Hydrochloride Solutions," Compt. Rend., 250, 3179 (1960); Chemical Abstracts, 54, 24468 b (1960).

5. Breck, D. W., "Crystalline Molecular Sieves," Journal of Chemical Education, 41, (No. 12), 678 (1964).

6. Breck, D. W., "Recent Advances in Zeolites, "Second International Conference on Molecular Sieve Zeolites, Worcester, Massachusetts, September (1970).

7. Cawley, C. M. and Hall, C. C., "Reactions of Cyclohexane and Decahydronaphthalene Under Hydrogenation - Cracking Conditions," Journal of the Society of Chemical Industry (London), 63, 33 (1944).

8. Ciapetta, F. G. and Hunter, J. B., "Isomerization of Saturated Hydrocarbons, Paraffins," Industrial and Engineering Chemistry, 45, 147 (1953).

9. Condon, F. E., "Catalytic Isomerization of Hydrocarbons," Catalysis, 6, 43, Reinhold Publishing Corp., New York, New York, 1958.

10. Egan, C. J., Langlois, G. E., and White, R. J., "Selective Hydrocracking of C_9 to C_{12} - Alkylcyclohexanes on Acidic Catalysts. Evidence for the Paring Reaction," Journal of the American Chemical Society, 84, 1204 (1962).

11. Gawalek, G., Schneider, G. and Koennecke, H. G., "Influence of Co-Catalysts on the Isomerization of Cyclohexane with $AlCl_3$ to Methylcyclopentane," Z. Physik. Chem., 223, 269 (1963).

12. Glazebrook, A. L., and Lovell, W. G., "The Isomerization of Cyclohexane and Methylcyclopentane," Journal of the American Chemical Society, 61, 1717 (1939).

13. Gonikberg, M. G. and Levistskii, I. I., "The Effect of Hydrogen Pressure on the Velocity of Heterogeneous Catalytic Isomerization of Cyclohexane. III. Study of the Causes of Inhibition of Isomerization by Increasing Hydrogen Pressure," Izvest. Akad. Nauk S.S.S.R., Otdel. Khim. Nauk, 1170 (1960); Chemical Abstracts 55, 25789a (1961).

14. Gonikberg, M. G., Levitskii, I. I., and Kazanskii, B. A., "Effect of the Hydrogen Pressure on the Rate of the Heterogeneous - Catalytic Isomerization of Cyclohexane. I. Kinetics for the Isomerization of Cyclohexane on a Tungsten Sulfide Catalyst," Izvest. Akad. Nauk S.S.S.R., Otdel., Khim. Nauk, 611 (1959); Chemical Abstracts, 54, 571 (1960).

15. Hatcher, W. J., "Hydrocracking of Normal Hexane and Cyclohexane Over Zeolite Catalysts," Ph.D. dissertation, Department of Chemical Engineering, Louisiana State University, 1968.

16. Hinden, S. G., Weller, S. W., and Mills, G. A., "Mechanically Mixed Dual Function Catalysts,: Journal of Physical Chemistry, 62, 244 (1958).

17. Hopper, J. R., "A Study of the Catalytic Hydroisomerization Reactions of N-Pentane and Cyclohexane Over Structurally Modified Mordenites," Ph.D. dissertation, Department of Chemical Engineering, Louisiana State University, 1969.

18. Iijima, K., Schimizu, S., Furukaw, T., and Yoshida, N., "Hydrodecyclization of Methylcyclopentane and Benzene in the Presence of a Reforming Catalyst," Bulletin of the Japan Petroleum Institute, 5, 1 (1963).

19. Kazantseva, V. M., Neudachina, V. I., and Kalechits, I. V., "Characteristics of Hydrocracking Catalysts in Experiments with Some Individual Hydrocarbons," Neftepererab. Neftekhim. (Moscow), 8, 23 (1968); Chemical Abstracts, 69, 108314u (1968).

20. Koch, H., and Gilfert, W., "The Isomerizing and Hydrogen Splitting of Hydrocarbons with Aluminum Chloride - Hydrogen Chloride. I. Pure Paraffins and Naphthenes," Brennstoff - Chem., 30, 413 (1960).

21. Levitskii, I. I., and Gonikberg, M. G. "Effect of Hydrogen Pressure on the Rate of the Heterogeneous Catalytic Isomerization of Cyclohexane. II. Relation of the Rate of Isomerization of Cyclohexane to the Partial Pressure of Hydrogen, Temperature, and Grain Size of the Tungsten Sulfide, Izvest. Akad. Nauk S.S.S.R., Otdel Khim. Nauk, 996 (1960); Chemical Abstracts, 54, 571 (1960).

22. Levitskii, I. I., and Gonikberg, M. G., "Effect of Oxygen and Water on the Hydrogenating and Isomerizing Activity of Tungsten Sulfide Catalyst," Doklady Akad. Nauk. S.S.S.R., 137, 609 (1961); Chemical Abstracts, 55, 19822a (1961).

23. Levitskii, I. I., Minachev, Kh.M., Bogomolov, V. I., and Udal'tsova, E. A., "Effect of Oxygen on the Hydrogenolysis of Methylcyclopentane on an Alumina-Chromium Oxide Catalyst," Neftkhimiya, 7, 330 (1967); Chemical Abstracts, 67, 116607r (1967).

24. Lien, A. P., D'Ouville, E. L., Evering, B. L., and Grubb, H. M., "Rate of Isomerization of Cyclohexane," Industrial and Engineering Chemistry, 44, (No. 1), 351 (1952).

25. Maslyanskii, G. N., "Kinetics of Isomerization of Cyclohexane at High Pressures," Journal of General Chemistry (U.S.S.R.), 13, 540 (1943).

26. Mihail, R. "Titanous Chloride as an Isomerization Catalyst," Angew. Chem., 70, 343 (1958); Chemical Abstracts, 53, 259e (1959).

27. Minachev, Kh. M., Garanin, V. I., and Isakov, Ya. I., "Synthetic Zeolites as Catalysts," Probl. Kinetiki i Kataliza, Akad. Nauk. S.S.S.R., 11, 214 (1966); Chemical Abstracts, 65, 18378h (1966).

28. Minachev, Kh. M., Garanin, V. I., Isakov, Ya. I., "Applications of Synthetic Zeolites (Molecular Sieves) in Catalysis," Usp. Khim., 35, 2151 (1966) (Russ.); Chemical Abstracts, 66, 49594Y (1967).

29. Mizushima, S., Morino, Y. and Fiyisiro, R., Science Papers Institute Physics Chemical Research (Tokyo), 38, 1034 (1941).

30. Nenitzescu, C. D., Avram, M. and Sliam, E., "The Catalytic Isomerization of Saturated Hydrocarbons. The Mechanism of Activation of Aluminum Chloride by Water," Bull. Soc. Chim. France, 1266 (1955).

31. Neudachina, V. I., and Kalechits, I. V., "Chemistry of the Conversion of Individual Hydrocarbons Under Hydrocracking Conditions in the Presence of Aluminum-Cobalt-Molybdenum and Platinum Catalysts," Neftepererab. Neftekhim., 1, 21 (1969); Chemical Abstracts, 70, 79686e (1969).

32. Pines, H., Abraham, B. M. and Ipatieff, V. N., "Isomerization of Saturated Hydrocarbons. V. The Effect of Cyclohexane Upon the Isomerization of Methylcyclopentane and Cyclohexane," Journal of the American Chemical Society, 70, 1742 (1948).

33. Pines, H., Aristoff, E., and Ipatieff, V. N., "Isomerization of Saturated Hydrocarbons. VIII. The Effect of Oxygen and Light Upon the Isomerization of Methylcyclopentane in the Presence of Aluminum Bromide," Journal of the American Chemical Society, 72, 4304 (1950).

34. Pines, H., Aristoff, E., and Ipatieff, V. N., "Isomerization of Saturated Hydrocarbons. VII. The Effect of Light Upon the Isomerization of Methylcyclopentane in the Presence of Aluminum Bromide - Hydrogen Bromide," Journal of the American Chemical Society, 72, 4055 (1950).

35. Pines, H., Aristoff, E., and Ipatieff, V. N., "Isomerization of Saturated Hydrocarbons. XII. The Effect of Experimental Variables, Alkyl Bromides and Light Upon the Isomerization of Methylcyclopentane in the Presence of Aluminum Bromide," Journal of the American Chemical Society, 75, 4775 (1953).

36. Rabo, J. A. and Poutsma, M. L., "Structural Aspects of Catalysis with Zeolites," Second International Conference on Molecular Sieve Zeolites, Worcester, Massachusettes, Septemper (1970)

37. Rossini, F. D., et.al., Selected Values of Physical and Thermodynamic Properties of Hydrocarbons and Related Compounds, Carnegie Press, Pittsburgh, Pa., 1953.

38. Russell, G. A., "Catalysis by Metal Halides. IV. Relative Efficiencies of Friedel - Crafts Catalysis in Cyclohexane - Methylcyclopentane Isomerization, Alkylation of Benzene, and Polymerization of Styrene," Journal of the American Chemical Society, 81, 4815 (1959).

39. Sabitova, V. F., Levinter, M. E., Tanatorov, M. A., Akhmetshina, M. N., "Comparison of the Kinetics of Coke Formation on Ca X Zeolites and Amorphous Aluminosilicates," Izv. Vyssh. Vcheb. Zaued., Neft. Gaz, 12, 59 (1969); Chemical Abstracts, 71, 103785e (1969).

40. Schuit, G. C. A., Hoog, H. and Verheva, J., "Investigation Into the Isomerizations of Aliphatics and Alicyclic Hydrocarbons," Recueil des Traveux Chimiques de Pays-Bas, 59, 793 (1940).

41. Shuikin, N. I., "The Contact - Catalytic Isomerization of Six - Membered into Five - Membered rings," Bulletin of the Academy of Science (U.S.S.R.), 440 (1944); Chemical Abstracts, 39, 4319 (1945).

42. Stevenson, D. P., and Morgan, J. H., "The Isomerization of Cyclohexane and Methylcyclopentane in the Presence of Aluminum Halides. II. Equilibrium and Side Reaction," Journal of the American Chemical Society, 70, 2773 (1948).

43. Swain, C. G., "Kinetic Evidence for a Termolecular Mechanism in Displacement Reactions of Thriphenylmethyl Halides in Benzene Solution," Journal of the American Chemical Society, 70, 1119 (1948).

44. Turkevich, J., "Zeolites as Catalysts," Catalysis Reviews, 1, 1 (1967).

45. Venuto, P. B., Landis, P., "Organic Catalysis Over Crystalline Aluminosilicates," Advances in Catalysis, 18, 259 (1968).

46. Zelinskii, N. D., Turova - Polyak, M. B., Tsvetkova, N. F. and Treshchova, E. G., "Isomerization of Cyclohexane by Aluminum Chloride," Zhur. Obshchei. Khim., 21, 2160 (1951); Chemical Abstracts, 46, 8024a (1952).

Patents

47. French Patent 1,314,358

48. French Patent 1,359,087

49. French Patent 1,510,098

50. U. S. Patent 3,069,482

51. U. S. Patent 3,108,974

52. U. S. Patent 3,299,153

CHAPTER III

CATALYST PREPARATION AND ANALYTICAL MEASUREMENTS

A. Introduction

A recent British patent by the Mobil Company (2) advocates steaming and ammonium exchanging to increase the catalytic activity of faujasites. Presumably, the objective of the steaming step is to dislodge the sodium from the faujasite structure. Ammonium exchanging replaces the dislodged sodium cations with ammonium cations.

Employing the general techniques described in the above mentioned patent, the Esso Research Laboratories at Baton Rouge, Louisiana, prepared a faujasite base, which they impregnated with 0.6% Pd to impart hydrogenation - dehydrogenation functionality. Upon calcination, ammonia was driven off resulting in the desired H-faujasite form.

B. Catalyst Preparation

The catalyst preparation consisted of three steps: (1) preparation of the H-faujasite base; (2) impregnation of the base with Pd; and (3) activation of the catalyst. The information on each step is summarized below.

1. Preparation of the Base

As already mentioned, this step was carried out at the Esso Research Laboratories employing the teachings of a recent British patent (2). The starting material was Na-faujasite (SK-40) obtained from the Union Carbide Company, Linde Division. The final base is NH_4-faujasite

of a low sodium content.

2. Impregnation of the Base with Pd

This step, also performed at the Esso Research Laboratories, involved the impregnation of the base with Pd $(NH_3)_4$ Cl_2 calculated to give about 0.6 wt.% of Pd in the finished catalyst.

3. Activation of the Catalyst

This final step was carried out at Louisiana State University, it involved the calcination of the catalyst to drive off water and ammonia in order to obtain the desired Pd-H-faujasite form. The calcination was conducted according with the following schedule:

a. The catalyst samples were placed in Vycor containers inside a furnace.

b. Purified air was passed over the catalyst during calcination. Hydrocarbons were removed from the air by converting them to carbon dioxide over a copper catalyst at 1000°F. Moisture is trapped in a bed of 13-X molecular sieve and indicating Drierite.

c. The furnace temperature was raised to about 350°F. at a rate of 100°F./hr and maintained there for 16 hours. This low temperature was employed to prevent damaging the zeolite crystal structure by sudden water movements.

d. The temperature was increased to 1000°F. at a rate of 100°F./hr and maintained there for 2 hours.

e. Finally, upon cooling the furnace to 400-450°F., the catalyst samples were removed, placed in sealed vials, weighed, and stored in a dessicator.

C. Analytical Measurements on the Catalyst

A summary of the analytical measurements obtained on a fresh calcined catalyst sample is as follows:

Analysis	Results
Na, wt.%	0.32
Surface area, m^2/gm	789*
Al_2O_3, wt.%	22.0
SiO_2, wt.%	75.6
Palladium, wt.%	0.624

Hopper (1), a former investigator in this project, has described the techniques employed in securing the above mentioned analysis.

---

* Langmuir

LIST OF REFERENCES - CHAPTER III

1. Hopper, J. R., "A Study of the Catalytic Hydroisomerization Reactions of N-Pentane and Cyclohexane Over Structurally Modified Mordenites," Ph.D. dissertation, Department of Chemical Engineering, Louisiana State University, 1969.

Patent

2. British Patent 1,141,955

CHAPTER IV

EXPERIMENTAL EQUIPMENT AND PROCEDURE

A. General

The equipment employed in this experimentation was obtained from the Esso Research Laboratories, Baton Rouge, Louisiana. All the experimental equipment is located in the Petroleum Processing Laboratory of the Chemical Engineering Department at Louisiana State University. This research program is sponsored by the Esso Research and Engineering Company. P. A. Bryant, the pioneer researcher in this project, designed the experimental units and supervised their construction. The system has been remodeled by R. G. Beecher, J. R. Hopper, and the author.

B. Equipment

1. Flow Diagram

A schematic flow diagram of the experimental equipment is shown in Figure 2. The unit is composed of three main sections: feed, reactor, and product recovery.

Excluding the Ruska pump and the gas cylinder, the unit is housed in a walk-in hood having a 3000 cfm exhaust fan and a sliding safety glass door. The equipment is mounted on a steel frame, three feet wide, three feet deep, and six feet high.

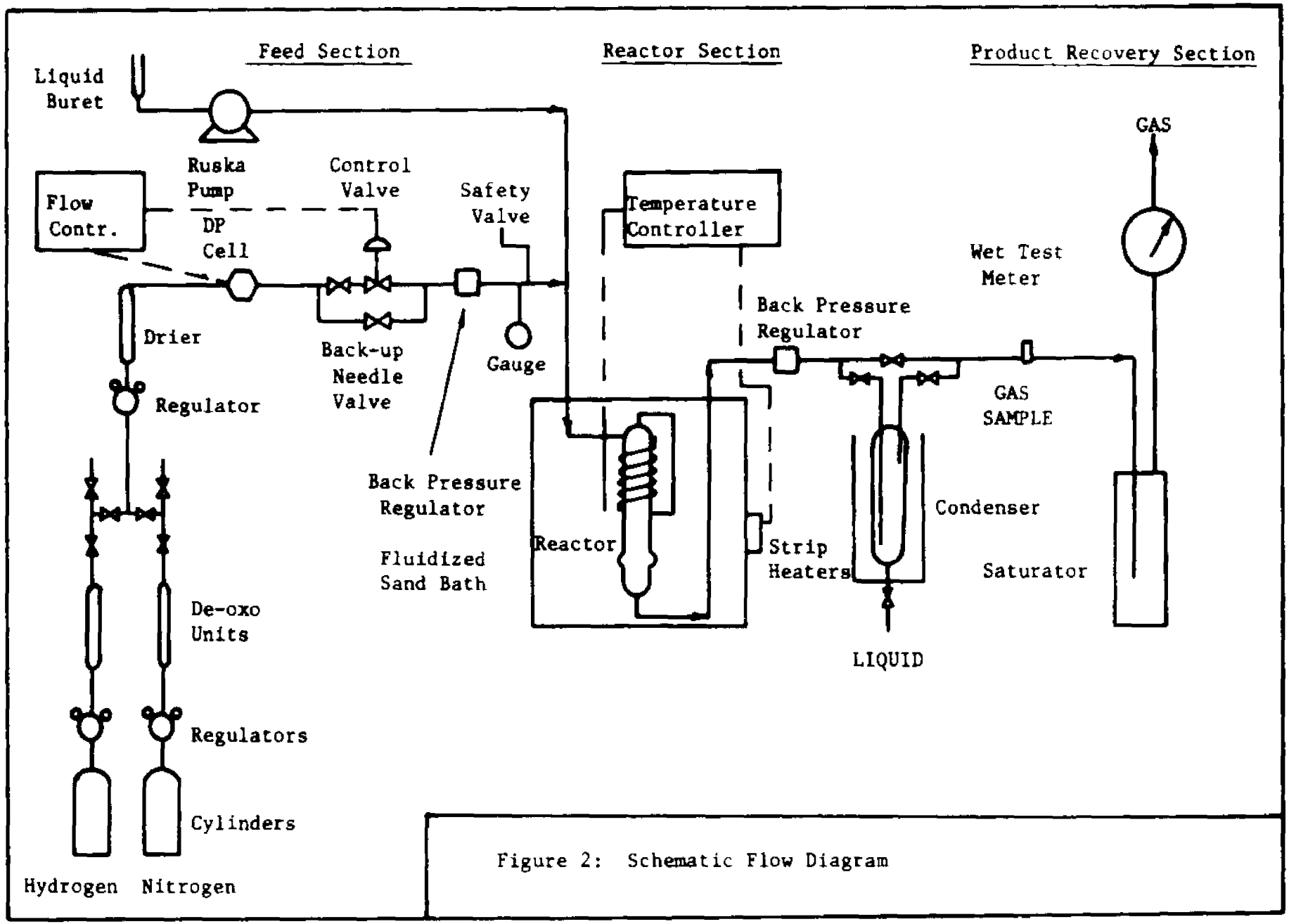

Figure 2: Schematic Flow Diagram

2. Feed Section

a. Hydrocarbons

The cyclohexane feed was obtained from Phillips as 99 + mole % pure. It was stored over 3A molecualr sieves in order to keep it free from moisture.

The hydrocarbon feed is introduced into the positive displacement Ruska pump through a graduated buret. Liquid flow rates can be varied between 2 and 240 cc/hr by manually changing the gear ratios of the pump. The maximum capacity of the pump is 250 cc.

b. Hydrogen and Nitrogen

Electrolytic hydrogen from a gas cylinder is fed through a regulator, into the deoxygenation units where oxygen traces are converted to water by means of a palladium-alumina catalyst. The water formed is trapped in a bed containing 3A molecular sieves and indicating Drierite.

Hydrogen flow rates are measured with the aid of a Foxboro jewel orifice (0.006") inserted in a differential pressure analyzer cell (DP Cell). A control valve is employed to regulate the hydrogen flow. Also, a back-up needle valve manifold is available to regulate the flow of hydrogen. Constant pressure drops across the "DP Cell" and the control valve are maintained with a "Mity-Mite" back pressure regulator. Unexpected pressure build-ups are taken care of by a safety release valve set at 1000 psig.

Similar facilities are available for the nitrogen flow which is primarily used to purge the reactor and the liquid feed system.

3. Reactor Section

An enlarged view of the reactor section is shown in Figure 3. The entire reactor is immersed in a fluidized bed of silica-alumina particles to insure isothermal conditions. Air is employed as the fluidization medium. It enters through a porous frit and is released in a cyclone separator in order to recover the silica-alumina fines. Heat is supplied to the bed by six 500-watt strip heaters. Half of the heaters are adjusted manually with a rheostat. The remaining heaters are automatically controlled by a Leeds and Northrup Electromax (C.A.T.) current-adjusting-type solid state temperature controller. A phaser* power controller is used as the final control element to regulate the voltage supplied to the sandbath heaters.

The hydrocarbon-hydrogen feed stream is vaporized and preheated to the desired reaction temperature within the fluidized sandbath. This is accomplished by coiling the inlet line several times around the reactor before the feed stream is brought in contact with the catalyst.

The reactor is made of 1/2" schedule 80 Inconel pipe. It can be easily opened by means of a temperature-compensated coupling. A pressure-tight seal is provided by a steel ring which is replaced after every run. Catalyst particles are contained within the reactor by two micro-metallic frits. The reactor can hold up to 40 cc of catalyst but the usual charge is 15 cc.

---

* Manufactured by R-I Controls of Minneapolis, Minnesota.

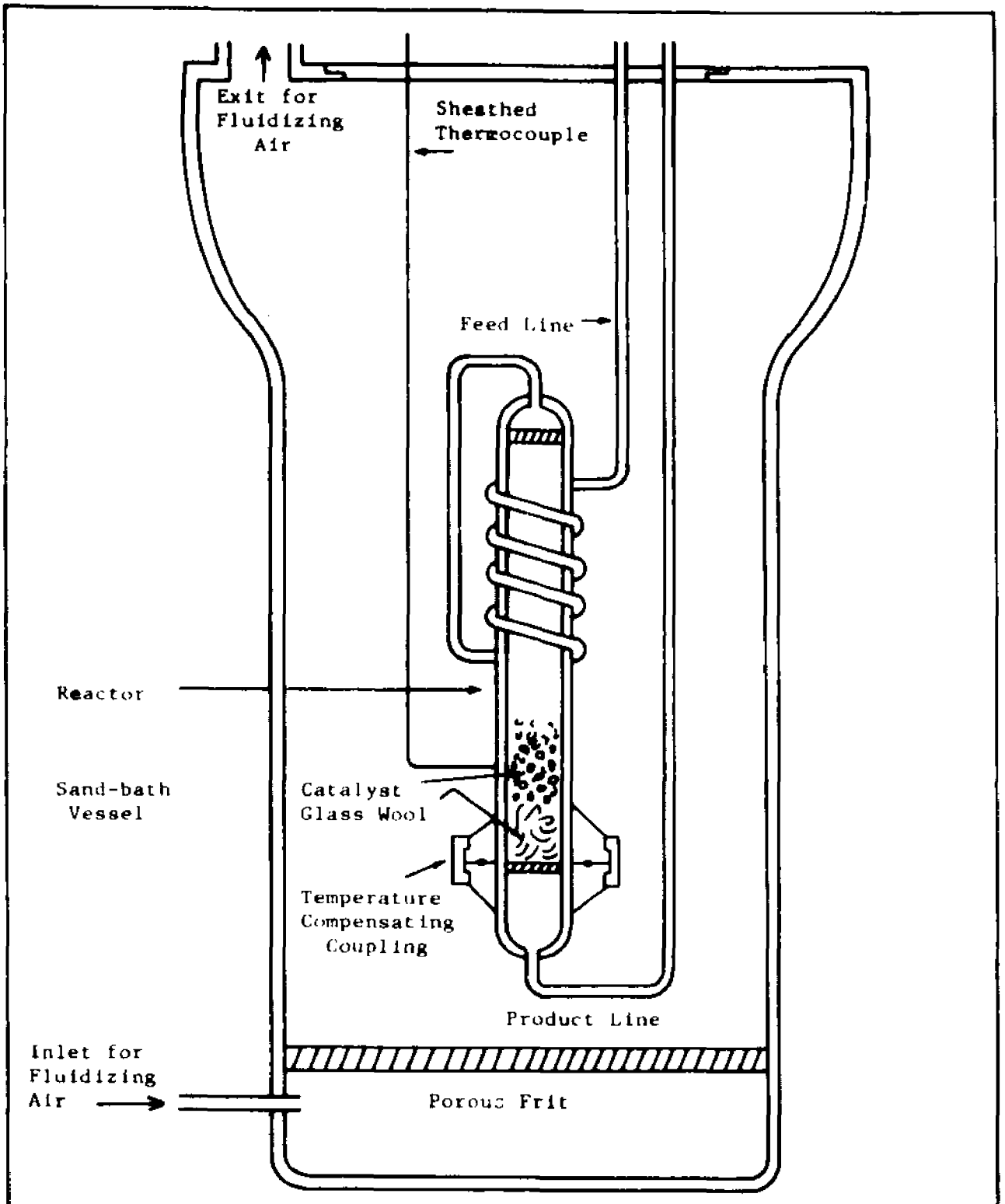

Figure 3: Enlarged View of Reactor Section.

Temperature in the catalyst bed is measured by a 1/16" iron-constantan thermocouple. It enters the reactor through a Conax fitting and its tip penetrates 1/4" into the catalyst bed. Actual temperatures were read off a Leeds and Northrup Speedomax H temperature indicator.

4. Sampling and Product Recovery Section

The reactor effluents are split into a gas and a liquid phase in an ice-cooled condenser. A "mity-mite" regulates the pressure in the reactor.

The liquid components are drained from the product accumulator; and the gases are saturated with water and circulated through a wet-test meter. Liquid product recovery was not required in the present study; because all of the product was in the gas phase. Gas samples were taken with a syringe and injected into a gas chromatograph for analysis.

5. Analytical

A dual-column F&M Model 810R chromatograph was used to analyze the products from the reactor. The separation of the hydrocarbon components was obtained by means of a ten foot x 1/4" aluminum column packed with 10% silicone-rubber (SE-30) on 90% white-chromosorb (80-100 mesh). An Infotronics Digital Integrator Model CRS-110 measured the area under each peak and recorded the elution times.

The gas chromatograph is equipped with an automatic temperature programming system in order to expedite the elution of the heavier hydrocarbon components. The temperature program in the present study consisted of an increase in temperature from 40°C. to 150°C. at a rate of 30°C. per minute. The temperature was then held at 150°C. for 8 min.

A detailed description of the gas chromatograph calibration constants has been given by Hopper (1).

C. Procedure

The steps followed on each experimental run were as follows:

1. A desired weight of calcined catalyst is put in a stoppered vial. If the apparent volume of the catalyst sample is less than 15 cc, the catalyst is diluted with mullite and vigorously shaken to form a well-dispersed mixture having an apparent volume of about 15 cc. The dilution is made to insure proper contact with the temperature measuring thermocouple.
2. The catalyst-mullite mixture is transferred to the reactor. A glass-wool plug is inserted behind the catalyst to serve as a support. The reactor is sealed with a new steel ring and the temperature-compensated coupling is secured with a flange.
3. The reactor is positioned outside the sand bath and tested for leaks at a pressure 20% higher than that required in the experimental run.
4. While the reactor is being pressure tested, the gear ratios of the Ruska pump are adjusted to obtain the desired flow rate. The hydrocarbon feed is loaded into the pump.
5. The reactor is depressured and placed in the sand bath. The system is purged with nitrogen.
6. The hydrogen flow rate is set by the control valve. The flow of hydrogen is checked with a stop watch and the wet

test meter.

7. After the catalyst temperature has reached 500°F., the hydrogen flow is maintained for 1 hour to reduce the palladium to the metallic form.
8. The temperature for the run is selected and the controller adjusted accordingly.
9. The system pressure is established and the unit is tested for leaks.
10. The liquid feed is started.
11. After reaching steady state (1 1/2-2 hours) a 15-30 minutes material balance is taken.
12. The information gathered during the experimentation is analyzed as shown in Appendix B.

LIST OF REFERENCES - CHAPTER IV

1. Hopper, J. R., "A Study of the Catalytic Hydroisomerization Reactions of N-Pentane and Cyclohexane Over Structurally Modified Mordenites," Ph.D. dissertation, Department of Chemical Engineering, Louisiana State University, 1969.

CHAPTER V

A SIMPLIFIED KINETIC MODEL FOR THE SIMULTANEOUS HYDROISOMERIZATION AND HYDROCRACKING OF CYCLOHEXANE

A. Introduction

There are two types of models; namely, theoretical or empirical. An empirical model is a simple mathematical formulation used only to correlate a given set of data. As a consequence, extreme care must be exercised in extrapolating an empirical model beyond the range of actual experimentation. On the other hand, the theoretical model may be simple or complex but it is based on some assumed mechanism. A theoretical model can be applied with more confidence over a wide-range of unexplored conditions. Most frequently, the researcher finds himself in a compromise between the empirical and theoretical approach.

In this chapter a kinetic model is developed for the simultaneous hydroisomerization and hydrocracking of cyclohexane based, as much as possible, on fundamental considerations.

B. Reactor Considerations

1. Choice of Experimental Reactor

The selection of a suitable experimental reactor is a critical step in obtaining meaningful kinetic data, and consequently it should be given careful consideration. Not only does the experimental reactor influence the mathematical development of the kinetic

model, but also the strategy involved in planning the experiments.

As noted by Petersen (18) an experimental reactor must be simple so as to allow the researcher to isolate purely kinetic effects from distracting extraneous phenomena; namely, mass transfer, internal diffusion within catalyst pores, eddy diffusivities, etc.

For gaseous fluid systems catalyzed by solids, as in the case in the present study, the tubular experimental reactor is the most frequently encountered (13). The tubular reactor can be operated in an integral or differential fashion. Plus marks for the differential reactor are compactness, easier temperature control, and more direct rate determination. However, the attractive features of the integral reactor are less analytical difficulties (since concentration changes are considerable), and a more straight-forward scale-up.

It seemed appropriate to use an integral tubular reactor with a fixed bed of catalyst to study the simultaneous hydroisomerization and hydrocracking of cyclohexane over a Pd-H-faujasite catalyst.

2. Axial Dispersion in Integral Tubular Reactor Employed in Present Study

Deviations from plug flow behavior are observed when axial dispersion becomes pronounced. Dispersion is another name for diffusion, and the axial dispersion rate equation is expressed as:

$$N_{di} = -E_d A_e \frac{dC_i}{dz} \qquad (1)$$

where

N_{di} = axial dispersion rate of species i,

E_d = axial dispersion coefficient,

A_e = empty cross sectional area,

C_i = concentration of species i,

z = longitudinal reactor length.

A dispersion group results from arranging in dimensionless form the differential equations describing dispersion and bulk motion in a packed-bed reactor. This dispersion group, or Peclet number, can be thought of as a measure of the ratio of the directed motion of the bulk stream to the random motion in the dispersive eddies.

A Peclet number of zero represents perfect mixing, and a Peclet number of infinity corresponds to ideal plug flow. Furthermore, Levenspiel (15) demonstrates that for Peclet numbers greater than — 20 deviations from plug flow conditions are small.

Tracer test studies were conducted by Bryant (3) in a packed bed reactor which was a duplicate of the one employed in the present study, and he concluded that plug flow conditions were very closely approximated. Bryant's data agree well with the correlations presented by Levenspiel and Bischoff (16).

3. Temperature Profiles Along the Catalyst Bed in Present Study

A short study was conducted to investigate temperature variations along the catalyst bed for a typical hydroisomerization and hydrocracking run over a Pd-H-Faujasite catalyst employing a special reactor equipped with an axial thermocouple. Axial temperature profiles were found to be negligible (< $1^{o}F$).

C. Simplified Kinetic Model

1. Model Conception

For the present study, it was expected that by reacting

cyclohexane over a Pd-H-faujasite catalyst one would obtain the corresponding methylcyclopentane isomer along with lower molecular weight hydrocarbons which will be referred to as "cracked products." At the conditions of temperature (490°F-550°F), pressure (250 psig-650 psig), and hydrogen to cyclohexane molar ratios (5-10 moles H_2/mole feed) investigated, negligible amounts of benzene are expected in the product. Accordingly, a set of experiments was designed which consisted in varying the cyclohexane feed space velocity at constant temperature (490°F), pressure (450 psig), and H_2/cyclohexane mole ratio (10). The results of such experiments are shown in Figure 4.

From Figure 4, it was observed that by increasing contact time (l/w/hr/w) cyclohexane disappeared continuously; methylcyclopentane was initially formed very fast and then went through a maximum before beginning to disappear. The cracked products were being produced rather slowly at the start but increased at an accelerated rate as the reactions proceeded.

In order to obtain a more precise idea of the reaction path, a similar set of experiments was conducted at a higher temperature level. This time the experiments were carried out starting with a pure cyclohexane feed, a pure methylcyclopentane feed, and an equilibrium mixture of cyclohexane and methylcyclopentane. The experimental results are conveniently represented in a triangular diagram as shown in Figure 5.

From Figure 5, it was noticed that the cyclohexane isomerization occurred very fast initially, However, as the contact time was increased, cracked products began to appear before equilibrium was reached between cyclohexane and methylcyclopentane. A similar be-

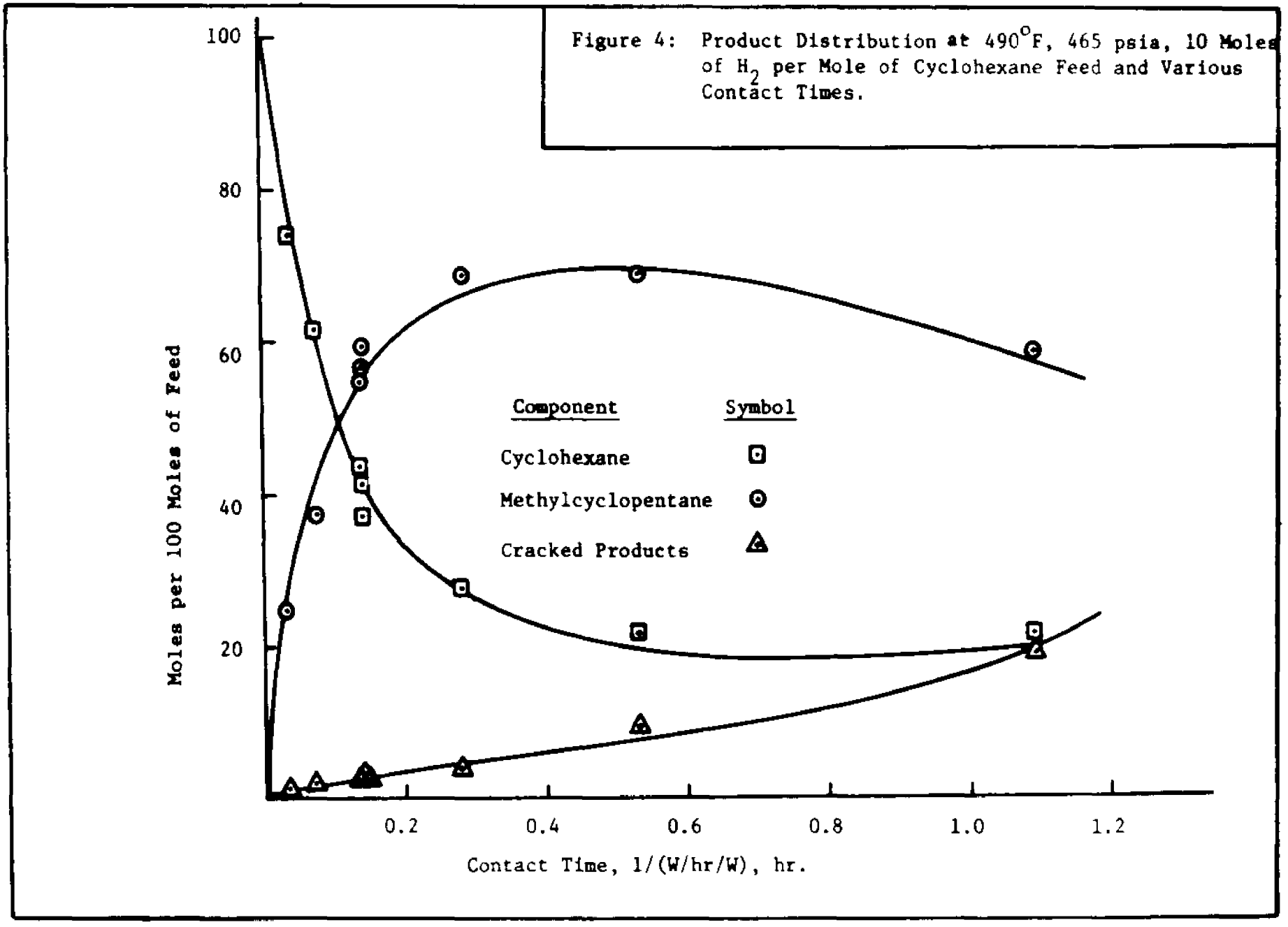
Figure 4: Product Distribution at 490°F, 465 psia, 10 Moles of H_2 per Mole of Cyclohexane Feed and Various Contact Times.
100
80
60
40
20
Moles per 100 Moles of Feed
Component
Symbol
Cyclohexane
Methylcyclopentane
Cracked Products
0.2
0.4
0.6
0.8
1.0
1.2
Contact Time, 1/(W/hr/W), hr.

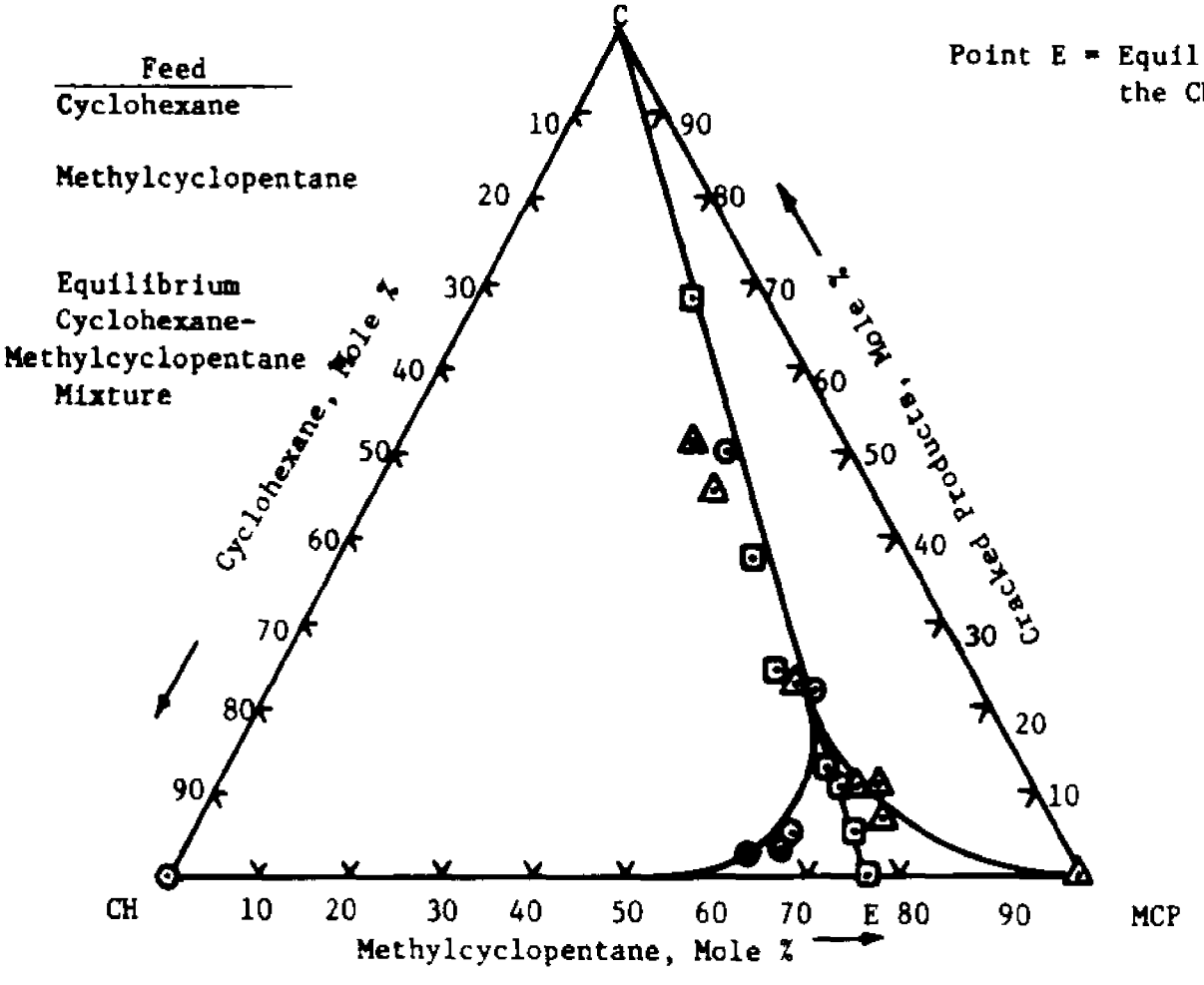

Figure 5: Reaction Path at 520°F, 465 psia, and 10 Moles of H_2 per Mole of Feed.

havior was demonstrated when starting with a methylcyclopentane feed.

Furthermore, it was noticed that the straight line CE, representing a constant cyclohexane/methylcyclopentane ratio, became at long contact times a good approximation for the reaction path from all three starting positions.

It was then concluded that a "reasonable" model for these reactions could be:

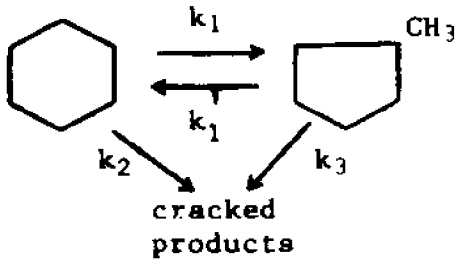

2. Competitive Mechanisms in Heterogeneously Catalyzed Reactions

In order for the surface reaction to occur the following steps must take place (12):

a. mass transfer of reactants from the bulk gas stream to the external surface of the catalyst,

b. diffusion of reactants into the catalyst pores,

c. adsorption of reactants,

d. surface chemical reaction,

e. desorption of products,

f. diffusion of products through catalyst pores to the external surface of the catalyst,

g. mass transfer of products from the catalyst surface to the bulk gas stream.

Steps a, b, f, and g can be eliminated from further consideration by adjusting the experimental conditions as will be demonstrated

in Chapter VI. The experimental kinetic data are interpreted in terms of steps c, d, and e as will also be shown in Chapter VI.

3. Mathematical Formulation

Based on the discussion of the previous sections, the following assumptions were made:

a. Plug flow prevails in the packed bed of the integral tubular reactor.

b. Isothermal conditions and negligible pressure drops exist along the catalyst bed.

c. The surface chemical reactions are the rate controlling step and they proceed according to the kinetic model.

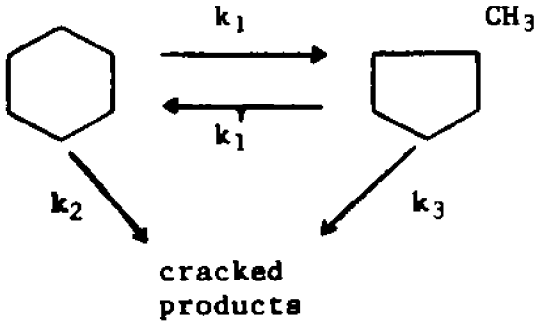

d. Steady state has been reached.

Now, consider an element of the packed bed tubular reactor containing the differential amount of catalyst ΔW_c.

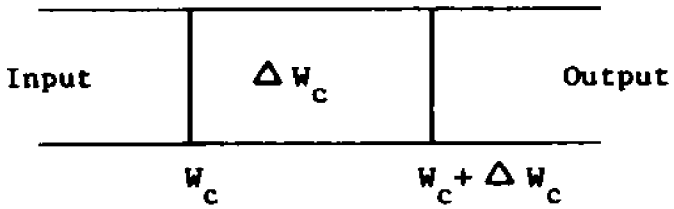

A material balance on cyclohexane yields:

$$N_{a|(W_c)} - N_{a|(W_c+\Delta W_c)} + r_A(\Delta W_c) = 0 \qquad (2)$$

where

N_a = gm moles of cyclohexane/sec,

W_c = gm of catalyst,

r_A = gm moles of cyclohexane/sec-gm catalyst.

Solving equation (2) for r_A, the following expression is obtained.

$$r_A = \frac{N_a|_{(W_c + \Delta W_c)} - N_a|_{(W_c)}}{\Delta W_c} \tag{3}$$

If the limit of equation (3) is taken as $\Delta W_c \longrightarrow 0$, the differential equation resulting is

$$r_A = \frac{dN_a}{dW_c} \tag{4}$$

The same reasoning can be repeated for methylcyclopentane to obtain the rate equation

$$r_B = \frac{dN_b}{dW_c} \tag{5}$$

where

r_B = gm moles of methylcyclopentane/sec-gm catalyst,

N_b = gm moles of methylcyclopentane/sec.

Incorporating the postulated reaction model into equations (4) and (5) results in the overall equations:

$$\frac{dN_a}{dW_c} = k_1' C_b - (k_1 + k_2) C_a \tag{6}$$

$$\frac{dN_b}{dW_c} = k_1 C_a - (k_1' + k_3) C_b \tag{7}$$

where

C_a = gm moles of cyclohexane/cc of total gas,

C_b = gm moles of methylcyclopentane/cc of total gas,

k_1, k_1', k_2, k_3 = cc of total gas/sec - gm of catalyst.

In this study, it was convenient to work with mole fractions instead of absolute concentrations. As a consequence, the following relationships were used:

$$C_a = y_a \frac{N}{V} , \tag{8}$$

$$C_b = y_b \frac{N}{V} , \tag{9}$$

$$N_a = y_a \; N \; , \tag{10}$$

and

$$N_b = y_b \; N \; , \tag{11}$$

where

y_a = mole fraction of cyclohexane,

N = gm moles of total gas/sec,

and V = cc of total gas/sec.

By substituting equations (8) through (11) into equations (6) and (7), upon rearrangement, the rate equations can be expressed in terms of mole fractions as:

$$\frac{dy_a}{d(W_c/V)} = k_1' \; y_b - (k_1 + k_2) y_a \tag{12}$$

and

$$\frac{dy_b}{d(W_c/V)} = k_1 \; y_a - (k_1' + k_3) y_b \tag{13}$$

Furthermore, the surface chemical reactions are carried out in the presence of hydrogen to keep the catalyst surface clean of carbonaceous materials commonly referred to as "coke." To facilitate the analytical interpretation of the experimental data, it is advantageous to express the mole fractions on a hydrogen-free basis by means of the relations:

$$Y_a = y_a \; (1 + R_H) \tag{14}$$

$$Y_b = y_b \; (1 + R_H) \tag{15}$$

where

Y_a = hydrogen-free mole fraction of cyclohexane,

Y_b = hydrogen-free mole fraction of methylcyclopentane,

R_H = moles of hydrogen per mole of hydrocarbons.

Substituting equations (14) and (15) into equations (12) and (13) yields:

$$\frac{dY_a}{d(W_c/V)} = k_1' Y_b - (k_1 + k_2)Y_a \tag{16}$$

$$\frac{dY_b}{d(W_c/V)} = k_1 Y_a - (k_1' + k_3)Y_b \tag{17}$$

Finally, the ratio (W_c/V) appearing in equations (16) and (17) can be expressed in terms of more easily measured parameters by letting

$$(W_c/V) = t_s = M_w\left(\frac{P}{RT}\right)\left(\frac{3600}{w/hr/w}\right)\left(\frac{1}{1 + R_H}\right) \tag{18}$$

where

t_s = superficial contact time based on catalyst weight, sec-gm/cc total gas,

M_w = molecular weight of hydrocarbons,

P = total pressure, psia,

T = temperature, ^oR,

R = gas low constant,

w/hr/w = weight space velocity, gm feed/hr-gm catalyst,

and

R_H = moles of hydrogen per mole of hydrocarbons.

The final form of the simultaneous differential equations is obtained by substituting equation (18) into equations (16) and (17), to obtain:

$$\frac{dY_a}{dt_s} = k_1' Y_b - (k_1 + k_2)Y_a \tag{19}$$

$$\frac{dY_b}{dt_s} = k_1 Y_a - (k_1' + k_3)Y_b \tag{20}$$

Recalling that the present study employs an integral reactor, the next step is to solve equations (19) and (20) simultaneously, for the hydrogen-free mole fractions of cyclohexane (Y_a), and methylcyclopentane (Y_b). Obviously, the hydrogen-free mole fraction of the cracked products (Y_c) is obtained by difference.

Wei and Prater (23) have solved the simultaneous differential equations for the general three component kinetic system.

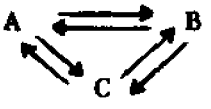

When their solution is expressed in terms of the nomenclature developed in the present chapter, the following equations result:

$$Y_a = Y_a^* + \frac{1}{(u_2-u_1)} \left\{ \left[(Y_a^o - Y_a^*) + u_1(Y_b^o - Y_b^*) \right] u_2 e^{-\lambda_1 t_s} - \left[(Y_a^o - Y_a^*) + u_2(Y_a^o - Y_a^*) \right] u_1 e^{-\lambda_2 t_s} \right\} \tag{21}$$

$$Y_b = Y_b^* + \frac{1}{(u_2-u_1)} \left\{ - \left[(Y_a^o - Y_a^*) + u_1(Y_b^o - Y_b^*) \right] e^{-\lambda_1 t_s} + \left[(Y_a^o - Y_a^*) + u_2(Y_b^o - Y_b^*) \right] e^{-\lambda_2 t_s} \right\} \tag{22}$$

$$Y_c = 1 - Y_a - Y_b, \tag{23}$$

where

$$k_a = k_1 + k_2, \tag{24}$$

$$k_b = k_1' + k_3, \tag{25}$$

$$k_c = k_1, \tag{26}$$

$$k_d = k_1', \tag{27}$$

$$\Delta = (k_a - k_b)^2 + 4\, k_c\, k_d, \tag{28}$$

$$u_1 = \frac{k_a - k_b - \sqrt{\Delta}}{2\, k_c}, \tag{29}$$

$$u_2 = \frac{k_a - k_b + \sqrt{\Delta}}{2\, k_c}, \tag{30}$$

$$\lambda_1 = \frac{(k_a + k_b + \sqrt{\Delta})}{2}, \tag{31}$$

$$\lambda_2 = \frac{(k_a + k_b - \sqrt{\Delta})}{2}, \tag{32}$$

Y_a^o = mole fraction of cyclohexane at $t_s = o$,

Y_a^* = mole fraction of cyclohexane at $t_s = \infty$,

Y_b^o = mole fraction of methylcyclopentane at $t_s = o$,

Y_b^* = mole fraction of methylcyclopentane at $t_s = \infty$,

and

Y_c = mole fraction of cracked products.

4. Evaluation of Rate Constants

From a mathematical standpoint, the method of solving the present problem was outlined in the previous section. However, there still remains the considerable task of evaluating the rate constants; namely, k_1, k_1', k_2, and k_3, from the experimental data.

In addition to equations (21) - (23), it is necessary to have the equilibrium equation relating k_1 and k_1'. The equilibrium constant could be calculated from the API-44 free energy data (22). However, the free energy change involved in the cyclohexane hydroisomerization is small; and erroneous results could be obtained when relying on a small difference between two large numbers. Consequently, the experimentally determined equilibrium constants obtained by

Hopper (11), in the range 400°F-600°F were used in the present study. The experimental equation relating K with temperature is as follows:

$$\ln K = -4810/(T) + 6.114 \tag{33}$$

where

K = equilibrium constant,

T = temperature, °R.

Due to the complexity of the mathematical system, it is impossible to solve the remaining rate constants k_1, k_2, and k_3 explicitly in terms of the process variables. Consequently, the approach taken was to calculate the rate constants by an iterative trial and error procedure, where the square of the residuals is minimized.

Consider the independent equations (21) and (22) and for simplicity write them as:

$$Y_a = P_1(k_1, k_2, k_3, t_s, \text{other variables}), \tag{34}$$

and

$$Y_b = P_2(k_1, k_2, k_3, t_s, \text{other variables}). \tag{35}$$

The objective is to find k_1, k_2, and k_3 such that the calculated functional values P_1 and P_2, would match the experimentally determined Y_a and Y_b. Mathematically, the problem is formulated as a square residual minimization by the equation

$$C = \sqrt{\sum_i (Y_i - P_i)^2}; \tag{36}$$

where C, represents the objective function to be minimized in successive iterations. To preserve physical significance, a constraint is imposed by requiring that all rate constants be positive.

The literature on optimization procedures is very recent. Some of the most important schemes developed in the last decade are

summarized in Table 3. A comparasion of several optimization procedures has been given by Box (2).

In general, it is hard to say "a priori," which optimization scheme will work best for a given system. In a two dimensional minimization problem, one can obtain a good idea of the contour surfaces and plan the optimization strategy accordingly. When more than two dimensions are involved, the problems of following the movements of a given optimization procedure are greatly increased. Wilde (24) has referred to this problem as the "curse of dimensionality."

For the present study, it was decided to use Pattern search, because no first derivatives evaluations are required, and the constraint equations can be easily handled. The Pattern search computer program employed was written by Dr. C. F. Moore and is available at the computer library of the Chemical Engineering Department of Louisiana State University. Allan (1) successfully used Pattern to calculate the rate constants for the dehydrogenation and hydroisomerization of cyclohexane.

For the present work, it was found that the convergence rate of Pattern was quite good, and the final value of the objective function was in the neighborhood of 10^{-6} for most of the cases investigated.

Upon analysis of the experimental data, it became apparent that the present model would predict the cyclohexane hydrocracking rate constant (k_2) to be equal to the methylcyclopentane hydrocracking rate constant (k_3). In other words, a two parameter model containing only two rate constants (k_1, k_2=k_3) would fit the data equally well. A comparison of the predictions obtained by the two parameter model, and

Table 3: Chronological Summary of Most Important Optimization Schemes

Procedure	Year	Literature Reference
Pattern	1960	(10)
Rotating Coordinates	1961	(21)
Partan	1961	(24)
Fletcher - Powell	1963	(5)
Powell Non-Derivative I	1964	(19)
Conjugate Gradients	1964	(6)
Powell Non-Derivative II	1965	(20)
Simplex	1965	(17)
Rotational Discrimination	1967	(14)
Davidon - Variance Algorithm	1968	(4)
Zangwill Non-Derivative	1968	(25)
Fletcher-Generalized Least Squares	1968	(7)
Variable Metric Methods	1970	(8)
Variational Means	1970	(9)

the three parameter model at two different temperature levels is presented in Table 4.

As a consequence, the kinetic model was finally reduced to

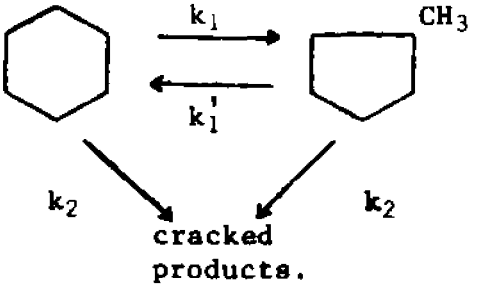

Obviously, all the previously developed yield equations are still applicable if k_3 is replaced by k_2. However, the optimization strategy is altered since k_2 can be solved for explicitly in terms of the operating conditions. Only k_1 needs to be obtained by trial and error by minimizing the objective function.

The manipulations carried out to obtain k_2 analytically can be quickly demonstrated. Consider the rate of formation of cracked products as:

$$\frac{dY_c}{dt_s} = k_2(Y_a + Y_b) = k_2(1-Y_c) \tag{37}$$

Upon integration and rearrangement of equation (37) k_2 is expressed as:

$$k_2 = \left(\frac{1}{t_s}\right) \left\{ \ln[1/(1-Y_c)] \right\} \tag{38}$$

A discussion of the overall effectiveness of the developed kinetic model is postponed until Chapter VI.

Table 4: A Comparison of the Two-Parameter Kinetic Model with the Three-Parameter Kinetic Model.

Reacting Conditions

Feed	Cyclohexane
Catalyst	Pd-Faujasite
Catalyst Particle Size, mm	0.417 - 1.168
Pressure, psia	465
Weight Space Velocity, (grm. feed)/(hr.)/(grm. cat.)	7
Moles of H_2 per Mole of Feed	10

Experimental Results

		Three-Parameter		
Run No.[1]	Temp. °F	Cyclohexane Hydroisomerization Rate Constant, k_1, cc./grm. sec.	Cyclohexane Hydrocracking Rate Constant, k_2, cc./grm. sec.	MCP[2] Hydrocracking Rate Constant, k_3, cc./grm. sec.
1A	490	0.327	0.012	0.012
4D	530	0.927	0.035	0.035

		Two-Parameter	
Run No.[1]	Temp. °F	Cyclohexane Hydroisomerization Rate Constant, k_1, cc./grm. sec.	[Cyclohexane + MCP][3] Hydrocracking Rate Constant, k_2, cc./grm. sec.
1A	490	0.327	0.012
4D	530	0.928	0.035

[1] Detailed data in Appendix A
[2] Methylcyclopentane
[3] Lumped cyclohexane and methylcyclopentane

LIST OF REFERENCES - CHAPTER V

1. Allan, D. E., "The Dehydrogenation and Isomerization of Cyclohexane over a Platinum Alumina Mordenite Catalyst," Ph.D. Dissertation, Department of Chemical Engineering, Louisiana State University, 1970.

2. Box, M. J., "A Comparison of Several Current Optimization Methods and the Use of Transformations in Constrained Problems," The Computer Journal, 9, 67 (1966).

3. Bryant, P. A., "Hydroisomerization of Normal Pentane over a Zeolite Catalyst, "Ph.D. Dissertation, Department of Chemical Engineering, Louisiana State University, 1966.

4. Davidon, W. C., "Variance Algorithm for Minimization," The Computer Journal, 10, 406 (1968).

5. Fletcher, R. and Powell, M. J. D.,"A Rapidly Convergent Descent Method for Minimization," The Computer Journal, 6, 163 (1963).

6. Fletcher, R. and Reeves, C. M., "Function Minimization by Conjugate Gradients," The Computer Journal, 7, 149 (1964).

7. Fletcher, R., "Generalized Inverse Methods for the Best Least Squares Solution of Systems of Non-Linear Equations," The Computer Journal, 10, 392 (1968).

8. Greenstadt, J., "Variations on Variable- Metric Methods," Mathematics of Computation, 24, 1 (1970).

9. Golfarb, D., "A Family of Variable-Metric Methods Derived by Variational Means," Mathematics of Computation, 24, 22 (1970).

10. Hooke, R. and Jeeves, T. A., "Direct Search Solution of Numerical and Statistical Problems," Journal Association of Computing Machinery, 8, 212 (1961).

11. Hopper, J. R., "A Study of the Catalytic Hydroisomerization Reactions of n-Pentane and Cyclohexane over Structurally Modified Mordenites," Ph.D Dissertation, Department of Chemical Engineering, Louisiana State University, 1969.

12. Hougen, O. A. and Watson, K. M., Chemical Process Principles, Part III, Kinetics and Catalysis, John Wiley and Sons, New York, New York, 1947.

13. Kramer, H. and Westerterp, K. R., Elements of Chemical Reactor Design and Operation, Academic Press Inc., New York, New York, 1963.

14. Law, V., "Rotational Discrimination," American Institute of Chemical Engineers National Meeting, Paper No. 30, Houston, 1967.

15. Levenspiel, O., Chemical Reaction Engineering, John Wiley and Sons, Inc. New York, New York, 1962.

16. Levenspiel, O. and Bischoff, K. B., "Patterns of Flow in Chemical Process Vessels," Advances in Chemical Engineering, 4, 75, Academic Press, New York, New York, 1963.

17. Nelder, J. A. and Mead, R., "A Simplex Method for Function Minimization," The Computer Journal, 7, 308 (1965).

18. Petersen, E. E., Chemical Reaction Analysis, Prentice-Hall, Inc., Englewood Cliffs, New Jersey, 1965.

19. Powell, M. J. D., "An Efficient Method for Finding the Minimum of a Function of Several Variables Without Calculating Derivatives," The Computer Journal, 7, 155 (1964).

20. Powell, M. J. D., "A Method for Minimizing a Sum of Squares of Non-Linear Functions Without Calculating Derivatives, The Computer Journal, 7, 303 (1965).

21. Rosenbrock, H. H., "Automatic Method for Finding the Greatest or Least Value of a Function," The Computer Journal, 3, 175 (1960).

22. Rossini, F. D., et al, Selected Values of Physical and Thermodynamic Properties of Hydrocarbons and Related Compounds, Carnegie Press, Pittsburgh, Pa., (1953).

23. Wei, J. and Prater, C. D., "Analysis of Complex Reactions," Advances in Catalysis, 13, 203 (1960).

24. Wilde, D. J., Optimum Seeking Methods, Prentice-Hall Inc., Englewood Cliffs, New Jersey, 1964.

25. Zangwill, W. I., "Minimizing a Function Without Calculating Derivatives," The Computer Journal, 10, 293 (1968).

CHAPTER VI

EXPERIMENTAL DATA AND ITS CORRELATION

A. Introduction

The objective of this chapter is to analyze the experimental data in accordance with the previously developed kinetic model. In the first part of the chapter, it is shown that mass transfer and internal diffusion do not have any influence on the reaction rate constants. Hence they are eliminated from further consideration.

Subsequently, a test on the assumed order of the hydroisomerization and hydrocracking reactions is presented and analyzed. With the aid of an Arrhenius-type correlation, activation energies for the above-mentioned reactions are obtained by a least squares technique and compared with the values reported in the literature. A study is also conducted to elucidate the proper adsorption-surface reaction-desorption mechanism for the present investigation.

Finally, the chapter is concluded with a discussion on the effectiveness of the overall kinetic model.

B. Effect of Mass Transfer and Intra-Particle Diffusion on the Reaction Rate Constants

The rate of mass transfer from the bulk fluid stream to the catalyst surface depends on the thickness of the boundary layer surrounding the catalyst particles. Therefore, by varying the fluid velocity alone, a range can be found where mass transfer does not have

any effect on the reaction rate. Accordingly, a set of experiments was conducted by varying the feed rate at otherwise constant conditions. The experimental results are summarized in Table 5 and Figure 6. As shown in Figure 6, it appears that the reaction rate constants are independent of fluid velocity for the feed rates commonly employed in the present study; namely, 16-60 cc/hr.

The intraparticle diffusion of the reacting molecules depends on the size of the catalyst particles or "macropore" accessibility. To investigate the effect of intraparticle diffusion, a set of experiments was conducted with different particle sizes but otherwise constant operating conditions. The experimental results are shown in Table 6 and Figure 7. As shown in Figure 7, intraparticle diffusion does not seem to have an effect on the reaction rate constants. However, the present test does not take into consideration the diffusion in the internal channels or "micropores" of the zeolite crystal.

C. A Test of the Postulated Reaction Order

The rate constants for the hydroisomerization and hydrocracking reactions should be a function of the catalyst, and the operating temperature and pressure. However, for a good kinetic model, they should be independent of contact time in the reactor.

For the purpose of investigating the effect of contact time on the reaction rate constants, a set of experiments was carried out where the weight space velocity (w/hr/w) was varied holding all other variables constant. The results of such experiments are summarized in Table 7 and Figure 8.

Within the precision of the experimental data, there seems to be

Table 5: Effect of Mass Transfer on the Hydroisomerization and Hydrocracking Rate Constants at 490°F and 465 psia over a Pd-Faujasite Catalyst.

Reacting Conditions

Feed	Cyclohexane
Catalyst	Pd-Faujasite
Catalyst Particle Size, mm	0.417 - 1.168
Temperature, °F	490
Pressure, psia	465
Weight Space Velocity, $\frac{\text{(grm. feed)}}{\text{(hr.) (grm. cat.)}}$	7
Moles of H_2 per Mole of Cyclohexane	10
Reactor Cross Sectional Area, cm^2	1.51

Experimental Results

Run No.[1]	Superficial Space Velocity, grm/cm^2 min.	Rate Constants, cc./grm. sec. Hydroisomerization k_1	Hydrocracking k_2
1A	0.442 (60)[2]	0.327	0.011
1B	0.221 (30)	0.385	0.011
1C	0.221 (30)	0.387	0.010
1D	0.105 (16)	0.387	0.013
1E	0.105 (16)	0.381	0.009

[1]Detailed data are given in Appendix A
[2]Corresponding feed rates, cc/hr

Figure 6: Mass Transfer Effect.

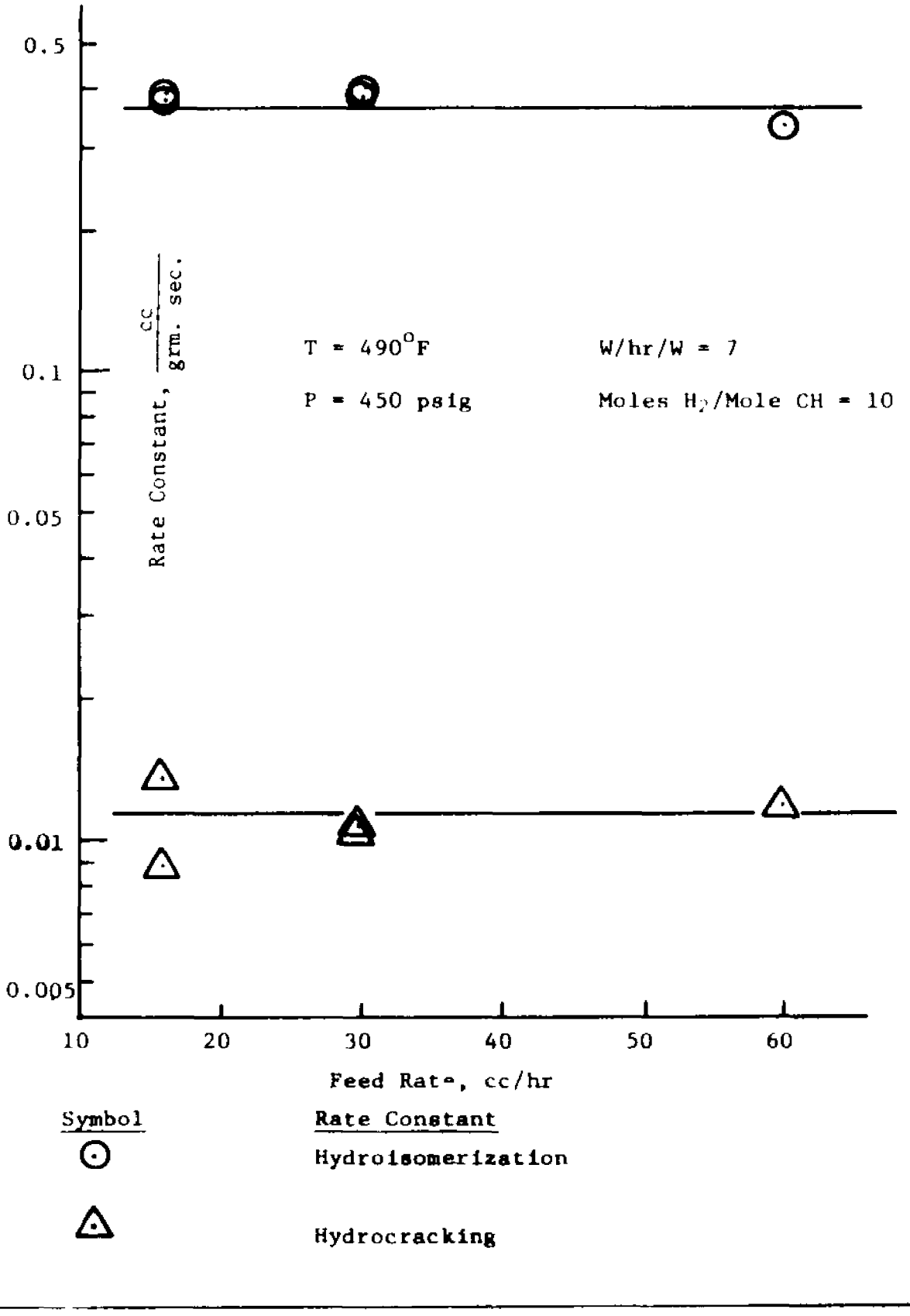

Table 6: Effect of Intraparticle Diffusion on the Hydroisomerization and Hydrocracking Rate Constants at 490°F and 465 psia over a Pd-Faujasite Catalyst.

Reacting Conditions

Feed	Cyclohexane
Catalyst	Pd-Faujasite
Temperature, °F	490
Pressure, psia	465
Weight Space Velocity, $\frac{\text{(grm. feed)}}{\text{(hr.) (grm. cat.)}}$	7
Moles of H_2 per Mole of Cyclohexane	10

Experimental Results

Run No.[1]	Particle Size, mm	Rate Constants, cc./grm. sec. Hydroisomerization k_1	Hydrocracking k_2
1D	0.417-1.168	0.387	0.013
1E	0.417-1.168	0.381	0.009
2A	0.295-0.417	0.381	0.010
2B	0.295-0.417	0.401	0.009
2C	0.074-0.147	0.376	0.009
2D	0.074-0.147	0.361	0.009

[1]Detailed data are given in Appendix A

Figure 7: Intraparticle Diffusion Effects.

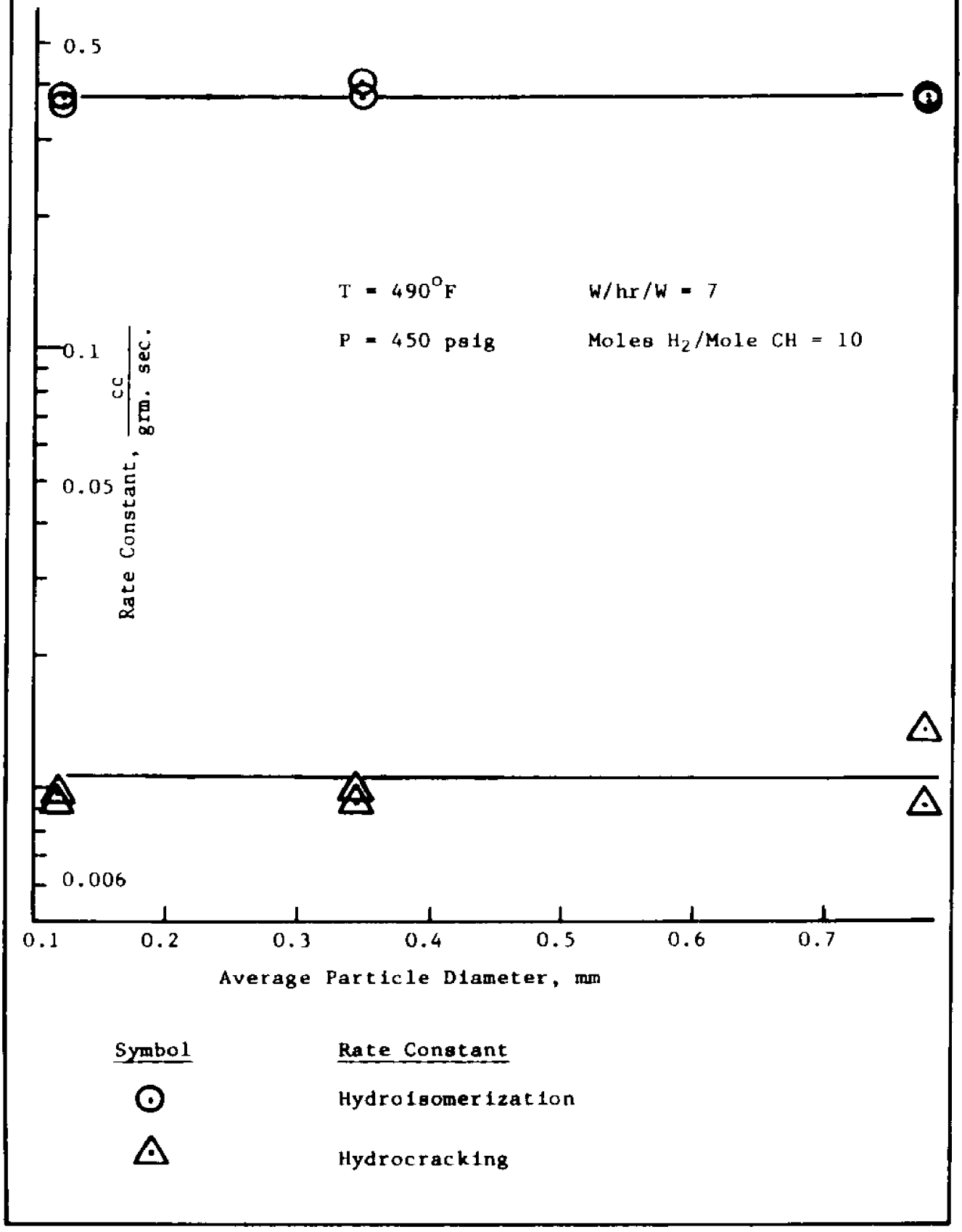

Table 7: Test of the Assumed Reaction Order for the Hydroisomerization and Hydrocracking of Cyclohexane at 490°F and 465 psia over a Pd-Faujasite Catalyst.

Reacting Conditions

Feed	Cyclohexane
Catalyst	Pd-Faujasite
Catalyst Particle Size, mm	0.417 - 1.168
Temperature, °F	490
Pressure, psia	465
Moles of H_2 per Mole of Cyclohexane	10

Experimental Results

Run No.[1]	Weight Space Velocity, grm. feed/hr./grm. cat.	Rate Constants, cc./grm. sec. Hydroisomerization k_1	Hydrocracking k_2
1B	6.98	0.384	0.011
1C	6.98	0.386	0.010
1D	6.99	0.387	0.013
3A	7.01	0.415	0.014
3B	3.50	0.393	0.008
3C	7.01	0.365	0.011
3D	26.28	0.364	0.013
3E	13.14	0.322	0.010
3F	7.00	0.363	0.009

[1]Detailed data in Appendix A

Figure 8: A Test of the Postulated Reaction Order

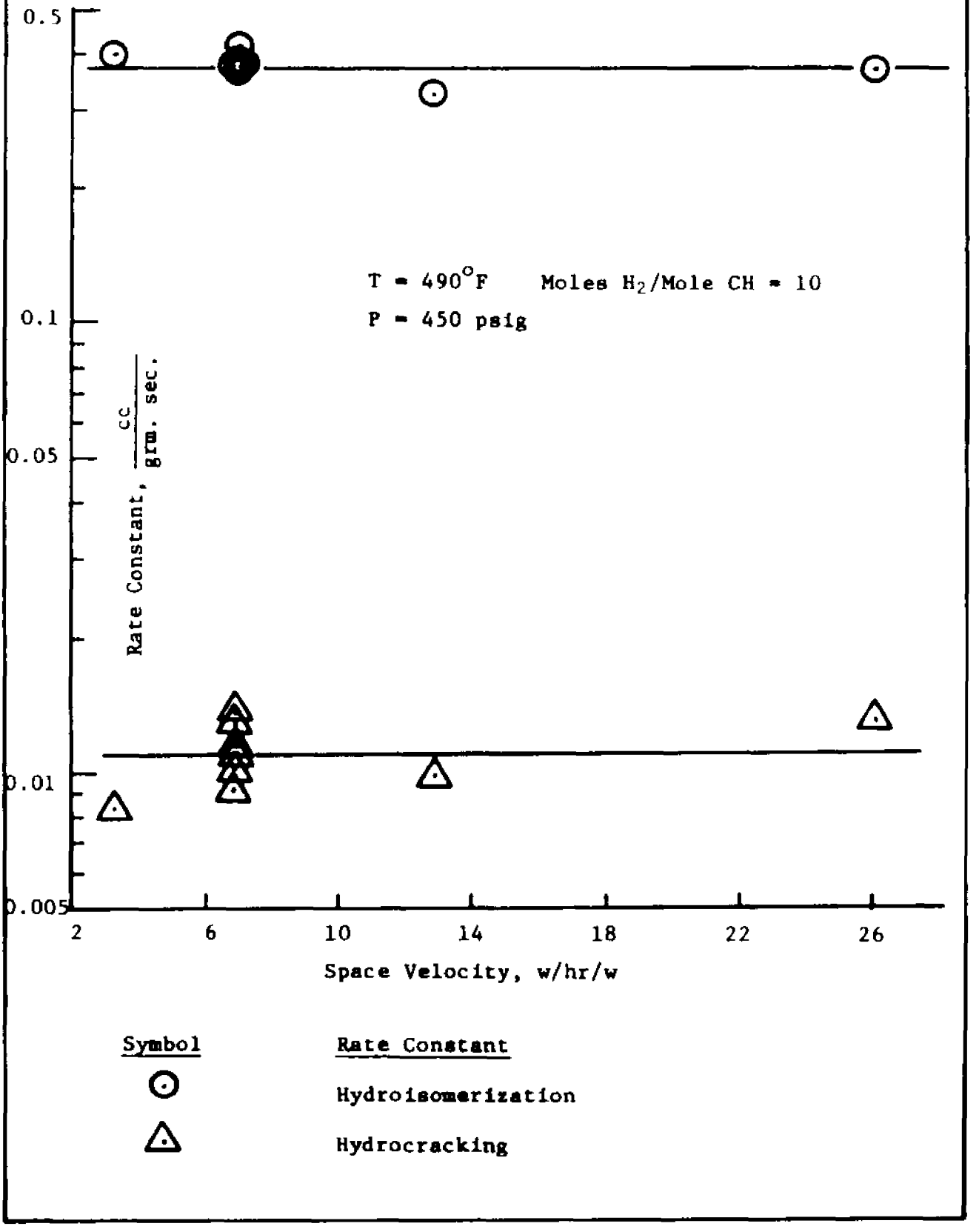

no correlation between the reaction rate constants and the weight space velocities.

D. Activation Energies for the Cyclohexane Hydroisomerization and Hydrocracking Reactions

The effect of temperature on the hydroisomerization and hydrocracking rate constants is shown in Table 8 and Figure 9. In accordance with Arrhenius, the relationship between the rate constants and the operating temperature is given by the following equations:

$$k_1 = k_o^1 \, e^{-\Delta E_1/RT} \qquad (1)$$

$$k_2 = k_o^2 \, e^{-\Delta E_2/RT} \qquad (2)$$

where

k_1, k_2 = hydroisomerization and hydrocracking rate constants,

k_o^1, k_o^2 = hydroisomerization and hydrocracking frequency factors,

ΔE_1, ΔE_2 = hydroisomerization and hydrocracking activation energies,

R = gas law constant,

and

T = absolute temperature.

Equations (1) and (2) can be arranged in linear form by taking the logarithm on both sides of the equations. The experimental data shown in Table 8 were fitted to the linear forms of equations (1) and (2) with the aid of a least squares scheme. A summary of the results obtained is shown in the following tabulation:

	Correlating Equation $\ln k = A + B/T$ ($^\circ$R)			Activation Energies (Kcal/gm-mole)	
Reaction	k	A	B	Present work	Literature
Hydroisomerization	k_1	22.0533	-21.8819×10^3	24(±1)	23-35(4,7,8)
Hydrocracking	k_2	27.0322	-30.0192×10^3	33(±3)	30-35(3,6)

Table 8: Effect of Temperature on the Hydroisomerization and Hydrocracking Rate Constants at 465 psia over a Pd-Faujasite Catalyst.

Reacting Conditions

Feed	Cyclohexane
Catalyst	Pd-Faujasite
Catalyst Particle Size, mm	0.417 - 1.168
Pressure, psia	465
Weight Space Velocity, $\frac{\text{(grm. feed)}}{\text{(hr.) (grm. cat.)}}$	7
Moles of H_2 per Mole of Cyclohexane	10

Experimental Results

Run No.[1]	Temp., $^{\circ}F$	Reciprocal Temperature, $1000/^{\circ}R$	Rate Constants, cc./grm. sec. Hydroisomerization k_1	Hydrocracking k_2
1A	490	1.053	0.327	0.011
1B	492	1.051	0.384	0.010
1C	491	1.052	0.386	0.010
1D	491	1.052	0.387	0.013
1E	490	1.053	0.381	0.009
4A	500	1.042	0.488	0.017
4B	510	1.031	0.620	0.014
4C	520	1.021	0.831	0.022
4D	530	1.011	0.928	0.034
4E	540	1.000	1.098	0.065

[1]Detailed data in Appendix A

Figure 9: Effect of Temperature on the Reaction Rate Constants.

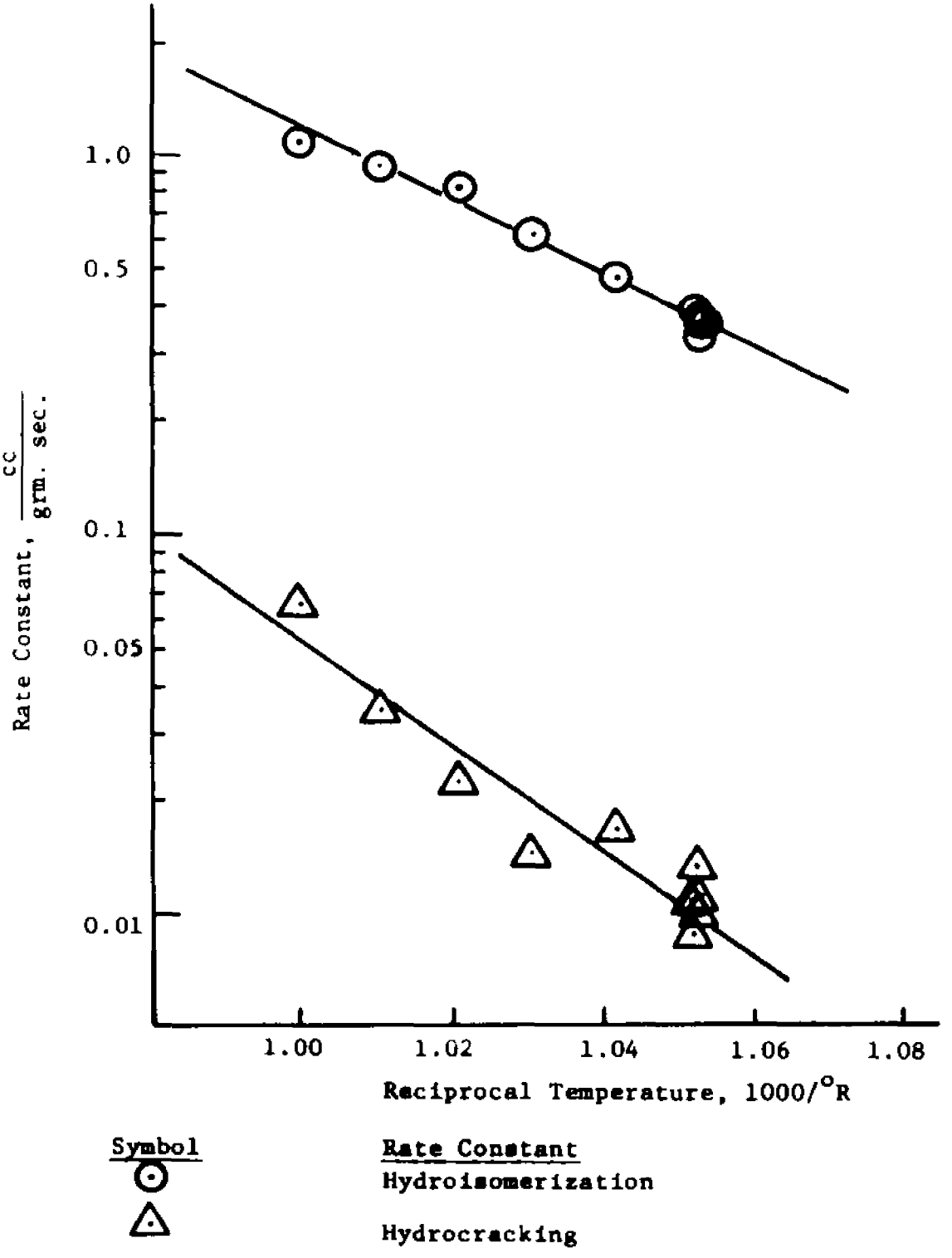

E. A Study of the Adsorption - Surface Reaction - Desorption Mechanisms

1. Effect of Total Pressure on the Reaction Rate Constants at Various Temperatures and Hydrogen Dilution Ratios

It was found that the hydroisomerization rate constant decreased as total pressure increased for all the hydrogen dilution ratios investigated. The results at 490°F are shown in Table 9 and Figure 10, whereas those at 520°F appear in Table 10 and Figure 11. At both temperature levels, the hydroisomerization rate constant increased with hydrogen dilution for a given total pressure.

A similar trend was found for the hydrocracking rate constants. The experimental results obtained at 490°F are shown in Table 11 and Figure 12. Similar results at 520°F appear in Table 12 and Figure 13. It is noticed that at 520°F, the total pressure seems to be the dominant variable.

2. Single and Dual Site Adsorption Mechanisms for Hydroismerization

To account for the effects of pressure on the reaction rate constants, the Langmuir - Hinshelwood - Hougen and Watson (5) adsorption theory is employed. If the rate controlling step is the surface chemical reaction with the adsorption - desorption steps being at equilibrium, the hydroisomerization rate constant can be expressed by the following equation:

$$k_1 = \frac{k_{01} K_{CH}}{(1 + K_{CH} P_{CH} + K_{MCP} P_{MCP} + K_C P_C + K_H P_H)^n} \qquad (3)$$

where

k_1 = hydroisomerization rate constant,

k_{01} = constant dependent on catalyst and temperature,

Table 9: Effect of Pressure on the Hydroisomerization Rate Constant at 490°F and Various Hydrogen to Cyclohexane Mole Ratios over a Pd-Faujasite Catalyst.

Reacting Conditions

Feed	Cyclohexane
Catalyst	Pd-Faujasite
Catalyst Particle Size, mm	0.417 - 1.168
Weight Space Velocity, $\frac{\text{(grm. feed)}}{\text{(hr.) (grm. cat.)}}$	7.0

Experimental Results

Run No.[1]	Temp., °F	Total Press., psia	Moles of H_2 per Mole of Feed	Partial Pressures		Hydroisomerization Rate Constant, cc./grm. sec.
				Hydrocarbons, psia	Hydrogen, psia	
5A	491	265	8.9	27	238	0.741
5B	490	365	8.9	37	328	0.562
5C	490	555	9.8	52	503	0.321
5D	490	665	9.8	62	603	0.235
5E	490	465	9.5	44	421	0.336
1B	492	465	9.2	46	419	0.384
1C	491	465	9.2	46	419	0.386
1D	491	465	8.6	48	416	0.387
3A	491	465	8.9	47	418	0.415

[1] Detailed data are given in Appendix A

Table 9 cont'd: Effect of Pressure on the Hydroisomerization Rate Constant at 490°F and Various Hydrogen to Cyclohexane Mole Ratios over a Pd-Faujasite Catalyst.

Experimental Results

Run No.[1]	Temp., °F	Total Press., psia	Moles of H_2 per Mole of Feed	Partial Pressures		Hydroisomerization Rate Constant, cc./grm. sec.
				Hydrocarbons, psia	Hydrogen, psia	
6A	490	465	20.3	22	443	0.559
6B	489	565	18.9	28	536	0.324
6C	491	665	18.6	34	631	0.343
6D	489	465	18.6	24	441	0.531
6E	490	265	18.3	14	251	0.882
7B	491	665	5.0	112	553	0.185
7C	491	565	5.6	86	478	0.215
7D	491	465	5.4	73	392	0.316
7E	491	370	5.3	58	311	0.405

[1]Detailed data are given in Appendix A

Figure 10: Effect of Total Pressure and Hydrogen Dilution on the Hydroisomerization Rate Constant at 490°F.

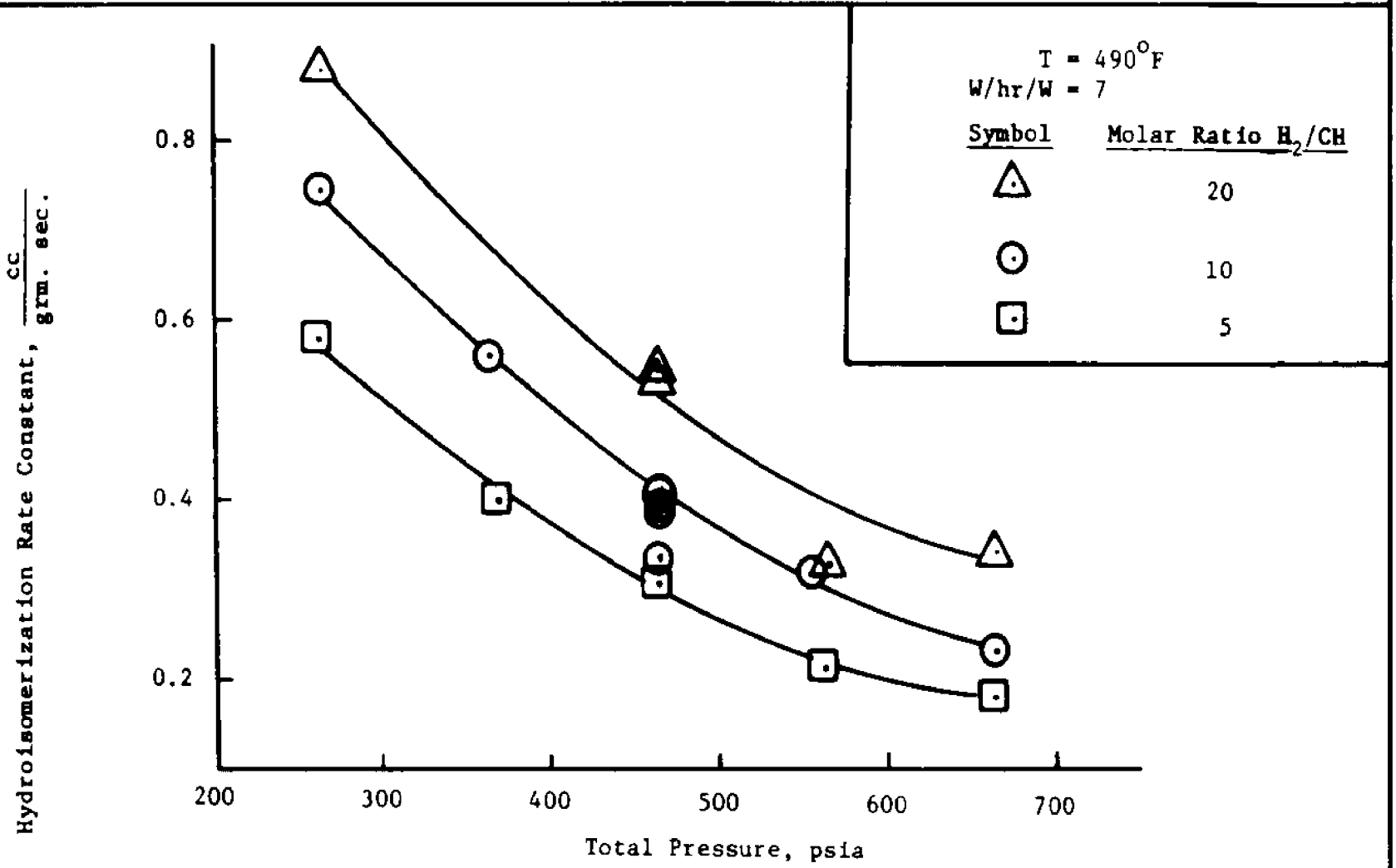

Table 10: Effect of Pressure on the Hydroisomerization Rate Constant at 520°F and Various Hydrogen to Cyclohexane Mole Ratios over a Pd-Faujasite Catalyst.

Reacting Conditions

Feed	Cyclohexane
Catalyst	Pd-Faujasite
Catalyst Particle Size, mm	0.417 - 1.168
Weight Space Velocity, $\frac{\text{(grm. feed)}}{\text{(hr.) (grm. cat.)}}$	7.0

Experimental Results

Run No.[1]	Temp., °F	Total Press., psia	Mole of H_2 per Mole of Feed	Partial Pressures		Hydroisomerization Rate Constant, cc./grm. sec.
				Hydrocarbons, psia	Hydrogen, psia	
8A	522	660	10.0	60	600	0.579
8B	520	565	9.8	52	512	0.618
8C	522	365	9.9	33	331	1.151
8D	521	265	10.2	24	241	1.142
8E	521	465	9.4	45	420	0.770
9A	519	665	19.7	32	633	0.713
9B	520	565	19.3	28	537	0.964
9C	520	465	19.1	23	442	1.091
9D	520	365	18.9	18	346	1.119
9E	519	275	19.4	13	261	1.623

[1]Detailed data are given in Appendix A

Table 10 cont'd: Effect of Pressure on the Hydroisomerization Rate Constant at 520°F and Various Hydrogen to Cyclohexane Mole Ratios over a Pd-Faujasite Catalyst.

Experimental Results

Run No.[1]	Temp., °F	Total Press., psia	Mole of H_2 per Mole of Feed	Partial Pressures		Hydroisomerization Rate Constant, cc./grm. sec.
				Hydrocarbons, psia	Hydrogen, psia	
10A	524	650	5.4	102	547	0.366
10B	520	565	5.5	87	478	0.444
10C	521	365	5.4	57	307	0.702
10D	520	465	5.2	75	390	0.502
10E	525	265	5.1	43	221	0.888

[1]Detailed data are given in Appendix A

Figure 11: Effect of Total Pressure and Hydrogen Dilution on the Hydroisomerization Rate Constant at 520°F.

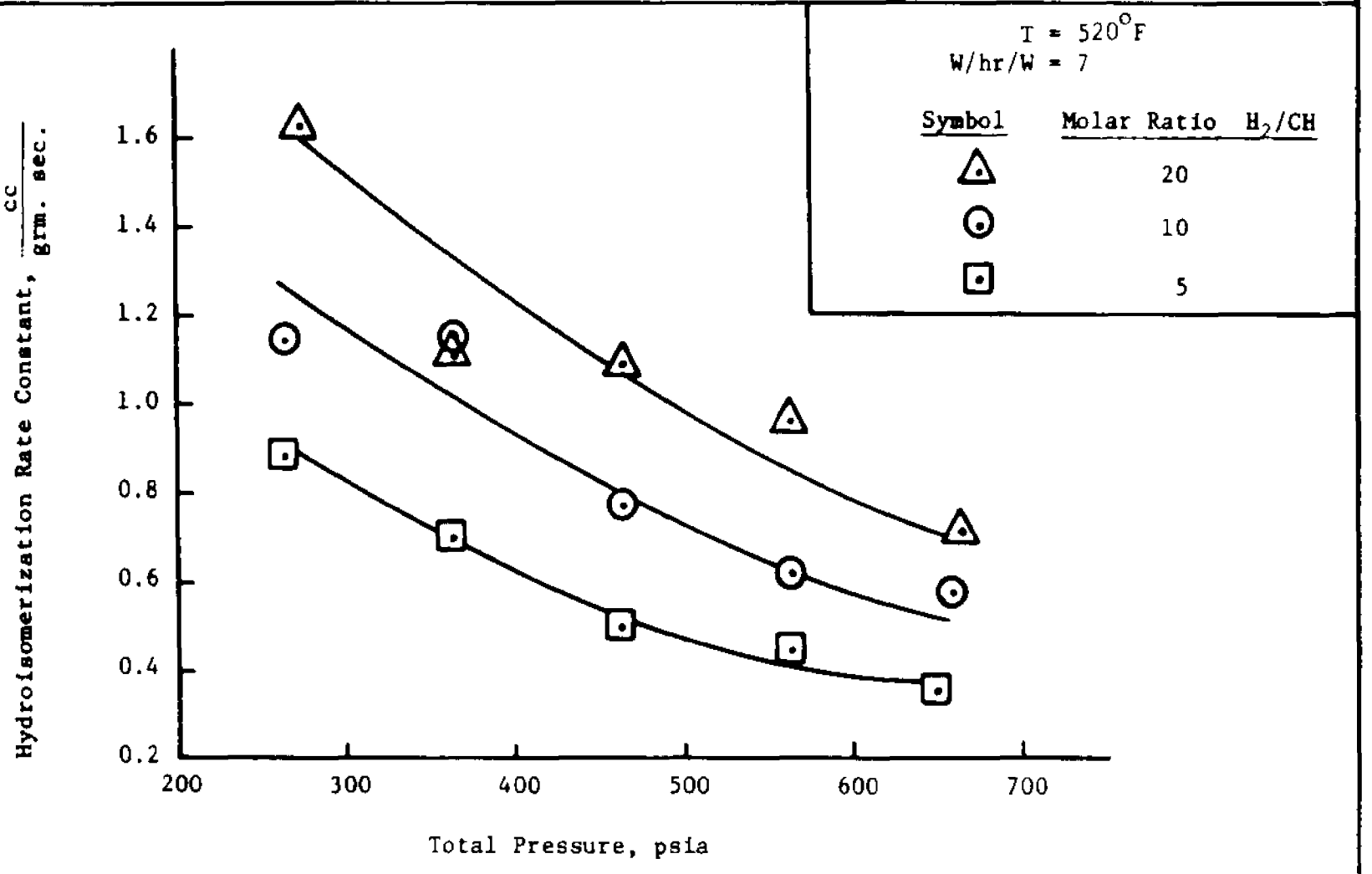

Table 11: Effect of Pressure on the Hydrocracking Rate Constant at 490°F and Various Hydrogen to Cyclohexane Mole Ratios over a Pd-Faujasite Catalyst.

Reacting Conditions

Feed	Cyclohexane
Catalyst	Pd-Faujasite
Catalyst Particle Size, mm	0.417 - 1.168
Weight Space Velocity, (grm. feed)/(hr.)/(grm. cat.)	7.0

Experimental Results

Run No.[1]	Temp., °F	Total Press., psia	Moles of H_2 per Mole of Feed	Partial Pressures		Hydrocracking Rate Constant, cc./grm. sec.
				Hydrocarbons, psia	Hydrogen, psia	
5A	491	265	8.89	27	238	0.018
5B	490	365	8.89	37	328	0.012
5C	490	555	9.75	52	503	0.007
5D	490	665	9.76	62	603	0.007
5E	490	465	9.54	44	421	0.012
1B	492	465	9.19	46	419	0.011
1C	491	465	9.19	46	419	0.010
1D	491	465	8.59	48	416	0.013
3A	491	465	8.92	47	418	0.014

[1] Detailed data are given in Appendix A

Table 11 cont'd: Effect of Pressure on the Hydrocracking Rate Constant at 490°F and Various Hydrogen to Cyclohexane Mole Ratios over a Pd-Faujasite Catalyst.

Experimental Results						
Run No.[1]	Temp., °F	Total Press., psia	Moles of H_2 per Mole of Feed	Partial Pressures		Hydrocracking Rate Constant, cc./grm. sec.
				Hydrocarbons, psia	Hydrogen, psia	
6A	490	465	20.3	22	443	0.041
6B	489	565	18.9	28	536	0.016
6C	491	665	18.6	34	631	0.010
6D	489	465	18.6	24	441	0.024
6E	490	265	18.3	14	251	0.106
7B	491	665	5.0	112	553	0.004
7C	491	565	5.6	86	478	0.005
7D	491	465	5.4	73	392	0.006
7E	491	370	5.3	58	311	0.011

[1] Detailed data are given in Appendix A

Figure 12: Effect of Total Pressure and Hydrogen Dilution on the Hydrocracking Rate Constant at 490°F.

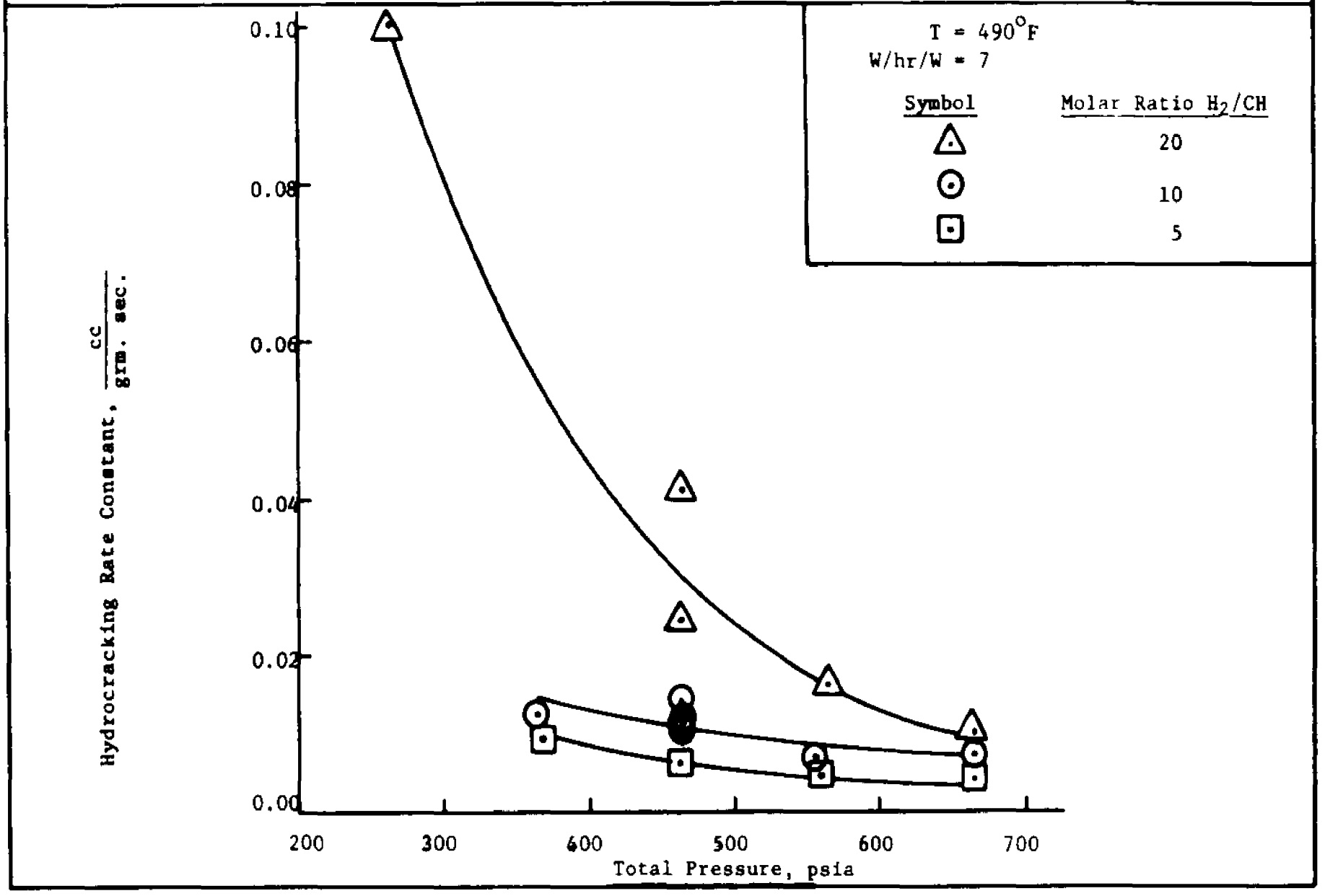

Table 12: Effect of Pressure on the Hydrocracking Rate Constant at 520°F and Various Hydrogen to Cyclohexane Mole Ratios over a Pd-Faujasite Catalyst.

Reacting Conditions

Feed	Cyclohexane
Catalyst	Pd-Faujasite
Catalyst Particle Size, mm	0.417 - 1.168
Weight Space Velocity, (grm. feed)/(hr.)/(grm. cat.)	7

Experimental Results

Run No.[1]	Temp., °F	Total Press., psia	Moles of H_2 per Mole of Feed	Partial Pressures		Hydrocracking Rate Constant, cc./grm. sec.
				Hydrocarbons, psia	Hydrogen, psia	
8A	522	660	10.0	60	600	0.017
8B	520	565	9.8	52	512	0.014
8C	522	365	9.9	33	331	0.044
8D	521	265	10.2	24	241	0.091
8E	521	465	9.4	45	420	0.030
9A	519	665	19.7	32	633	0.029
9B	520	565	19.3	28	537	0.029
9C	520	465	19.1	23	442	0.019
9D	520	365	18.9	18	346	0.059
9E	519	275	19.4	13	261	0.093

[1]Detailed data are given in Appendix A

Table 12 cont'd: Effect of Pressure on the Hydrocracking Rate Constant at 520°F and Various Hydrogen to Cyclohexane Mole Ratios over a Pd-Faujasite Catalyst.

Experimental Results

Run No.[1]	Temp., °F	Total Press., psia	Moles of H_2 per Mole of Feed	Partial Pressures		Hydrocracking Rate Constant, cc./grm. sec.
				Hydrocarbons, psia	Hydrogen, psia	
10A	524	650	5.4	102	547	0.019
10B	520	565	5.5	87	478	0.025
10C	521	365	5.4	57	307	0.070
10D	520	465	5.2	75	390	0.027
10E	525	265	5.1	43	221	0.131

[1]Detailed data are given in Appendix A

Figure 13: Effect of Total Pressure and Hydrogen Dilution on the Hydrocracking Rate Constant at 520°F.

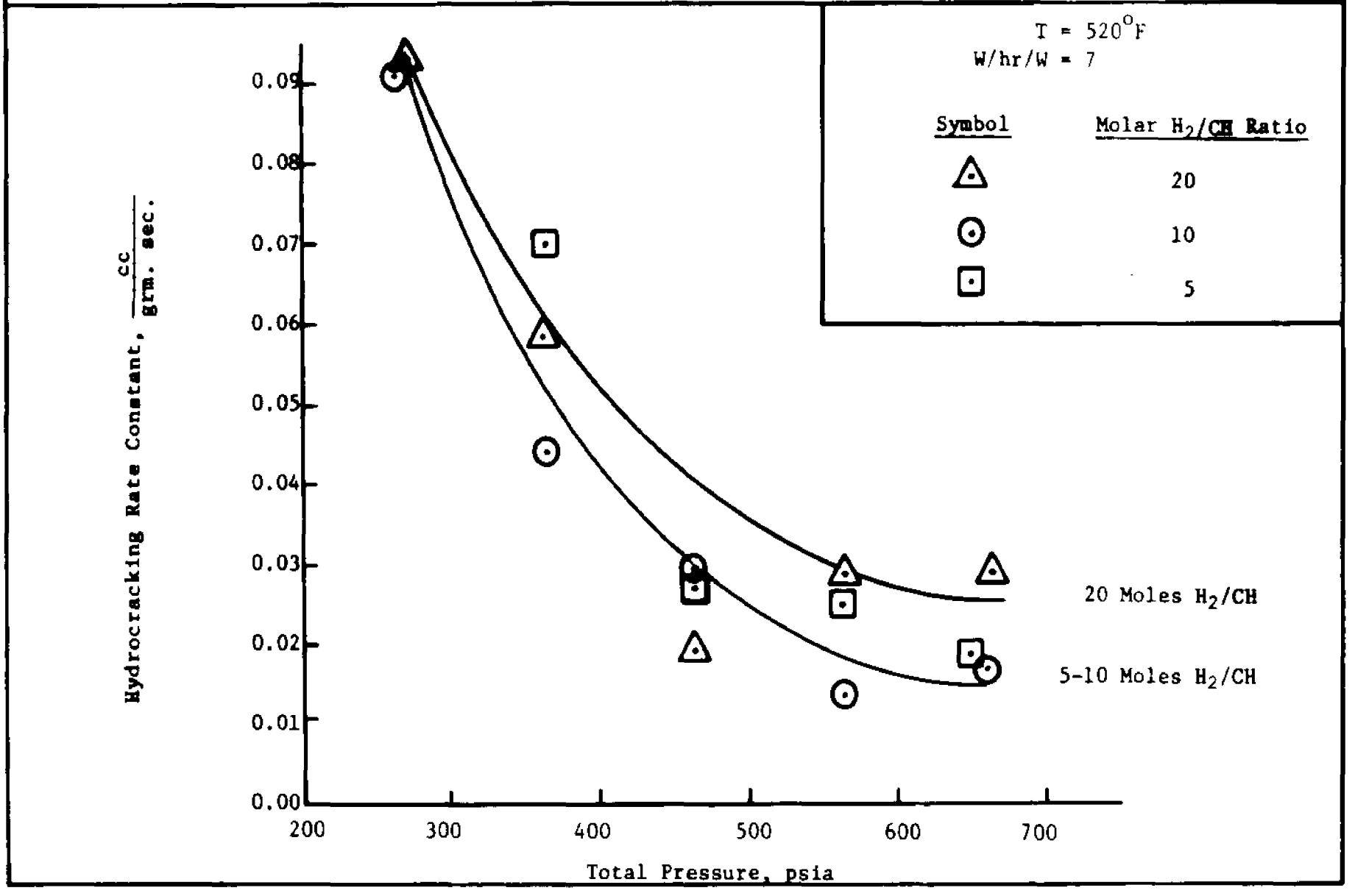

K_{CH}, K_{MCP}, K_C, K_H = adsorption coefficients for cyclohexane, methylcyclopentane, cracked products, and hydrogen respectively,

P_{CH}, P_{MCP}, P_C, P_H = partial pressures of cyclohexane, methylcyclopentane, cracked products, and hydrogen respectively,

and

n = 1 for single site, 2 for dual site.

It seemed reasonable to assume that the adsorption coefficients for the hydrocarbon components were approximately equal (1,3,4). Consequently, equation 3 can be expressed as

$$k_1 = \frac{k_{01} K_O}{(1 + K_O P_O + K_H P_H)^n} \tag{4}$$

where

$$K_O \cong K_{CH} \cong K_{MCP} \cong K_C \tag{5}$$

and

$$P_O = (P_{CH} + P_{MCP} + P_C) \tag{6}$$

Equation (4) can be arranged in a linear form to obtain the following equations for the single and dual site mechanisms.

$$\frac{1}{k_1} = \frac{1}{(k_{01} K_O)} + \frac{K_O}{(k_{01} K_O)} P_O + \frac{K_H}{(k_{01} K_O)} P_H \tag{7}$$

$$\frac{1}{\sqrt{k_1}} = \frac{1}{\sqrt{(k_{01} K_O)}} + \frac{K_O}{\sqrt{(k_{01} K_O)}} P_O + \frac{K_H}{\sqrt{(k_{01} K_O)}} P_H \tag{8}$$

For graphical presentation, it is convenient to express equations (7) and (8) in terms of total pressure with parameters of temperature and hydrogen dilution ratios.

The temperature parameters are tied up with the adsorption coefficients. The hydrogen mole ratios are related to the partial pressures by the following equation

$$R_H = \frac{P_H}{P_O} \tag{9}$$

where

R_H = molar ratio of hydrogen to hydrocarbons

Obviously, the hydrogen and hydrocarbon partial pressures must add up to the total pressure as given by

$$P_O + P_H = \pi \tag{10}$$

where

π = total pressure

Finally, by substituting equations (9) and (10) into equations (7) and (8), the following relationships are obtained:

$$\frac{1}{k_1} = \frac{1}{(k_{01}\ K_O)} + \left[\frac{K_O}{(k_{01}\ K_O)} + \frac{K_H}{(k_{01}\ K_O)}\ R_H\right] \frac{\pi}{(1 + R_H)} \tag{11}$$

$$\frac{1}{\sqrt{k_1}} = \frac{1}{\sqrt{(k_{01}\ K_O)}} + \left[\frac{K_O}{\sqrt{(k_{01}\ K_O)}\sqrt{(k_{01}\ K_O)}} + \frac{K_H}{\sqrt{(k_{01}\ K_O)}}\ R_H\right] \frac{\pi}{(1 + R_H)} \tag{12}$$

The hydroisomerization rate constants obtained at 20 moles of hydrogen per mole of hydrocarbon and various temperatures and total pressures are shown in Table 13. In Figures 14 and 15, the hydroisomerization rate constants are correlated with the total pressure in accordance with the single and dual site mechanisms. Negative intercepts are obtained for the single site mechanism which are unrealistic. However, the experimental data are compatible with the dual site mechanism.

A similar behavior was observed at 10 moles of hydrogen per mole of hydrocarbon and various temperatures and total pressures as

Table 13: Single and Dual Site Adsorption Mechanisms for Hydroisomerization at 20 Moles of H_2 per Mole of Cyclohexane and Various Temperatures.

Reacting Conditions

Feed	Cyclohexane
Catalyst	Pd-Faujasite
Catalyst Particle Size, mm	0.417 - 1.168
Weight Space Velocity, (grm. feed)/(hr.)/(grm. cat.)	7

Experimental Results

Run No.[1]	Temp., °F	Total Press., psia	Moles of H_2 per Mole of Feed	Hydroisomerization Rate Constant, k_1, cc./grm. sec.	$\frac{1}{k_1}$	$\frac{1}{\sqrt{k_1}}$
6A	490	465	20.2	0.559	1.788	1.336
6B	489	565	18.8	0.324	3.091	1.754
6C	491	665	18.6	0.343	2.919	1.706
6D	489	465	18.5	0.531	1.885	1.371
6E	490	265	18.3	0.882	1.135	1.064
9A	519	665	19.7	0.713	1.405	1.184
9B	520	565	19.3	0.964	1.039	1.018
9C	520	465	19.1	1.092	0.916	0.957
9D	520	365	18.9	1.119	0.894	0.945
9E	519	275	19.4	1.623	0.616	0.784

[1] Detailed data are given in Appendix A

Figure 14: Single Site Mechanism for Hydroisomerization at 20 Moles of Hydrogen per Mole of Feed and Various Temperatures.

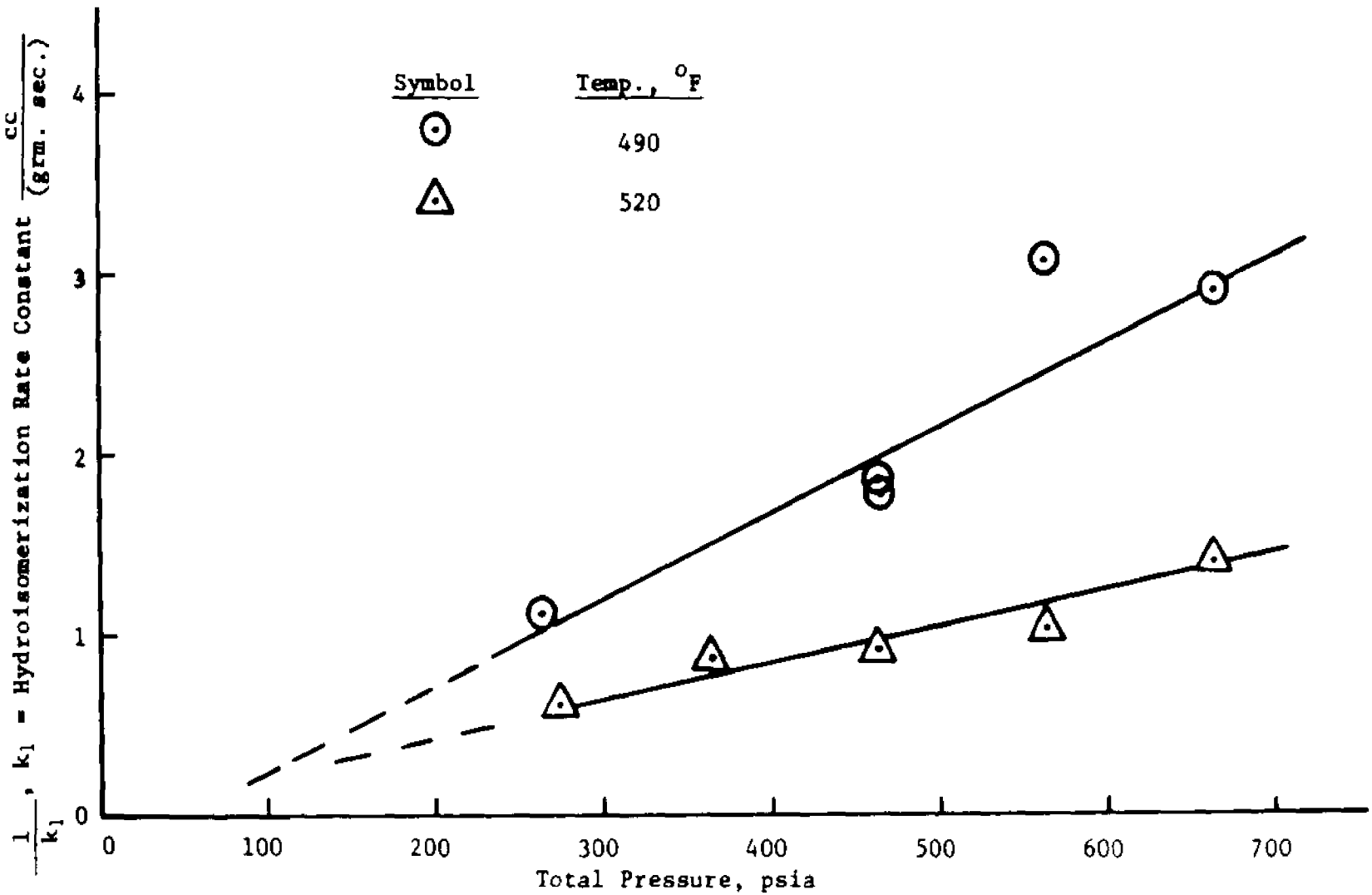

Figure 15: Dual Site Mechanism for Hydroisomerization at 20 Moles of Hydrogen per Mole of Feed and Various Temperatures.

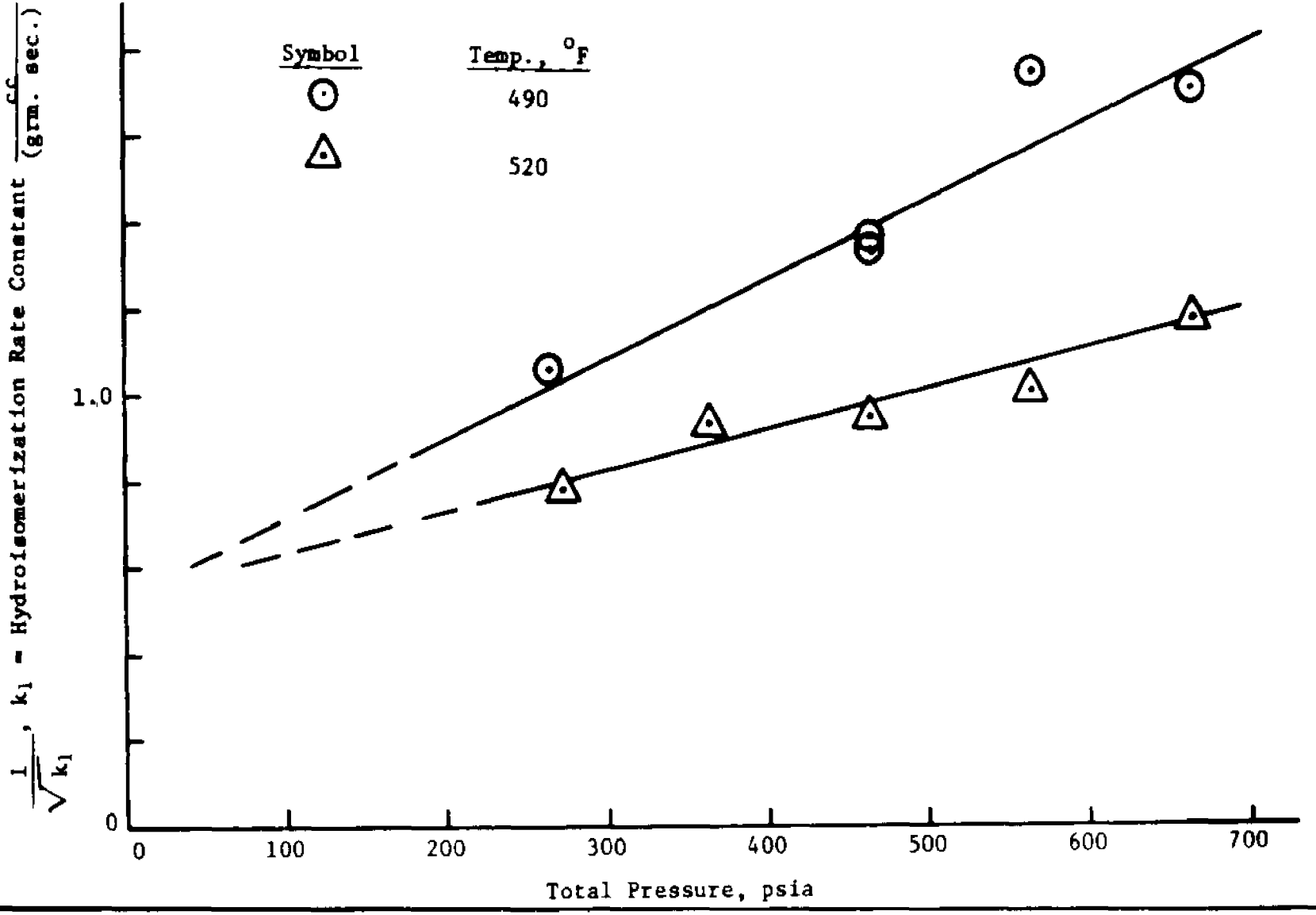

presented in Table 14, Figure 16, and Figure 17. The same conclusions are also valid at 5 moles of hydrogen per mole of hydrocarbon as demonstrated in Table 15, Figure 18, and Figure 19.

A detailed least squares analysis of the data is postponed until Section 5 of this discussion.

3. Single and Dual Site Adsorption Mechanisms for Hydrocracking

The development followed for hydroisomerization was also applied to hydrocracking to obtain the following equations for the single and dual site mechanisms.

$$\frac{1}{k_2} = \frac{1}{(k_{02}\ K_O)} + \left[\frac{K_O}{(k_{02}\ K_O)} + \frac{K_H}{(k_{02}\ K_O)}\ R_H\right] \frac{\pi}{(1 + R_H)} \qquad (13)$$

$$\frac{1}{\sqrt{k_2}} = \frac{1}{\sqrt{(k_{02}\ K_O)}} + \left[\frac{K_O}{\sqrt{(k_{02}\ K_O)}} + \frac{K_H}{\sqrt{(k_{02}\ K_O)}}\ R_H\right] \frac{\pi}{(1 + R_H)} \qquad (14)$$

where

k_2 = hydrocracking rate constant,

k_{02} = constant dependent on catalyst and temperature.

The experimental data at 20 moles of hydrogen per mole of hydrocarbon and various temperatures and total pressures are presented in Table 16, Figure 20, and Figure 21. Similarly, the results obtained at 10 and 5 moles of hydrogen per mole of hydrocarbon are shown in Table 17, Figure 22, Figure 23, Table 18, Figure 24, and Figure 25.

As was the case with hydroisomerization, the single site mechanism gives negative intercepts for the hydrocracking adsorption model which are unrealistic. However, the experimental data can be interpreted in terms of the dual site mechanism. This conclusion is valid for all the hydrogen to hydrocarbon molar ratios investigated.

A detailed least square analysis of the different adsorption

Table 14: Single and Dual Site Adsorption Mechanisms for Hydroisomerization at 10 Moles of H_2 per Mole of Cyclohexane and Various Temperatures

Reacting Conditions

Feed	Cyclohexane
Catalyst	Pd-Faujasite
Catalyst Particle Size, mm	0.417 - 1.168
Weight Space Velocity, (grm. feed)/(hr.)/(grm. cat.)	7

Experimental Results

Run No.[1]	Temp., °F	Total Press., psia	Moles of H_2 per Mole of Feed	Hydroisomerization Rate Constant, k_1, cc./grm. sec.	$\frac{1}{k_1}$	$\frac{1}{\sqrt{k_1}}$
5A	491	265	8.9	0.741	1.349	1.161
5B	490	365	8.9	0.562	1.780	1.333
5C	490	555	9.8	0.321	3.119	1.765
5D	490	665	9.8	0.235	4.260	2.060
5E	490	465	9.5	0.336	2.979	1.723
1B	492	465	9.2	0.384	2.605	1.612
1C	491	465	9.2	0.386	2.591	1.608
1D	491	465	8.6	0.387	2.585	1.606
3A	491	465	8.9	0.415	2.412	1.552
8A	522	660	10.0	0.579	1.729	1.314
8B	520	565	9.8	0.618	1.620	1.272
8C	522	365	9.9	1.151	0.869	0.931
8D	521	265	10.2	1.143	0.874	0.935
8E	521	465	9.4	0.770	1.300	1.139

[1] Detailed data are given in Appendix A

Figure 16: Single Site Mechanism for Hydroisomerization at 10 Moles of Hydrogen per Mole of Feed and Various Temperatures.

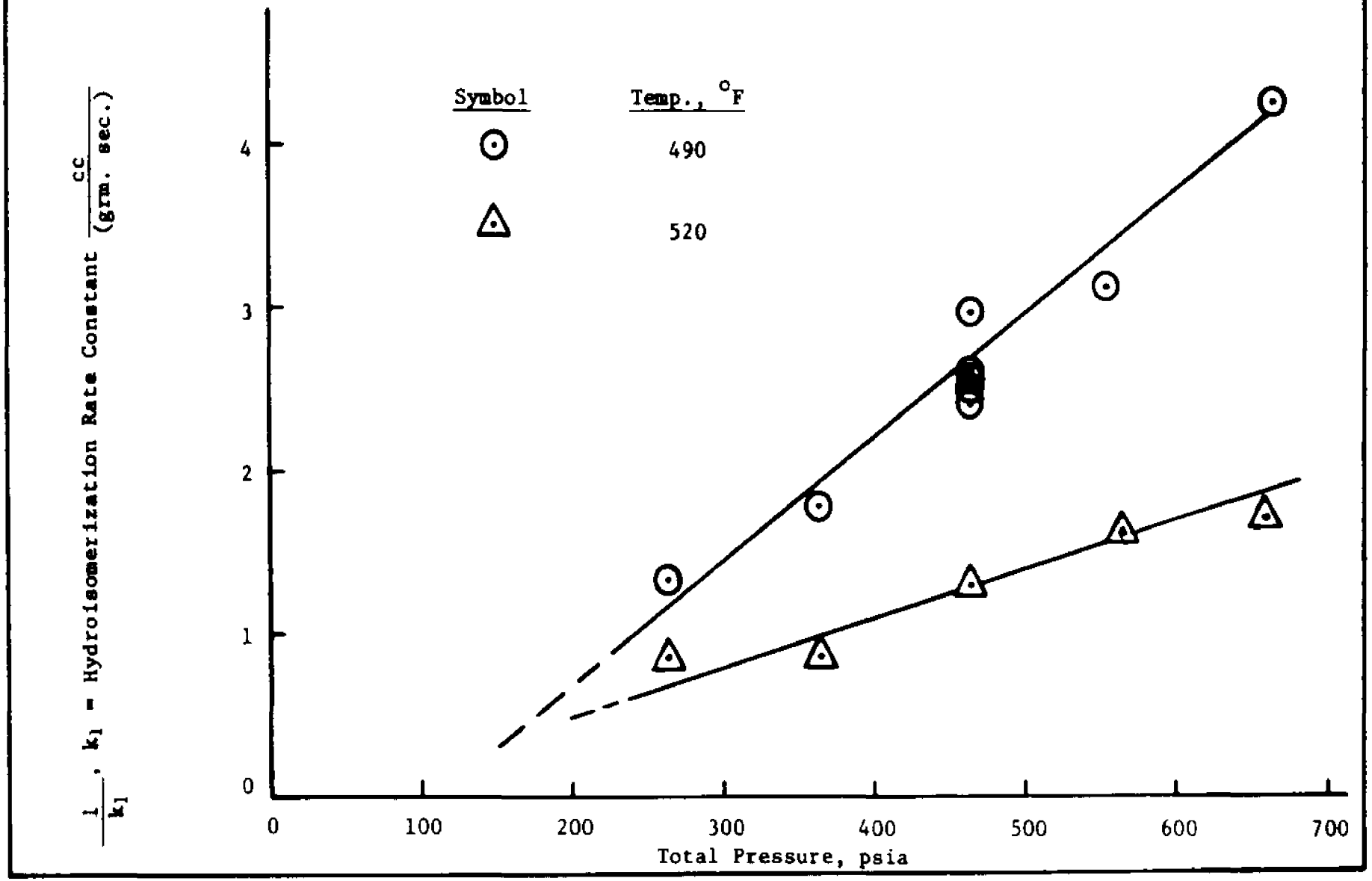

Figure 17: Dual Site Mechanism for Hydroisomerization at 10 Moles of Hydrogen per Mole of Feed and Various Temperatures.

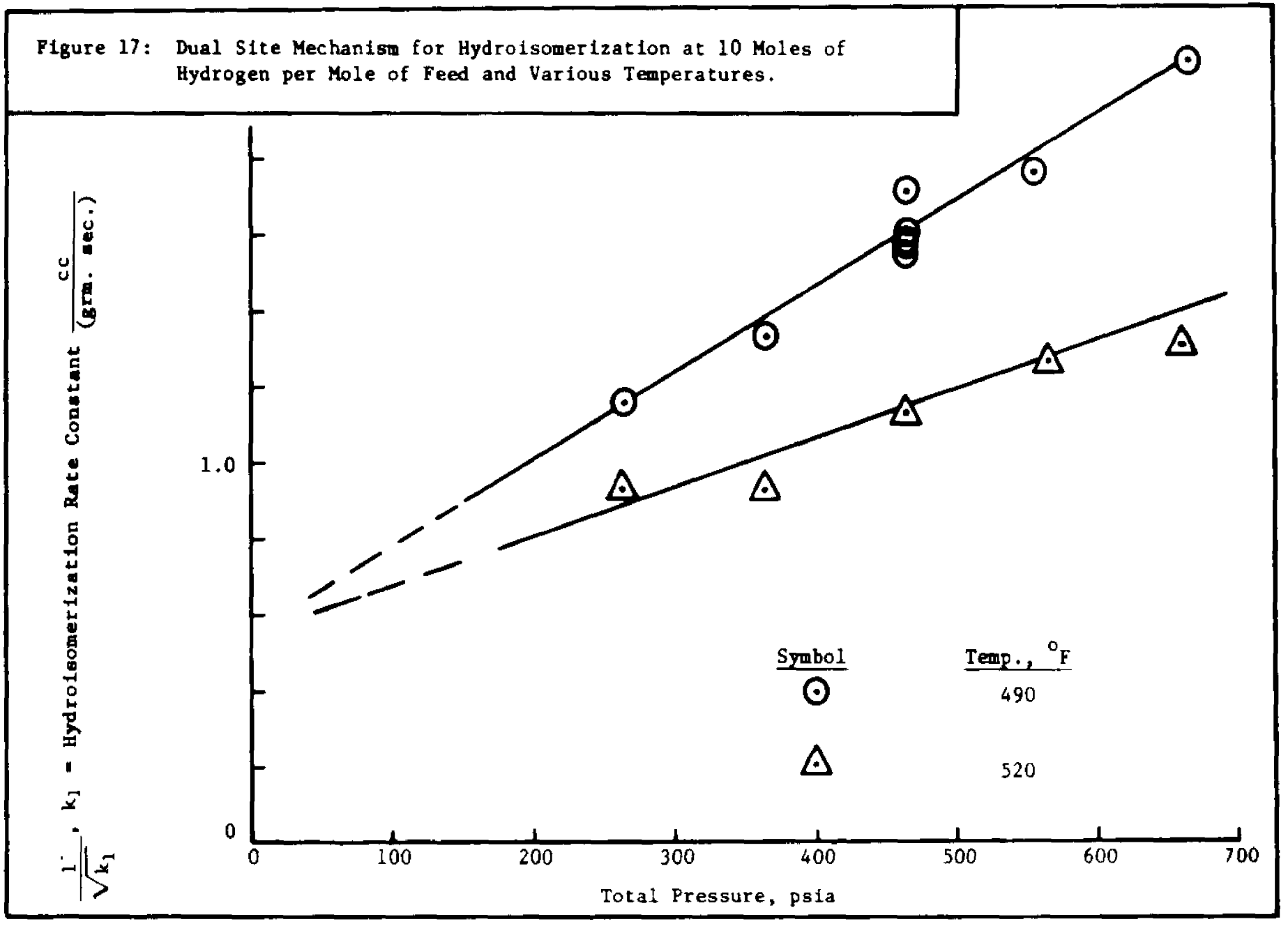

Table 15: Single and Dual Site Adsorption Mechanisms for Hydroisomerization at 5 Moles of H_2 per Mole of Cyclohexane and Various Temperatures

Reacting Conditions

Feed	Cyclohexane
Catalyst	Pd-Faujasite
Catalyst Particle Size, mm	0.417 - 1.168
Weight Space Velocity, (grm. feed)/(hr.)/(grm. cat.)	7

Experimental Results

Run No.[1]	Temp., °F	Total Press., psia	Moles of H_2 per Mole of Feed	Hydroisomerization Rate Constant, k_1, cc./grm. sec.	$\frac{1}{k_1}$	$\frac{1}{\sqrt{k_1}}$
7B	491	665	5.0	0.185	5.410	2.324
7C	491	565	5.6	0.215	4.650	2.155
7D	491	465	5.4	0.317	3.159	1.776
7E	491	370	5.3	0.405	2.471	1.570
7F	491	265	5.7	0.581	1.725	1.312
10A	524	650	5.4	0.367	2.730	1.651
10B	520	565	5.5	0.444	2.257	1.501
10C	521	365	5.4	0.702	1.425	1.193
10D	520	465	5.2	0.502	1.995	1.412
10E	525	265	5.1	0.888	1.128	1.061

[1]Detailed data are given in Appendix A

Figure 18: Single Site Mechanism for Hydroisomerization at 5 Moles of Hydrogen per Mole of Feed and Various Temperatures.

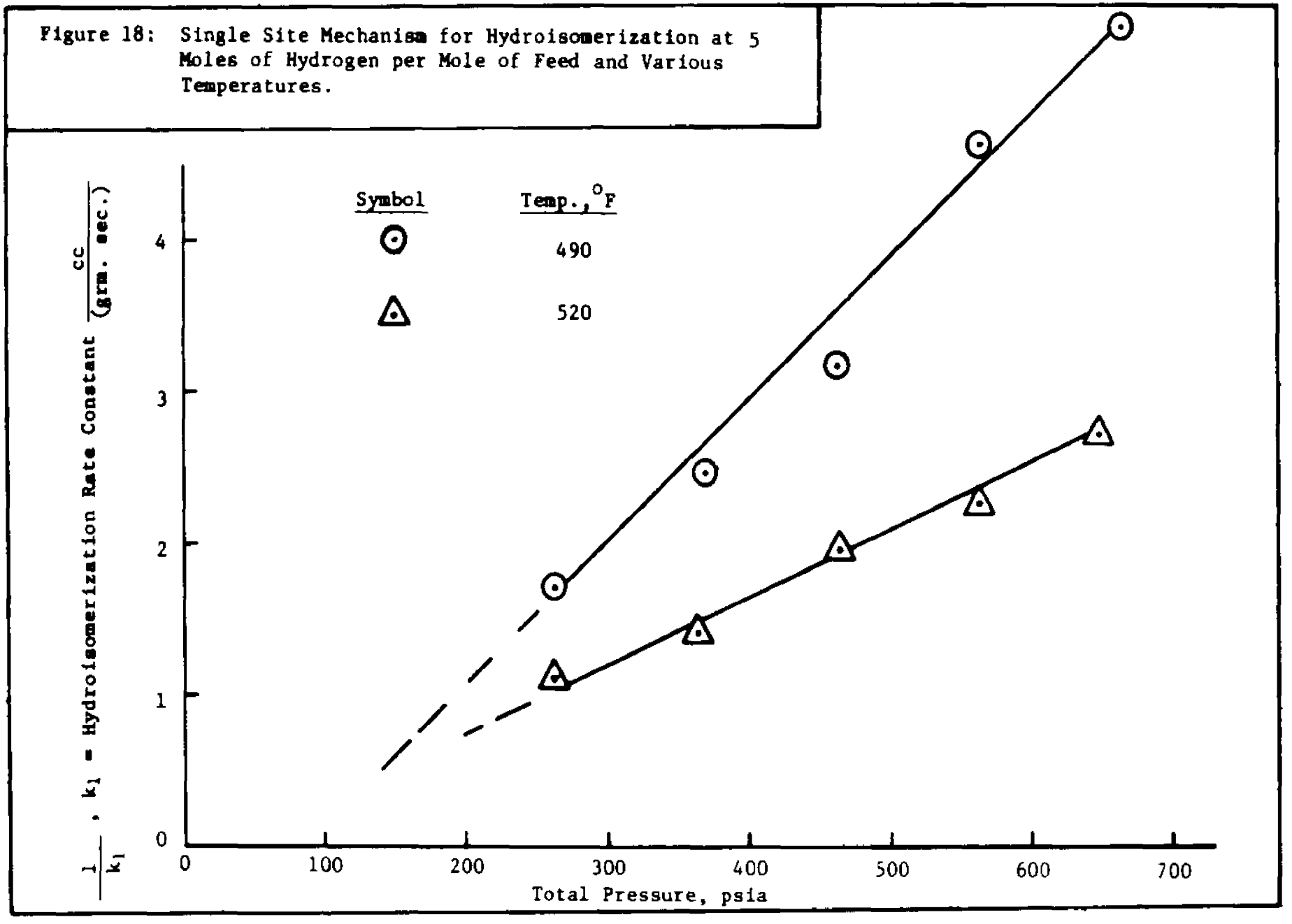

Figure 19: Dual Site Mechanism for Hydroisomerization at 5 Moles of Hydrogen per Mole of Feed and Various Temperatures.

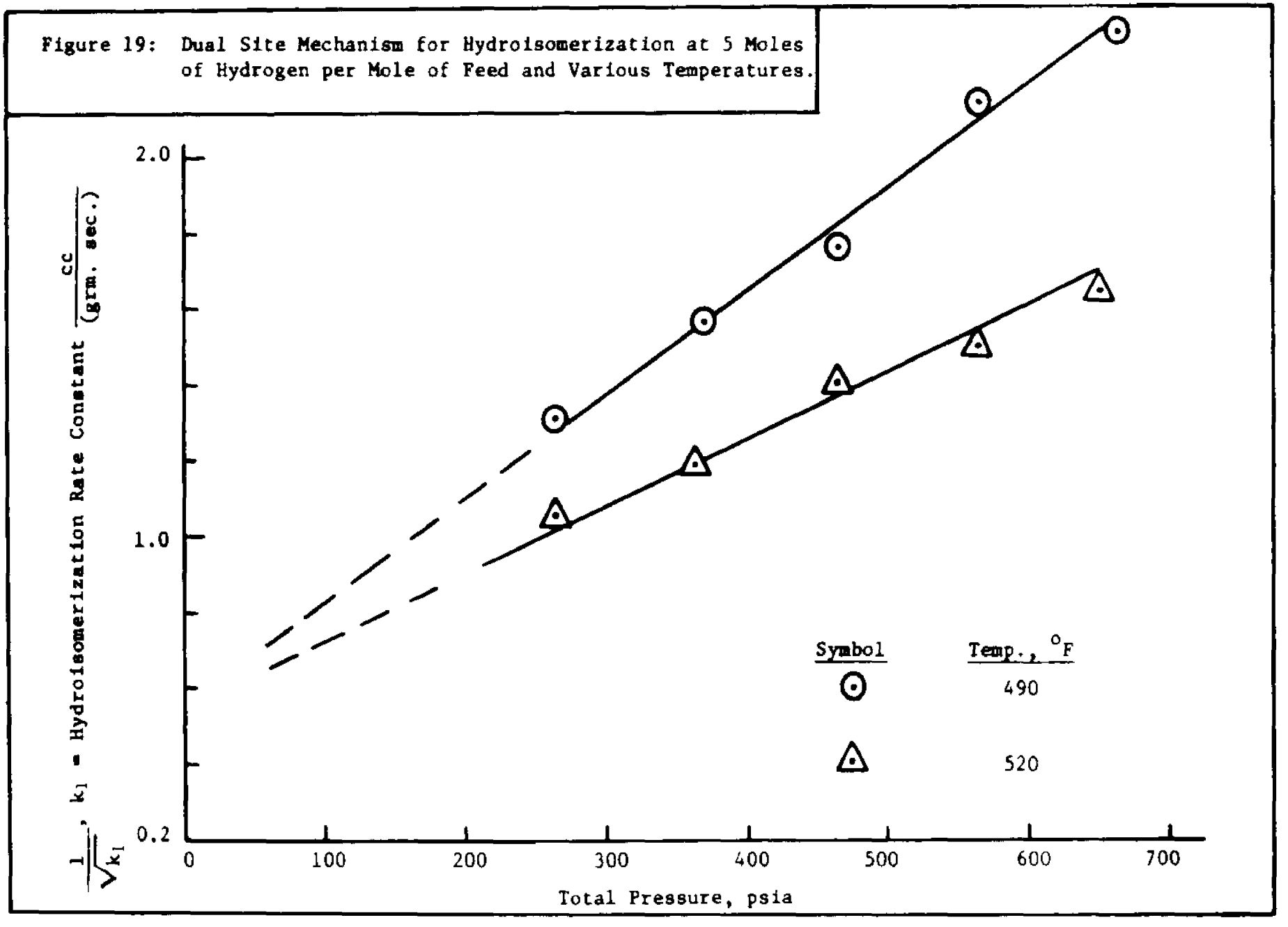

Table 16: Single and Dual Site Adsorption Mechanisms for Hydrocracking at 20 Moles of H_2 per Mole of Cyclohexane and Various Temperatures.

Reacting Conditions

Feed	Cyclohexane
Catalyst	Pd-Faujasite
Catalyst Particle Size, mm	0.417 - 1.168
Weight Space Velocity, (grm. feed)/(hr.)/(grm. cat.)	7

Experimental Results

Run No.[1]	Temp., °F	Total Press., psia	Moles of H_2 per Mole of Feed	Hydrocracking Rate Constant, k_2, cc./grm. sec.	$\frac{1}{k_2}$	$\frac{1}{\sqrt{k_2}}$
6A	490	465	20.3	0.041	24.70	4.966
6B	489	565	18.9	0.016	63.30	7.950
6C	491	665	18.6	0.010	100.00	10.110
6D	489	465	18.6	0.024	42.30	6.508
6E	490	265	18.3	0.106	9.41	3.066
9A	519	665	19.7	0.029	34.39	5.853
9B	520	565	19.3	0.028	34.99	5.913
9C	520	465	19.1	0.019	51.60	7.186
9D	520	365	18.9	0.059	17.10	4.133
9E	519	275	19.4	0.093	10.78	3.278
13A	535	665	20.7	0.033	30.79	5.540
13B	533	565	20.4	0.029	34.19	5.841
13C	535	465	20.1	0.050	19.89	4.455
13D	535	365	19.5	0.067	14.91	3.861
13E	535	265	19.3	0.084	12.13	3.450

[1]Detailed data are given in Appendix A

Figure 20: Single Site Mechanism for Hydrocracking at 20 Moles of Hydrogen per Mole of Feed and Various Temperatures.

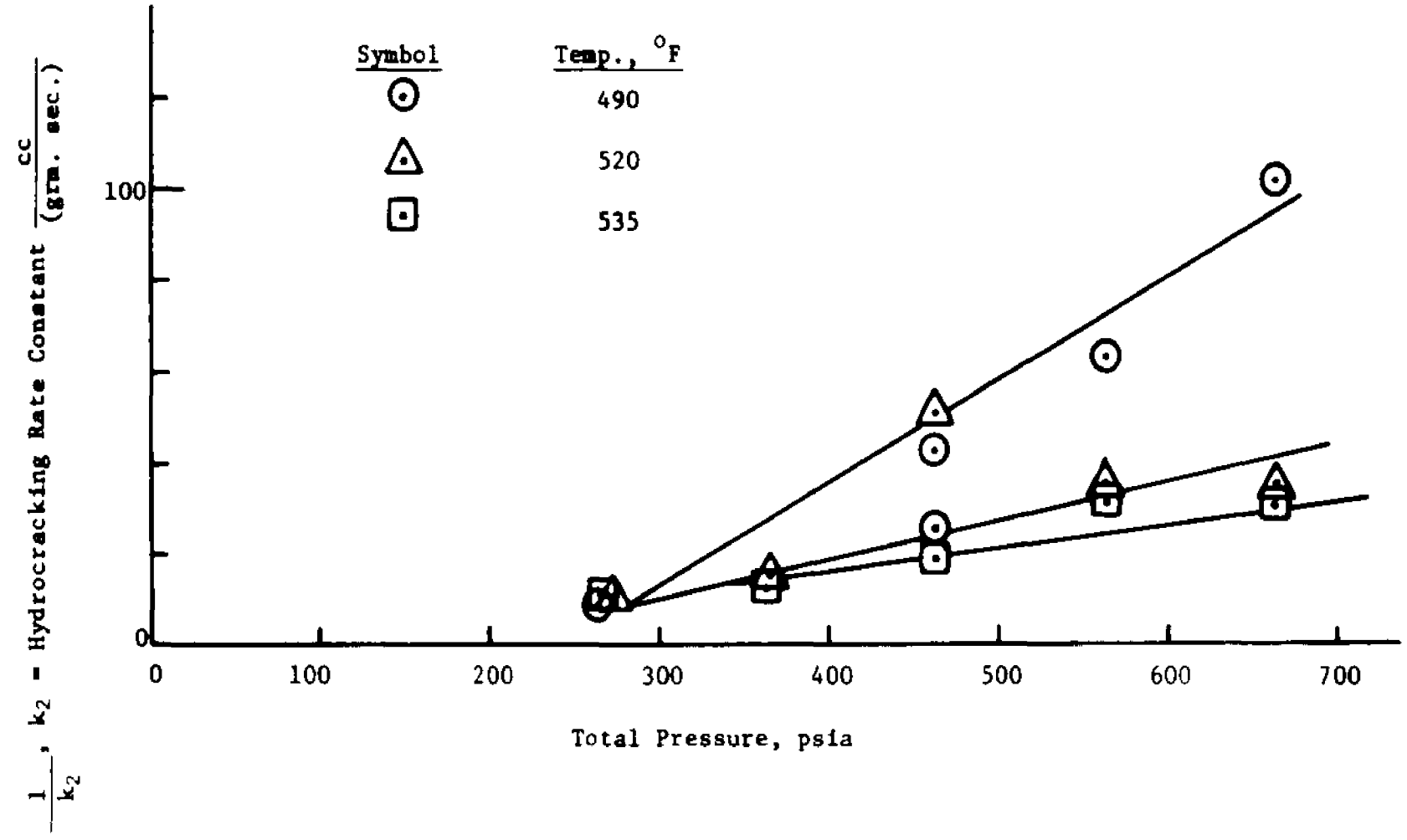

Figure 21: Dual Site Mechanism for Hydrocracking at 20 Moles of Hydrogen per Mole of Feed and Various Temperatures.

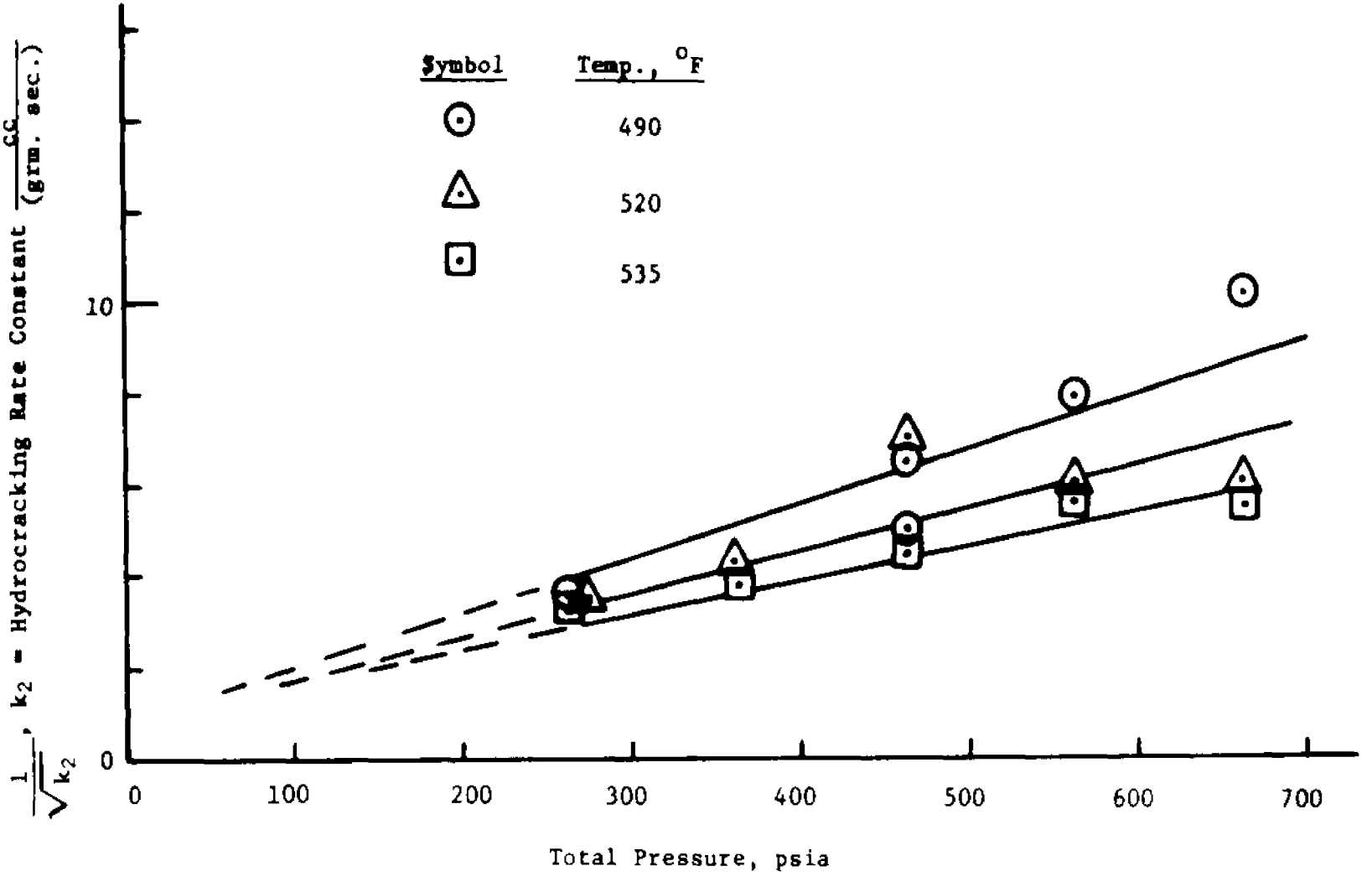

Table 17: Single and Dual Site Adsorption Mechanisms for Hydrocracking at 10 Moles of H_2 per Mole of Cyclohexane and Various Temperatures.

Reacting Conditions

Feed	Cyclohexane
Catalyst	Pd-Faujasite
Catalyst Particle Size, mm	0.417 - 1.168
Weight Space Velocity, (grm. feed)/(hr.)/(grm. cat.)	7

Experimental Results

Run No.[1]	Temp., °F	Total Press., psia	Moles of H_2 per Mole of Feed	Hydrocracking Rate Constant, k_2, cc./grm. sec.	$\frac{1}{k_2}$	$\frac{1}{\sqrt{k_2}}$
5A	491	265	8.9	0.018	56.00	7.477
5B	490	365	8.9	0.012	82.90	9.097
5C	490	555	9.8	0.007	144.80	12.034
5D	490	665	9.8	0.007	140.70	11.848
5E	490	465	9.5	0.012	83.41	9.125
1B	492	465	9.2	0.011	92.30	9.605
1C	491	465	9.2	0.010	98.4	9.926
1D	491	465	8.6	0.014	73.65	8.577
3A	491	465	8.9	0.014	72.30	8.500
8A	522	660	10.0	0.017	60.61	7.774
8B	520	565	9.8	0.014	73.70	8.581
8C	522	365	9.9	0.044	22.68	4.755
8D	521	265	10.2	0.092	10.92	3.303
8E	521	465	9.4	0.030	33.90	5.815

[1]Detailed data are given in Appendix A

Table 17 cont'd: Single and Dual Site Adsorption Mechanisms for Hydrocracking at 10 Moles of H_2 per Mole of Cyclohexane and Various Temperatures.

Experimental Results

Run No.[1]	Temp., °F	Total Press., psia	Moles of H_2 per Mole of Feed	Hydrocracking Rate Constant, k_2, cc./grm. sec.	$\frac{1}{k_2}$	$\frac{1}{\sqrt{k_2}}$
11A	552	665	10.3	0.080	12.48	3.527
11B	551	565	10.2	0.100	10.00	3.155
11C	552	465	10.3	0.158	6.36	2.519
11D	550	365	10.3	0.187	5.36	2.314
12A	538	465	10.2	0.082	12.25	3.501
12B	535	665	10.4	0.055	18.20	4.261
12C	535	565	10.3	0.061	16.51	4.064
12D	537	365	10.4	0.202	4.94	2.221

[1]Detailed data are given in Appendix A

Figure 22: Single Site Mechanism for Hydrocracking at 10 Moles of Hydrogen per Mole of Feed and Various Temperatures.

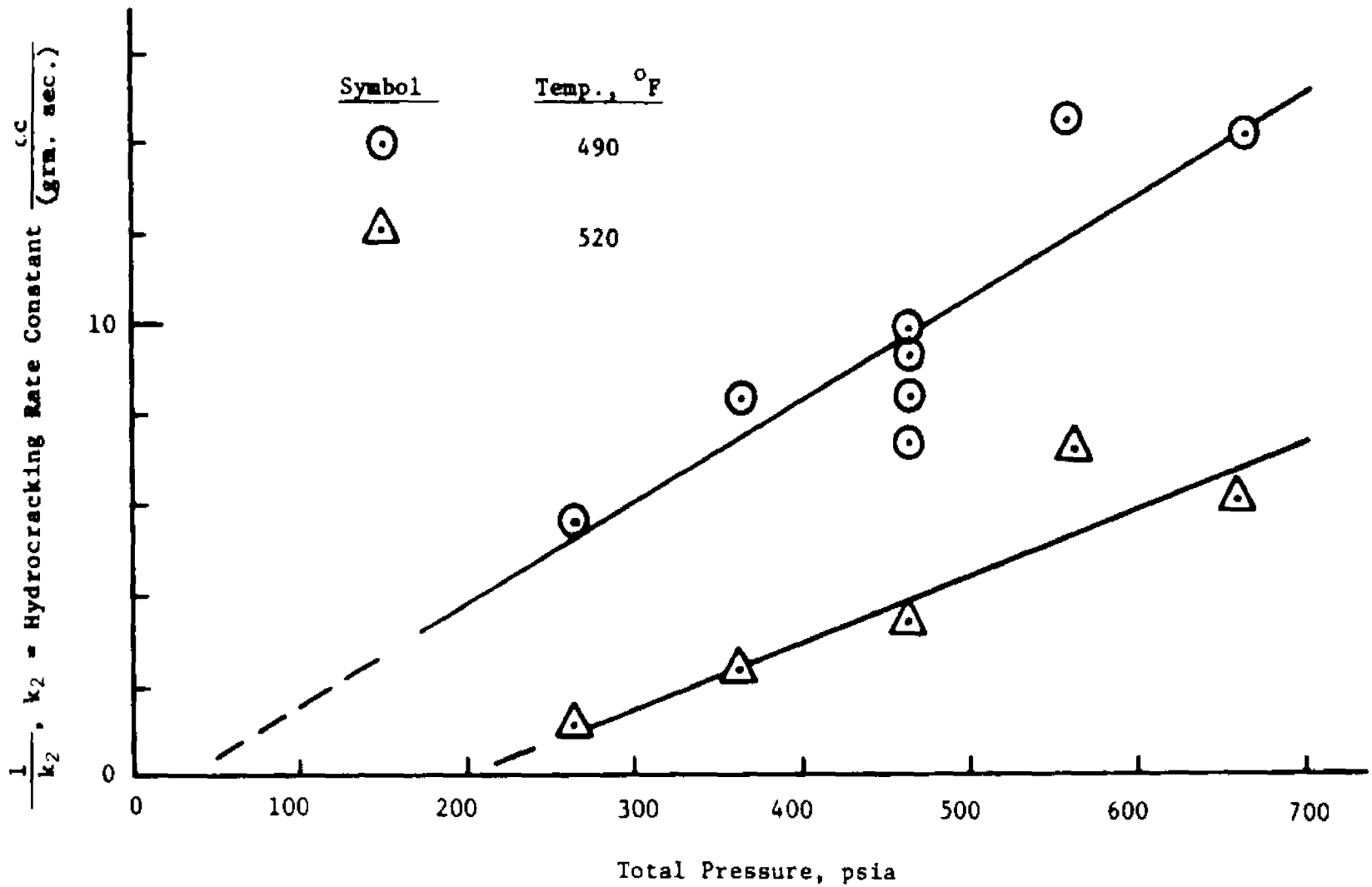

Figure 23: **Dual Site Mechanism** for Hydrocracking at 10 Moles of Hydrogen per Mole of Feed and Various Temperatures.

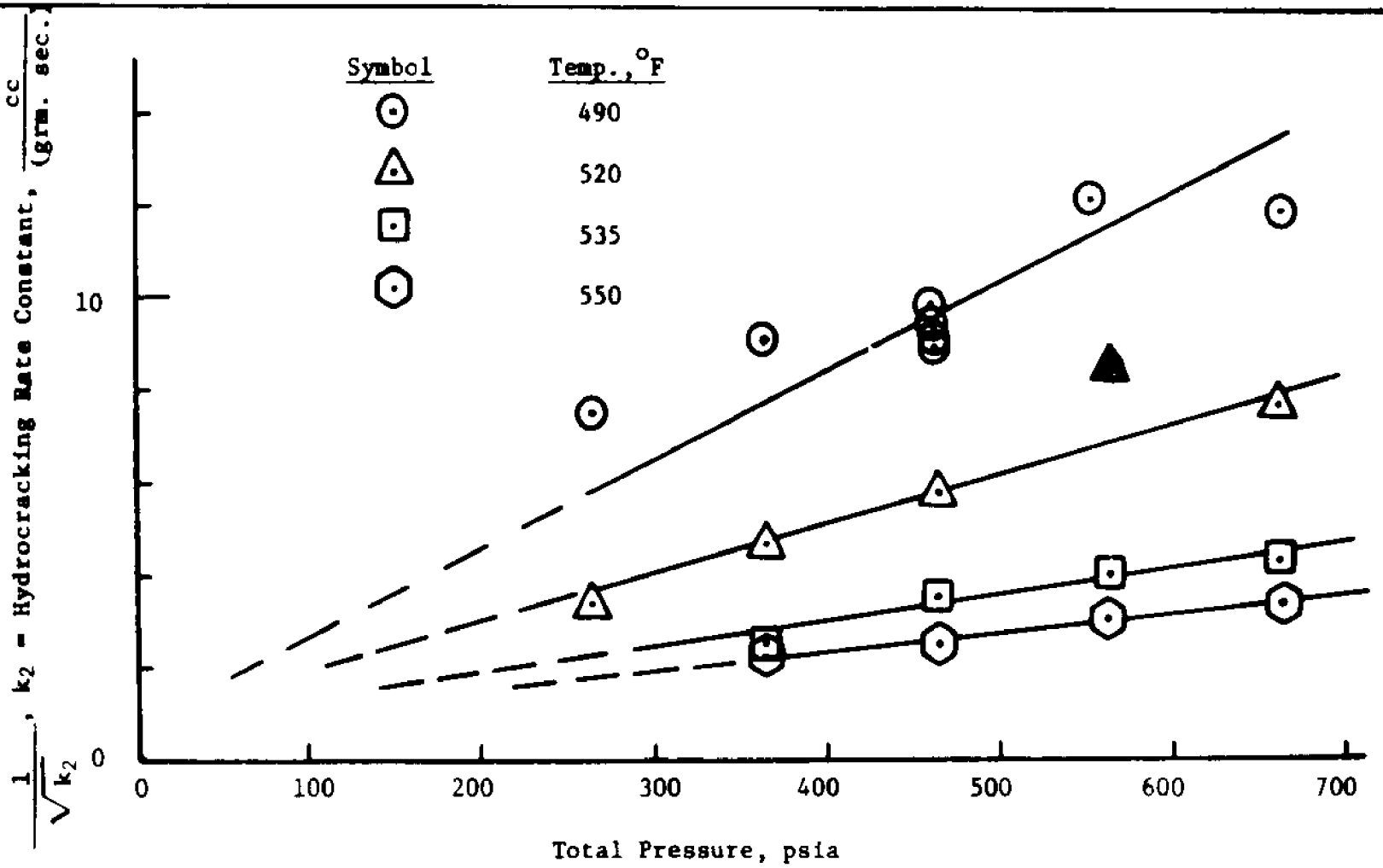

Table 18: Single and Dual Site Adsorption Mechanisms for Hydrocracking at 5 Moles of H_2 per Mole of Cyclohexane and Various Temperatures.

Reacting Conditions

Feed	Cyclohexane
Catalyst	Pd-Faujasite
Catalyst Particle Size, mm	0.417 - 1.168
Weight Space Velocity, (grm. feed)/(hr.)/(grm. cat.)	7

Experimental Results

Run No.[1]	Temp., °F	Total Press., psia	Moles of H_2 per Mole of Feed	Hydrocracking Rate Constant, k_2, cc./grm. sec.	$\frac{1}{k_2}$	$\frac{1}{\sqrt{k_2}}$
7B	491	665	5.0	0.0041	240	15.629
7C	491	565	5.5	0.0048	285	14.447
7D	491	465	5.4	0.0057	176	13.213
7E	491	370	5.3	0.0107	94	9.685
7F	491	265	5.7	0.0211	47	6.876
10A	524	650	5.4	0.0197	51	7.122
10B	520	565	5.5	0.0251	40	6.308
10C	521	365	5.4	0.0701	14	3.775
10D	520	465	5.2	0.0277	36	6.006
10E	525	265	5.1	0.1312	8	2.761

[1]Detailed data are given in Appendix A

Figure 24: Single Site Mechanism for Hydrocracking at 5 Moles of Hydrogen per Mole of Feed and Various Temperatures.

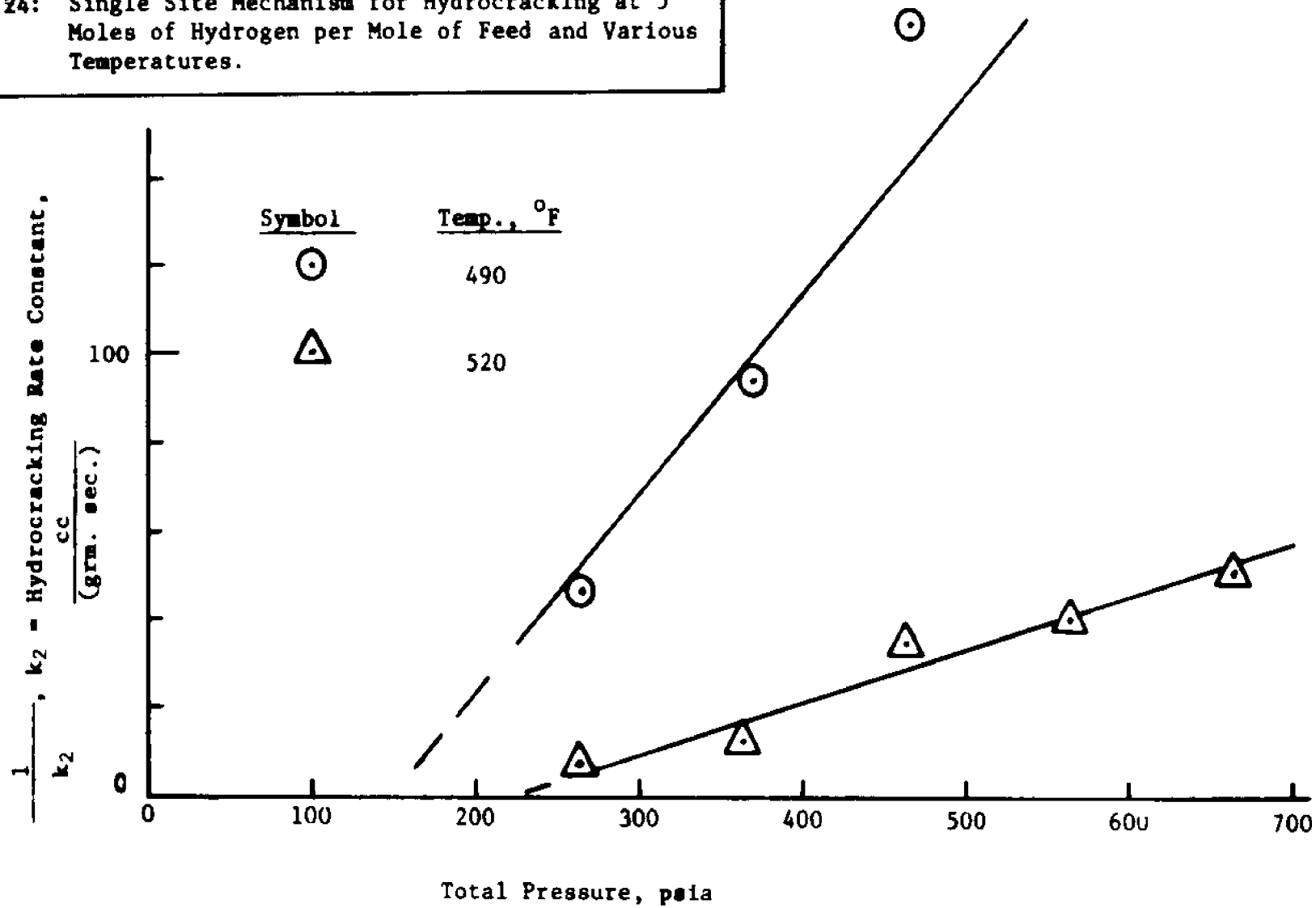

Figure 25: Dual Site Mechanism for Hydrocracking at 5 Moles of Hydrogen per Mole of Feed and Various Temperatures.

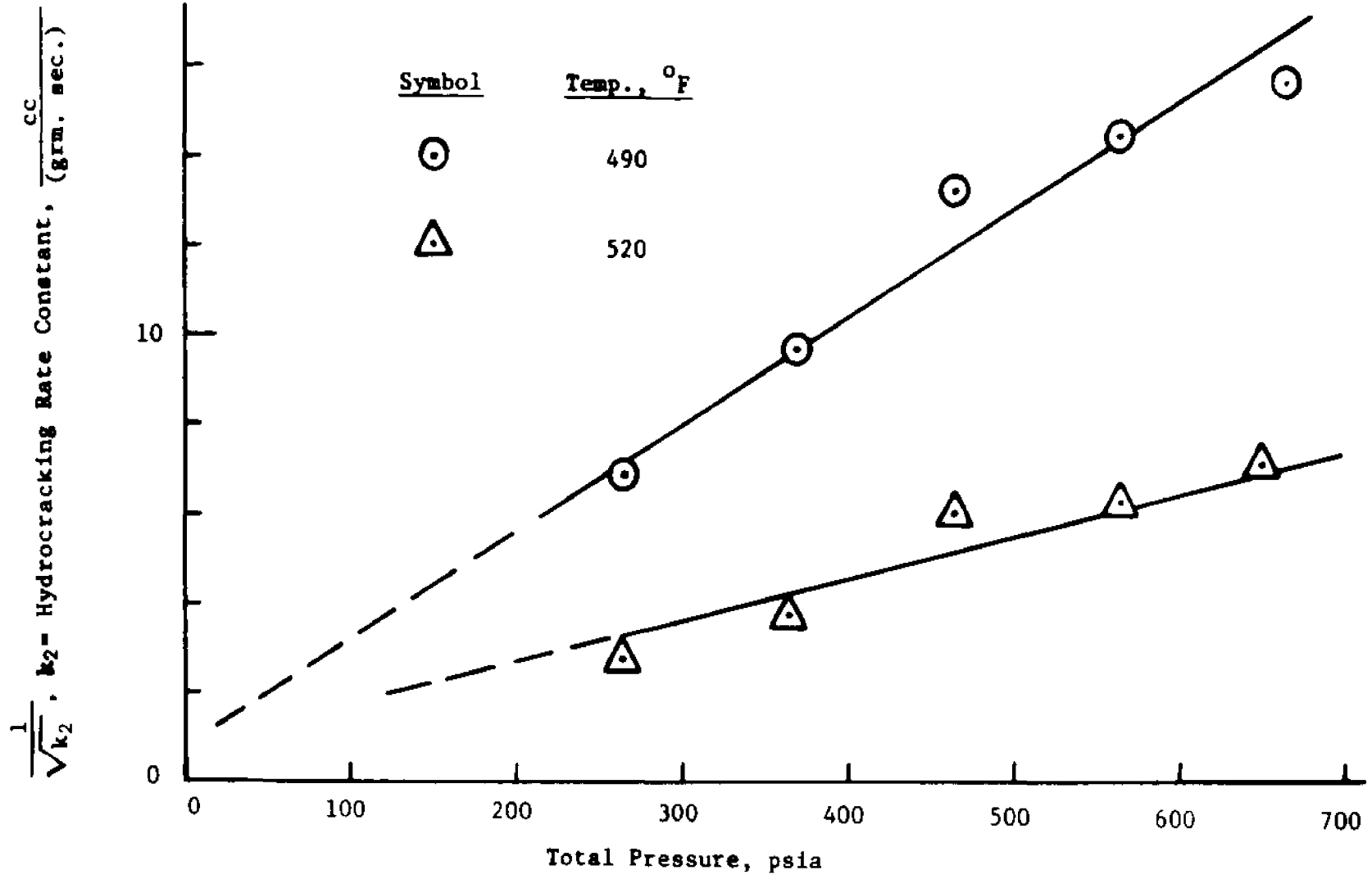

mechanisms studied for hydrocracking is presented in the following section.

4. Effectiveness of the Adsorption Model

The experimental data gathered to study the adsorption - surface reaction - desorption mechanisms were obtained at the following conditions:

Run No.	Temp, ^{o}F	Moles of H_2/Mole of Hydrocarbon Feed	Total Pressure, psig
5A - 7E	490	10	250 - 650
		20	250 - 650
		5	250 - 650
8A - 10E	520	10	250 - 650
		20	250 - 650
		5	250 - 650
12A - 13D	535	10	250 - 650
		5	250 - 650
11A - 11D	550	10	250 - 650

In order to develop an adsorption model, a least squares analysis was performed at each temperature level to obtain the "best fitted" (2) adsorption parameters for the single and dual site mechanisms. These adsorption parameters were then correlated with temperature by means of an Arrhenius - type formulation.

A summary of the results obtained for the hydroisomerization rate constant is shown in Table 19. For the single site mechanism, it is observed that negative parameters were obtained at $490^{o}F$ and $550^{o}F$. The negative parameter obtained at $550^{o}F$ is not very relevant since only one degree of freedom is involved. However, the negative parameters obtained at $490^{o}F$, where 15 degrees of freedom exist, suggest that the single site mechanism does not properly represent all the hydroisomerization data.

Table 19: Adsorption Mechanisms for Hydroisomerization

Correlating Equation: $$\frac{1}{(k_1)^{1/n}} = \frac{1}{(k_{01}\,K_O)^{1/n}} + \frac{K_O}{(k_{01}\,K_O)^{1/n}}\,P_O + \frac{K_H}{(k_{01}\,K_O)^{1/n}}\,P_H$$

Mechanism	Temp., °F	Fitted Parameters			Statistical Significance	
		k_{01}	K_O	K_H	D. F.[1]	R^2
Single Site	490	3.039×10	-4.428×10^{2}	-6.062×10^{3}	15	0.973
n = 1	520	4.958×10	2.622×10^{-1}	1.175×10^{-2}	12	0.988
	535	5.555×10	1.168×10^{-1}	6.690×10^{-3}	5	0.936
	550	2.930×10	9.464×10^{-3}	-3.316×10^{-3}	1	0.999
Dual Site	490	1.917×10^{2}	1.637×10^{-2}	2.585×10^{-3}	15	0.976
n = 2	520	2.046×10^{2}	1.348×10^{-2}	7.037×10^{-4}	12	0.988
	535	2.079×10^{2}	1.268×10^{-2}	7.871×10^{-4}	5	0.929
	550	7.684×10^{1}	2.414×10^{-2}	-1.111×10^{-3}	1	0.999

[1]Degrees of freedom = No. of data points - No. of parameters

[2]Multiple Correlation Coefficient = $$\frac{\sum(Y_{actual} - \bar{Y})^2 - \sum(Y_{actual} - Y_{pred.})^2}{\sum(Y_{actual} - \bar{Y})^2}$$

As shown in Table 17, positive parameters were obtained with the dual site mechanism excluding the results at 550°F, where a negative K_H was calculated. Since only one degree of freedom is available at 550°F, and since reasonable parameters were obtained at all the other temperature levels, the dual site mechanism was adopted for hydroisomerization. The final model employed for hydroisomerization is summarized in Table 20.

The hydroisomerization rate constants predicted by the adsorption model are compared with those obtained experimentally in Figure 26 for all the temperature levels investigated (490–550°F). The agreement between the actual and predicted values seems to be very good.

The dotted lines shown in Figure 20 represent the experimental uncertainties associated with the hydroisomerization rate constant (% σ/value = 8.2) as determined from the set of duplicate runs shown in Table 21.

A summary of the adsorption mechanisms studied for hydrocracking is presented in Table 22. Two main formulations were studied, namely, an adsorption equation relating the hydrocracking rate constant with the hydrocarbon and hydrogen partial pressures, and an adsorption equation relating the hydrocracking rate constant with the total pressure.

As shown in Table 22, the adsorption equation expressed in terms of the hydrocarbon partial pressure and hydrogen partial pressure yields unrealistic negative parameters for the single site mechanism at all temperature levels investigated. The dual site mechanism performed satisfactorily at 490°F and 520°F but gave negative coefficients at

Table 20: Final Adsorption Model for Hydroisomerization

Dual Site Equation: $$k_1 = \frac{k_{01} \; K_O}{(1 + K_O \; P_O + K_H \; P_H)^2}$$

Adsorption Parameter Equations:

$$\ln k_{01} = 7.103 - (1.752 \times 10^3)/^{\circ}R$$

$$\ln K_O = -9.871 + (5.466 \times 10^3)/^{\circ}R$$

$$\ln K_H = -34.837 + (2.734 \times 10^4)/^{\circ}R$$

Figure 26: Adsorption Model Predictions of the Hydroisomerization Rate Constant.

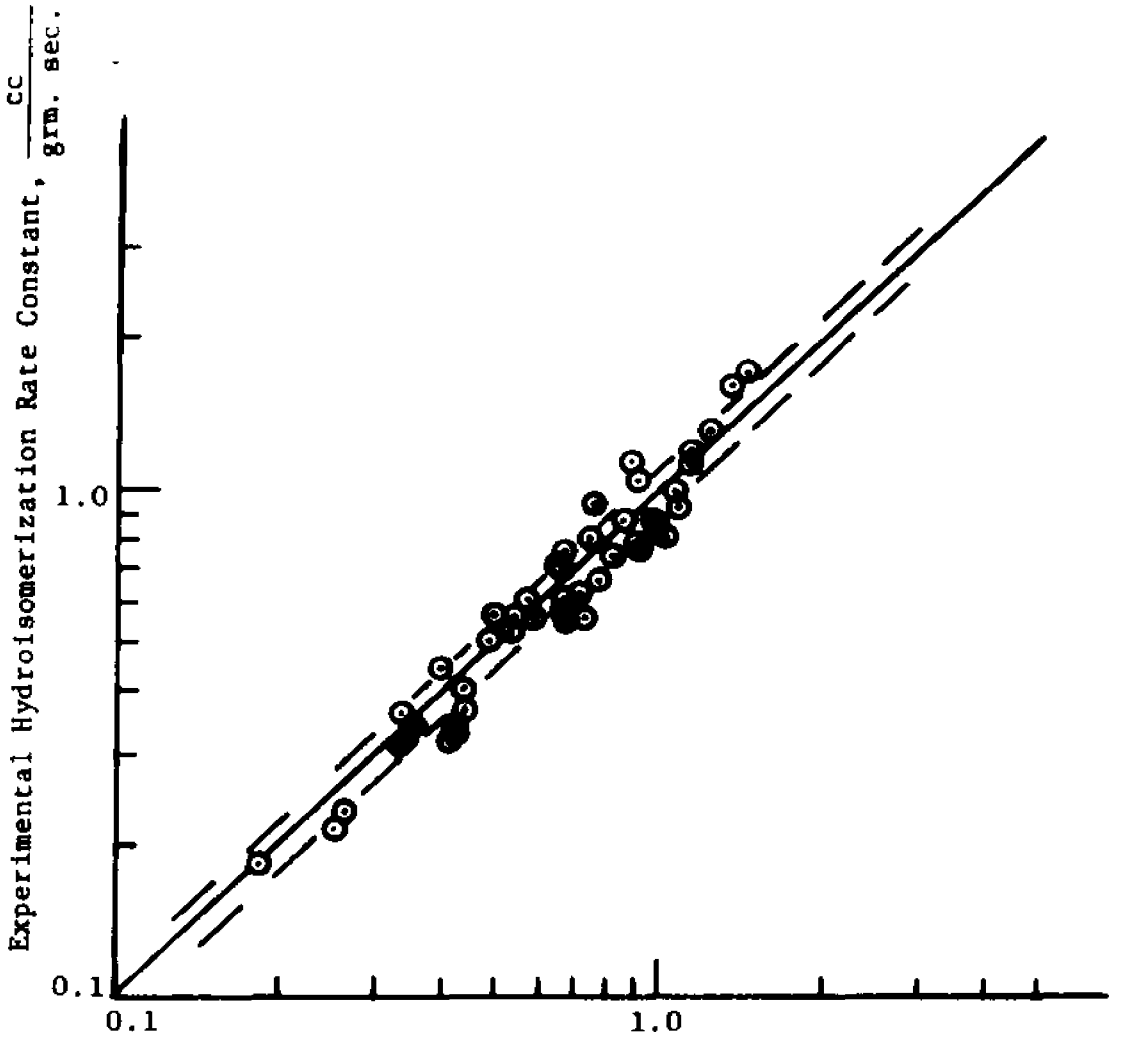

Symbol	Correlating Equation	Temp., °F
⊙	$k_1 = \frac{k_{01} K_O}{(1 + K_O P_O + K_H P_H)^2}$	490,520,535,550

Table 21: Reproducibility of Experimental Results at 490°F, 465 psia and 10 Moles of H_2/Mole Cyclohexane

Run No.	Reaction Rate Constants, cc/grm. sec. Hydroisomerization	Hydrocracking
1A	0.3272	0.0119
1B	0.3847	0.0108
1C	0.3867	0.0101
1D	0.3874	0.0135
1E	0.3810	0.0088
3A	0.4150	0.0138
3C	0.3656	0.0106
3F	0.3638	0.0087
5E	0.3366	0.0120
6F	0.3505	0.0118
7A	0.4058	0.0163
7G	0.3726	0.0104
Standard Deviation, σ	0.0261	0.0021
σ/ave. Value, %	8.2	17.1

Table 22: Adsorption Mechanisms for Hydrocracking

Correlating Equation: $$\frac{1}{(k_2)^{1/n}} = \frac{1}{(k_{02}\ K_O)^{1/n}} + \frac{K_O}{(k_{02}\ K_O)^{1/n}} P_O + \frac{K_H}{(k_{02}\ K_O)^{1/n}} P_H$$

Mechanism	Temp., °F	Fitted Parameters k_{02}	K_O	K_H	Statistical Significance D. F.[1]	R^2
Single Site	490	4.390×10^{-1}	-5.079×10^{-2}	-1.882×10^{-2}	15	0.962
n = 1	520	7.812	-6.977×10^{-3}	-5.957×10^{-3}	12	0.808
	535	1.145×10^{1}	-1.135×10^{-2}	5.882×10^{-3}	5	0.950
	550	3.662	-6.876×10^{-2}	------*	1	0.981
Dual Site	490	4.870	5.893×10^{-2}	3.004×10^{-3}	15	0.938
n = 2	520	1.405×10^{2}	1.859×10^{-2}	1.685×10^{-2}	12	0.852
	535	-2.175×10^{1}	-5.880×10^{-2}	1.213×10^{-2}	5	0.941
	550	1.315×10^{1}	1.235×10^{-1}	-6.352×10^{-3}	1	0.986

Correlating Equation: $$\frac{1}{(k_2)^{1/n}} = \frac{1}{(k_{02}\ K_\pi)^{1/n}} + \frac{K_\pi}{(k_{02}\ K_\pi)^{1/n}} \pi$$

		k_{02}	K_π		
Dual Site					
n = 2	490	4.147×10^{1}	1.179×10^{-2}	16	0.640
	520	1.530×10^{2}	1.697×10^{-2}	13	0.850
	535	1.804×10^{2}	7.764×10^{-3}	6	0.686
	550	3.417×10^{2}	6.201×10^{-3}	2	0.983

[1] D. F. = (No. of data points - No. of parameters)

[2] Multiple Correlation Coefficient = $$\frac{\sum(Y_{actual} - \bar{Y})^2 \quad \sum(Y_{actual} - Y_{pred.})^2}{\sum(Y_{actual} - \bar{Y})^2}$$

* Not Significant

535°F and 550°F. Since the dual site mechanism adequately represented most of the data (33 out of 42 experimental points) it was further investigated to explain the behavior of the hydrocracking rate constants at the higher temperature levels, 535°F and 550°F.

A dual site adsorption mechanism based on the total pressure gave meaningful coefficients at all temperature levels investigated. When this model is compared with the dual site mechanism expressed in terms of the hydrocarbon partial pressure and the hydrogen partial pressure, it is observed that at 490°F the total pressure model yielded a worse fit (R = 0.6). However, at 520°F, the multiple correlation coefficients (R) are equivalent. Furthermore, the adsorption coefficients K_O, K_H, and K_π approach each other, making the two equations compatible.

The indications are that at the low temperature levels (490°F, 520°F) the hydrocracking rate constant is dependent on both the hydrogen and the hydrocarbon partial pressures. As the temperature increases (520°F and above), the hydrocracking rate constant appears to be mostly dependent on the total pressure.

The final adsorption model adopted to represent the hydrocracking rate constants is shown in Table 23. It is based on a dual site mechanism, but represents a compromise between the partial pressures and the total pressure formulations.

A comparison between the hydrocracking rate constants obtained experimentally and those predicted by the adsorption model is shown in Figure 27. The dotted lines corresponds to the experimental uncertainties associated with the hydrocracking rate constants as shown in Table 21. There is some scatter in the predictions but they

Table 23: Final Adsorption Model for Hydrocracking

Dual Site Equations:

$$k_2 = \frac{k_{O2}\, K_O}{(1 + K_O\, P_O + K_H\, P_H)^2} \qquad T \leq 520^\circ F$$

$$k_2 = \frac{k'_{O2}\, K_\pi}{(1 + K_\pi\, \pi)^2} \qquad T \geq 520^\circ F$$

Adsorption Parameter Equations:

$$\ln k_{O2} = 112.38 - 1.053 \times 10^5 / {}^\circ R$$

$$\ln K_O = -40.359 + 3.565 \times 10^4 / {}^\circ R$$

$$\ln K_H = 50.778 - 5.375 \times 10^4 / {}^\circ R$$

$$\ln k'_{O2} = 38.128 - 3.263 \times 10^4 / {}^\circ R$$

$$\ln K_\pi = -15.767 + 1.097 \times 10^4 / {}^\circ R$$

Figure 27: Adsorption Model Predictions of the Hydrocracking Rate Constant.

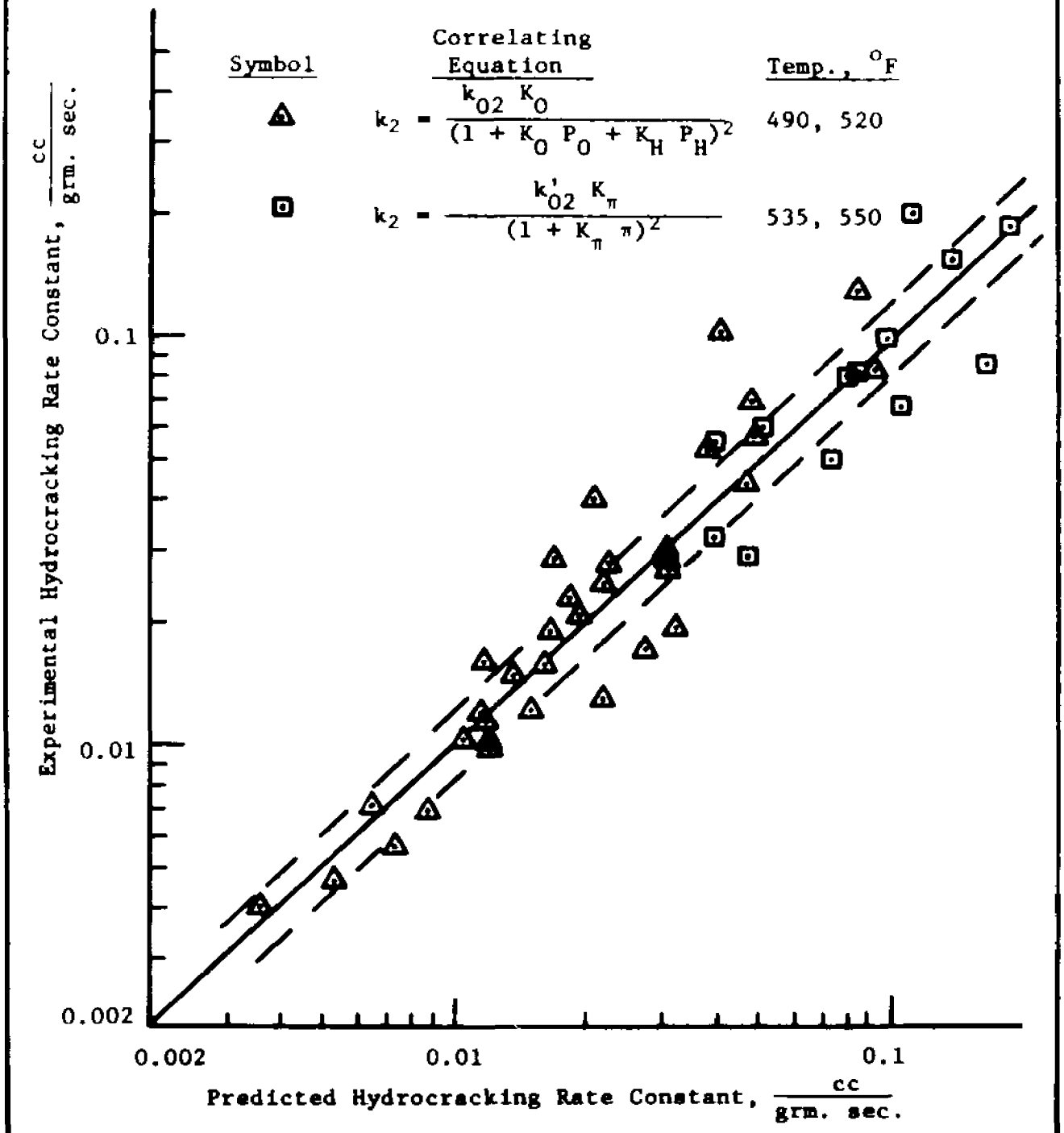

do not appear to be biased.

The effectiveness of the overall kinetic model is demonstrated in Figure 28. The solid lines correspond to the kinetic model predictions employing the rate constants calculated from the adsorption mechanisms for hydroisomerization and hydrocracking. The agreement seems to be quite good.

Figure 28: Overall Kinetic Model Yield Predictions at 490°F, 450 psig, and 10 Moles of H_2 per Mole of Cyclohexane Feed.

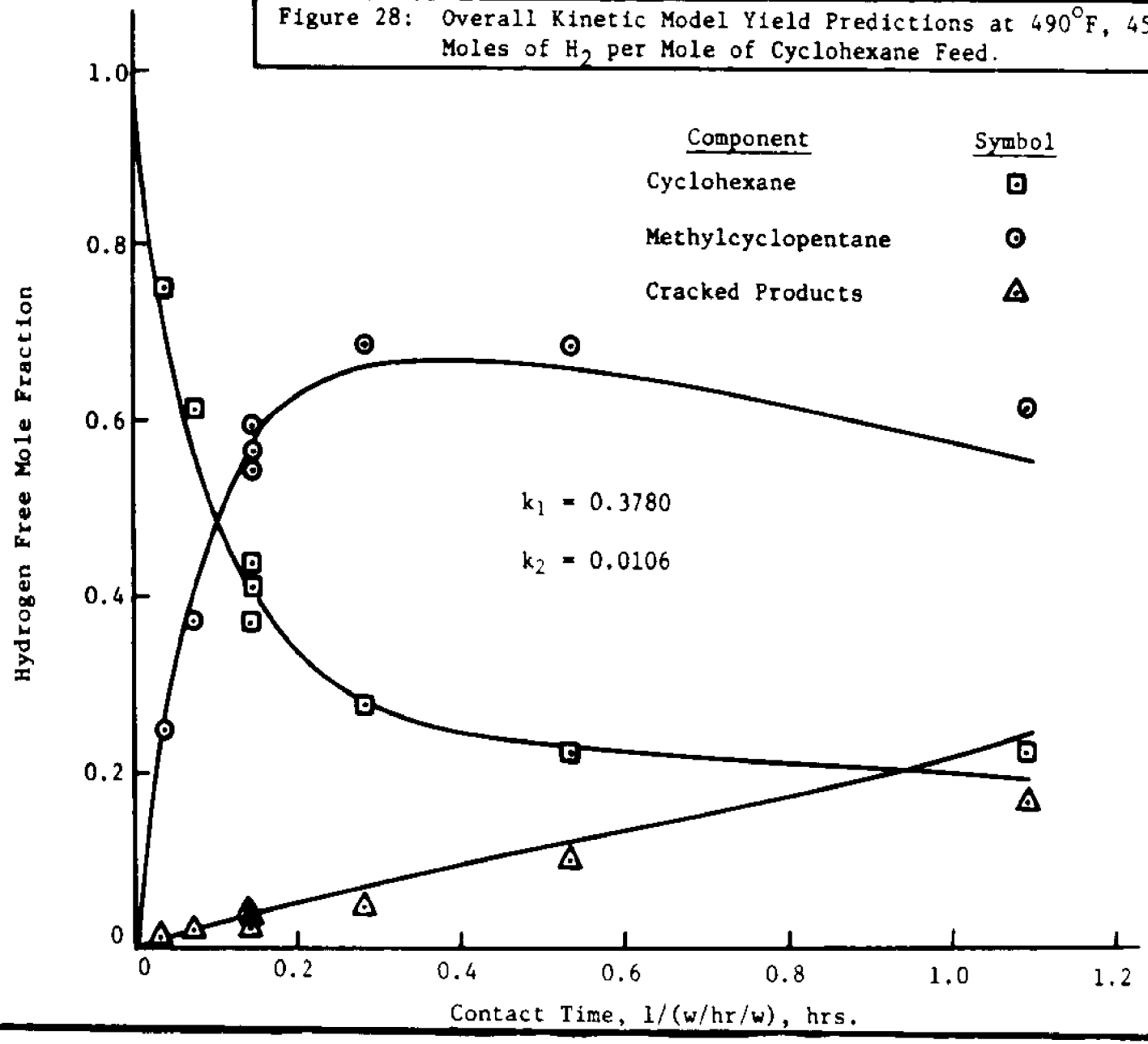

LIST OF REFERENCES - CHAPTER VI

1. Allan, D. E., "The Dehydrogenation and Isomerization of Cyclohexane over a Platinum Alumina Mordenite Catalyst," Ph.D. dissertation, Department of Chemical Engineering, Louisiana State University, 1970.

2. Chou, C. H., "Least Squares," Industrial and Engineering Chemistry, 50 (No. 5), 799 (1958).

3. Hatcher, W. J., "Hydrocracking of Normal Hexane and Cyclohexane over Zeolite Catalysts, "Ph.D. dissertation, Department of Chemical Engineering, Louisiana State University, 1968.

4. Hopper, J. R., "A Study of the Catalytic Hydroisomerization Reactions of N-Pentane and Cyclohexane over Structurally Modified Mordenites," Ph.D. dissertation, Department of Chemical Engineering, Louisiana State University, 1969.

5. Hougen, O. A. and Watson, K. M., Chemical Process Principles, Part III, Kinetics and Catalysis, John Wiley and Sons, New York, New York, 1947.

6. Iijima, K., Schimizu, S., Furukawa, T., and Yashida, N., "Hydrodecyclization of Methylcyclopentane and Benzene in the Presence of a Reforming Catalyst," Bulletin of the Japan Petroleum Institute, 5, 1 (1963).

7. Levitskii, I. I. and Gronikberg, M. G., Izvest. Akad. Nauk. S. S. S. R., Otdel. Khim. Nauk., 1960, 996-1000; Chemical Abstracts, 56, 10973e.

8. Maslyanskii, G. N., "Kinetics of Isomerization of Cyclohexane Under Elevated Pressures," Journal of General Chemistry, 13, 540 (1943); Universal Oil Products Company Translation 465, September 15, 1944.

CHAPTER VII

CONCLUSIONS AND RECOMMENDATIONS

A. Conclusions

1. The Pd-H-faujasite catalyst prepared by steaming and ammonium exchanging was found to be a very effective catalyst for hydroisomerizing cyclohexane in the temperature range 490°-550°F. It was demonstrated that as the severity of operations was increased, by increasing either temperature or contact time, the hydrocracking reactions became more pronounced.

2. A kinetic model was developed to describe the simultaneous hydroisomerization and hydrocracking of cyclohexane. The kinetic model is based on the first order reversible hydroisomerization of cyclohexane to methylcyclopentane and on the first order irreversible hydrocracking of cyclohexane and methylcyclopentane to lower molecular weight hydrocarbons or "cracked products." It was shown that the hydrocracking rate constants for cyclohexane and methylcyclopentane, over the Pd-H-faujasite catalyst studied, were essentially the same. The kinetic model was extensively tested and it was found to be in close agreement with the experimental data.

3. It was demonstrated that mass transfer from the bulk gas stream to the surface of the catalyst had no effect on the hydroisomerization and hydrocracking rate constants.

4. Intraparticle diffusion or "macropore" accesibility was shown not to be a limiting step for the hydroisomerization and hydrocracking reactions.

5. Activation energies for the cyclohexane hydroisomerization and hydrocracking reactions were computed from a least squares fitting of the experimental data. They were determined to be 23($\pm$1) Kcal/gmole and 33($\pm$3) Kcal/gmole respectively. These values agree favorably with those reported in the literature.

6. The cyclohexane hydroisomerization rate constant was found to be compatible with a dual site adsorption mechanism. The dual site mathematical model was formulated in terms of the individual partial pressures of the hydrogen and the hydrocarbons. Temperature effects were accounted for by the adsorption parameters.

7. The hydrocracking rate constant was also found to be compatible with a dual site adsorption mechanism. At temperatures below 520^{o}F., it was observed that the hydrocracking rate constant depended on both the hydrogen partial pressure and the hydrocarbon partial pressure. However, at temperatures in excess of 520^{o}F. the hydrocracking rate constant appeared to be mostly dependent on the total system pressure.

B. Recommendations

1. The mechanism for the cyclohexane hydroisomerization and hydrocracking reactions involves hydrogenation-dehydrogenation as well as isomerization of the olefin intermediate. These hydrogenation-dehydrogenation steps take place at the metallic sites of the catalyst as opposed to isomerization taking place on the acidic faujasite sites. It would be interesting to investigate the effect of adding additional hydrogenation-dehydrogenation activity to the Pd-H-faujasite catalyst

studied in this work. Extra hydrogenation-dehydrogenation functionality can be incorporated in the catalyst by additional impregnation with palladium or another metal.

2. Carbonium ions are necessary intermediates in the cyclohexane isomerization reaction whether it is conducted over acidic halides or dual function catalysts. In the case of acidic halides, it has been established in the literature that an initiator or promoter is required to set in motion the formation of carbonium ions. On the other hand, for the dual function Pd-H-faujasites the first step involves dehydrogenation of cyclohexane to form an olefin followed by rearrangement of the olefin via a carbonium ion.

It could be advantageous to utilize a hybrid acidic-halide-Pd-H-faujasite catalyst by incorporating halide funtionality into the Pd-H-faujasite thus speeding up the formation of carbonium ions by two independent routes.

3. Modified faujasites can be prepared by varying the silica to alumina mole ratios. The dependency of the cyclohexane hydroisomerization and hydrocracking rates on the silica to alumina mole ratios would be a very worthwhile correlation.

APPENDIX A

DETAILED EXPERIMENTAL DATA

TABLE A

RUN DATA

Run Number	1A	1B	1C
Catalyst Type	← Pd-H-Faujasite →		
Size, mm	← 0.417 - 1.168 →		
Temperature, °F	490	492	491
Pressure, psia	465	465	465
Feed:	← Cyclohexane →		
Partial Pressure, psia	45	46	46
W/hr/W	6.98	6.98	6.98
Hydrogen:			
Partial Pressure, psia	420	419	419
Moles H_2/Mole Feed	9.29	9.19	9.19
Minutes on Feed	143	99	155
Product, moles per 100 moles feed			
Hydrogen	949.30	916.52	916.62
Methane	0.00	0.00	0.00
Ethane	0.47	0.61	0.54
Propane	0.00	1.51	1.46
I-Butane	1.30	0.00	0.00
N-Butane	0.00	0.00	0.00
I-Pentane	0.73	0.69	0.56
N-Pentane	0.00	0.00	0.00
I-Hexanes	0.71	0.37	0.39
N-Hexane	0.44	0.17	0.21
Methylcyclopentane	53.56	58.19	58.36
Cyclohexane	43.66	39.73	39.68
Cyclohexane +	0.00	0.00	0.00
Isomerization, %	53.56	58.19	58.36
Rate Constant, k_1, cc./grm. sec.	0.3272	0.3847	0.3867
Cracking, %	2.78	2.08	1.96
Rate Constant, k_2, cc./grm. sec.	0.0119	0.0108	0.0102
Hydrogen Balance, %	101.6	100.1	100.3

TABLE A

RUN DATA

Run Number	1D	1E	2A
Catalyst Type	← Pd-H-Faujasite →		
Size, mm	← 0.417-1.168 →		0.295-0.417
Temperature, °F	491	490	490
Pressure, psia	465	465	465
Feed:	← Cyclohexane →		
Partial Pressure, psia	48	49	47
W/hr/W	6.99	6.99	6.97
Hydrogen:			
Partial Pressure, psia	416	416	418
Moles H_2/Mole Feed	8.59	8.56	8.96
Minutes on Feed	105	157	101
Product, moles per 100 moles feed			
Hydrogen	858.73	862.27	874.97
Methane	0.00	0.00	0.00
Ethane	0.39	0.63	0.16
Propane	2.29	0.26	0.75
I-Butane	0.00	1.02	1.11
N-Butane	0.00	0.00	0.00
I-Pentane	0.98	0.32	0.59
N-Pentane	0.00	0.00	0.00
I-Hexanes	0.53	0.41	0.48
N-Hexane	0.27	0.26	0.19
Methylcyclopentane	59.19	59.42	58.33
Cyclohexane	37.92	38.62	39.35
Cyclohexane +	0.00	0.00	0.00
Isomerization, %	59.19	59.42	58.33
Rate Constant, k_1, cc./grm. sec.	0.3873	0.3810	0.3808
Cracking, %	2.89	1.96	2.32
Rate Constant, k_2, cc./grm. sec.	0.0135	0.0088	0.0103
Hydrogen Balance, %	100.28	100.6	98.8

TABLE A

RUN DATA

Run Number	2B	2C	2D
Catalyst Type	← Pd-H-Faujasite →		
Size, mm	0.295-0.417	← 0.074-0.147 →	
Temperature, °F	490	491	491
Pressure, psia	465	465	465
Feed:	← Cyclohexane →		
Partial Pressure, psia	47	48	47
W/hr/W	6.97	6.98	6.98
Hydrogen:			
Partial Pressure, psia	418	417	417
Moles H_2/Mole Feed	8.93	8.75	8.80
Minutes on Feed	131	129	155
Product, moles per 100 moles feed			
Hydrogen	883.04	859.10	856.03
Methane	0.00	0.00	0.00
Ethane	0.07	0.45	0.95
Propane	0.60	1.41	0.99
I-Butane	1.04	0.00	0.00
N-Butane	0.00	0.00	0.00
I-Pentane	0.56	0.00	0.43
N-Pentane	0.00	0.00	0.00
I-Hexanes	0.37	0.95	0.42
N-Hexane	0.21	0.19	0.23
Methylcyclopentane	59.70	58.74	57.73
Cyclohexane	38.23	39.26	40.45
Cyclohexane +	0.00	0.00	0.00
Isomerization, %	59.70	58.74	57.73
Rate Constant, k_1, cc./grm. sec.	0.4009	0.3766	0.3609
Cracking, %	2.07	2.00	1.82
Rate Constant, k_2, cc./grm. sec.	0.0089	0.0093	0.0094
Hydrogen Balance, %	99.5	99.1	98.6

TABLE A

RUN DATA

Run Number	3A	3B	3C
Catalyst Type	← Pd-H-Faujasite →		
Size, mm	← 0.417-1.168 →		
Temperature, °F	491	489	490
Pressure, psia	465	465	465
Feed:	← Cyclohexane →		
Partial Pressure, psia	47	46	45
W/hr/W	7.01	3.50	7.01
Hydrogen:			
Partial Pressure, psia	418	419	420
Moles H_2/Mole Feed	8.92	9.11	9.29
Minutes on Feed	136	420	1211
Product, moles per 100 moles feed			
Hydrogen	891.72	875.28	907.84
Methane	0.00	0.00	0.00
Ethane	0.60	0.31	0.61
Propane	1.23	1.66	1.26
I-Butane	0.00	0.00	0.00
N-Butane	0.00	0.00	0.00
I-Pentane	1.14	1.28	0.59
N-Pentane	0.00	0.00	0.00
I-Hexanes	0.75	0.88	0.42
N-Hexane	0.66	0.70	0.19
Methylcyclopentane	59.72	68.58	56.60
Cyclohexane	37.12	27.61	41.29
Cyclohexane +	0.00	0.00	0.17
Isomerization, %	59.72	68.58	56.60
Rate Constant, k_1, cc./grm. sec.	0.4150	0.3932	0.3656
Cracking, %	3.16	3.80	2.11
Rate Constant, k_2, cc./grm. sec.	0.0138	0.0082	0.0106
Hydrogen Balance, %	100.3	97.9	98.8

TABLE A

RUN DATA

Run Number	3D	3E	3F
Catalyst Type	←——— Pd-H-Faujasite ———→		
Size, mm	←——— 0.417-1.168 ———→		
Temperature, °F	490	489	490
Pressure, psia	465	465	465
Feed:	←——— Cyclohexane ———→		
Partial Pressure, psia	46	45	42
W/hr/W	26.28	13.14	7.0
Hydrogen:			
Partial Pressure, psia	419	419	423
Moles H_2/Mole Feed	9.07	9.25	10.13
Minutes on Feed	110	410	545
Product, moles per 100 moles feed			
Hydrogen	891.06	916.7	993.95
Methane	0.00	0.00	0.00
Ethane	0.87	0.39	0.17
Propane	0.00	0.00	0.53
I-Butane	0.00	0.00	0.83
N-Butane	0.00	0.00	0.00
I-Pentane	0.00	0.70	0.29
N-Pentane	0.00	0.00	0.00
I-Hexanes	0.10	0.44	0.42
N-Hexane	0.15	0.04	0.23
Methylcyclopentane	24.88	37.43	54.75
Cyclohexane	74.58	61.36	43.49
Cyclohexane +	0.00	0.00	0.00
Isomerization, %	24.88	37.43	54.75
Rate Constant, k_1, cc./grm. sec.	0.3647	0.3228	0.3638
Cracking, %	0.54	1.21	1.76
Rate Constant, k_2, cc./grm. sec.	0.0133	0.0097	0.0087
Hydrogen Balance, %	99.0	99.5	99.0

TABLE A

RUN DATA

Run Number	3G	3H	4A
Catalyst Type	← Pd-H-Faujasite →		
Size, mm	← 0.417-1.168 →		
Temperature, °F	490	491	500
Pressure, psia	465	465	465
Feed:	← Cyclohexane →		
Partial Pressure, psia	45	51	44
W/hr/W	1.87	0.91	7.0
Hydrogen:			
Partial Pressure, psia	419	413	421
Moles H_2/Mole Feed	9.24	8.05	9.57
Minutes on Feed	526	1107	77
Product, moles per 100 moles feed			
Hydrogen	917.99	757.19	948.74
Methane	0.00	0.00	0.00
Ethane	0.33	0.26	0.38
Propane	0.53	0.98	2.36
I-Butane	1.99	4.31	0.00
N-Butane	0.92	0.85	0.00
I-Pentane	1.32	1.86	0.96
N-Pentane	0.53	0.63	0.00
I-Hexanes	3.32	7.04	0.67
N-Hexane	1.57	2.95	0.22
Methylcyclopentane	68.61	58.68	61.97
Cyclohexane	21.91	21.45	34.66
Cyclohexane +	0.72	1.47	0.32
Isomerization, %	68.61	58.68	61.97
Rate Constant, k_1, cc./grm. sec.	0.3782	0.3812	0.4882
Cracking, %	9.47	19.87	3.37
Rate Constant, k_2, cc./grm. sec.	0.0081	0.0068	0.0167
Hydrogen Balance, %	100.17	97.58	99.8

TABLE A

RUN DATA

Run Number	4B	4C	4D
Catalyst Type	← Pd-H-Faujasite →		
Size, mm	← 0.417-1.168 →		
Temperature, °F	510	520	530
Pressure, psia	465	465	465
Feed:	← Cyclohexane →		
Partial Pressure, psia	44	44	44
W/hr/W	7.00	6.98	7.00
Hydrogen:			
Partial Pressure, psia	421	420	421
Moles H_2/Mole Feed	9.53	9.51	9.57
Minutes on Feed	183	310	354
Product, moles per 100 moles feed			
Hydrogen	947.28	907.73	929.41
Methane	0.00	0.00	0.00
Ethane	0.40	0.38	0.39
Propane	0.44	0.00	0.66
I-Butane	1.12	2.22	2.30
N-Butane	0.00	0.00	1.04
I-Pentane	0.52	0.00	1.53
N-Pentane	0.00	1.55	0.57
I-Hexanes	0.86	1.51	1.72
N-Hexane	0.29	0.76	0.38
Methylcyclopentane	66.96	69.86	69.45
Cyclohexane	29.91	24.97	22.82
Cyclohexane +	0.40	0.00	0.92
Isomerization, %	66.96	69.86	69.45
Rate Constant, k_1, cc./grm. sec.	0.6207	0.8317	0.9283
Cracking, %	3.13	5.16	7.72
Rate Constant, k_2, cc./grm. sec.	0.0138	0.0223	0.0345
Hydrogen Balance, %	99.8	97.6	98.8

TABLE A

RUN DATA

Run Number	4E	5A	5B
Catalyst Type	← Pd-H-Faujasite →		
Size, mm	← 0.417-1.168 →		
Temperature, °F	540	491	490
Pressure, psia	465	265	365
Feed:	← Cyclohexane →		
Partial Pressure, psia	44	27	37
W/hr/W	7.00	6.97	6.97
Hydrogen:			
Partial Pressure, psia	421	238	328
Moles H_2/Mole Feed	9.60	8.89	8.89
Minutes on Feed	462	110	228
Product, moles per 100 moles feed			
Hydrogen	908.8	870.59	873.09
Methane	0.00	0.00	0.00
Ethane	0.31	0.58	0.41
Propane	0.98	0.36	0.00
I-Butane	4.64	1.24	1.18
N-Butane	1.12	0.00	0.00
I-Pentane	2.43	0.00	0.65
N-Pentane	0.72	0.00	0.00
I-Hexanes	4.65	0.51	0.40
N-Hexane	1.32	0.24	0.15
Methylcyclopentane	65.84	60.81	61.71
Cyclohexane	19.54	36.87	36.00
Cyclohexane +	1.30	0.31	0.25
Isomerization, %	65.84	60.81	61.71
Rate Constant, k_1, cc./grm. sec.	1.0981	0.7418	0.5626
Cracking, %	14.62	2.32	2.29
Rate Constant, k_2, cc./grm. sec.	0.0659	0.0178	0.0121
Hydrogen Balance, %	97.8	99.0	99.1

TABLE A

RUN DATA

Run Number	5C	5D	5E
Catalyst Type	← Pd-H-Faujasite →		
Size, mm	← 0.417-1.168 →		
Temperature, °F	490	490	490
Pressure, psia	555	665	465
Feed:	← Cyclohexane →		
Partial Pressure, psia	52	62	44
W/hr/W	6.97	6.97	6.97
Hydrogen:			
Partial Pressure, psia	503	603	421
Moles H_2/Mole Feed	9.75	9.76	9.54
Minutes on Feed	578	675	732
Product, moles per 100 moles feed			
Hydrogen	962.19	966.08	1348.51
Methane	0.00	0.00	0.00
Ethane	0.67	1.09	1.22
Propane	0.00	0.00	0.00
I-Butane	0.90	1.15	1.24
N-Butane	0.00	0.00	0.00
I-Pentane	0.23	0.20	0.31
N-Pentane	0.00	0.00	0.00
I-Hexanes	0.39	0.28	0.36
N-Hexane	0.18	0.20	0.15
Methylcyclopentane	57.05	53.72	53.92
Cyclohexane	41.29	44.41	43.70
Cyclohexane +	0.06	0.08	0.32
Isomerization, %	57.05	53.72	53.92
Rate Constant, k_1, cc./grm. sec.	0.3210	0.2355	0.3366
Cracking, %	1.65	1.87	2.37
Rate Constant, k_2, cc./grm. sec.	0.0069	0.0071	0.0120
Hydrogen Balance, %	99.3	99.6	105.5

TABLE A

RUN DATA

Run Number	6A	6B	6C
Catalyst Type	← Pd-H-Faujasite →		
Size, mm	← 0.417-1.168 →		
Temperature, °F	490	489	491
Pressure, psia	465	565	665
Feed:	← Cyclohexane →		
Partial Pressure, psia	22	28	34
W/hr/W	6.97	6.97	6.97
Hydrogen:			
Partial Pressure, psia	443	536	631
Moles H_2/Mole Feed	20.25	18.88	18.6
Minutes on Feed	189	279	415
Product, moles per 100 moles feed			
Hydrogen	1999.6	1858.87	1829.03
Methane	0.00	0.00	0.00
Ethane	4.33	2.84	1.91
Propane	0.00	0.00	0.00
I-Butane	0.00	0.00	0.00
N-Butane	0.00	0.00	0.00
I-Pentane	0.00	0.00	0.00
N-Pentane	0.00	0.00	0.00
I-Hexanes	0.00	0.00	0.20
N-Hexane	1.72	0.25	0.16
Methylcyclopentane	48.56	41.96	48.29
Cyclohexane	48.28	56.85	50.71
Cyclohexane +	0.00	0.00	0.00
Isomerization, %	48.56	41.96	48.29
Rate Constant, k_1, cc./grm. sec.	0.5596	0.3246	0.3433
Cracking, %	3.16	1.19	1.0
Rate Constant, k_2, cc./grm. sec.	0.0405	0.0158	0.0098
Hydrogen Balance, %	99.3	98.9	98.8

TABLE A

RUN DATA

Run Number	6D	6E	6F
Catalyst Type	← Pd-H-Faujasite →		
Size, mm	← 0.417-1.168 →		
Temperature, °F	489	490	490
Pressure, psia	465	265	465
Feed:	← Cyclohexane →		
Partial Pressure, psia	24	14	44
W/hr/W	6.97	6.97	6.97
Hydrogen:			
Partial Pressure, psia	441	251	421
Moles H_2/Mole Feed	18.57	18.33	9.57
Minutes on Feed	468	719	845
Product, moles per 100 moles feed			
Hydrogen	1831.88	1819.82	946.39
Methane	0.00	0.00	0.00
Ethane	1.16	1.12	1.88
Propane	0.00	1.95	0.00
I-Butane	1.12	5.45	0.81
N-Butane	0.00	0.00	0.00
I-Pentane	0.00	0.00	0.23
N-Pentane	0.00	0.00	0.00
I-Hexanes	1.44	0.00	0.28
N-Hexane	0.10	1.07	0.15
Methylcyclopentane	49.60	46.65	55.09
Cyclohexane	47.74	47.03	42.91
Cyclohexane +	0.00	0.23	0.18
Isomerization, %	49.60	46.65	55.09
Rate Constant, k_1, cc./grm. sec.	0.5313	0.8824	0.3505
Cracking, %	2.66	6.32	2.00
Rate Constant, k_2, cc./grm. sec.	0.0236	0.1063	0.0118
Hydrogen Balance, %	99.1	99.8	99.6

TABLE A

RUN DATA

Run Number	7A	7B	7C
Catalyst Type	← Pd-H-Faujasite →		
Size, mm	← 0.417-1.168 →		
Temperature, °F	490	491	491
Pressure, psia	465	665	565
Feed:	← Cyclohexane →		
Partial Pressure, psia	44	112	86
W/hr/W	6.84	6.97	6.97
Hydrogen:			
Partial Pressure, psiz	421	553	478
Moles H_2/Mole Feed	9.65	4.96	5.55
Minutes on Feed	100	80	196
Product, moles per 100 moles feed			
Hydrogen	867.99	474.34	467.77
Methane	0.00	0.00	0.00
Ethane	0.34	1.44	0.31
Propane	1.62	0.00	0.00
I-Butane	0.00	0.42	0.41
N-Butane	0.00	0.00	0.00
I-Pentane	1.36	0.22	0.21
N-Pentane	0.00	0.00	0.00
I-Hexanes	0.67	0.47	0.39
N-Hexane	0.83	0.33	0.29
Methylcyclopentane	57.86	61.81	59.14
Cyclohexane	38.48	36.18	38.25
Cyclohexane +	0.09	0.22	1.19
Isomerization, %	57.86	61.81	59.14
Rate Constant, k_1, cc./grm. sec.	0.4058	0.1850	0.2152
Cracking, %	3.65	2.01	2.61
Rate Constant, k_2, cc./grm. sec.	0.0163	0.0041	0.0047
Hydrogen Balance, %	94.1	98.3	92.7

TABLE A

RUN DATA

Run Number	7D	7E	7F
Catalyst Type	← Pd-H-Faujasite →		
Size, mm	← 0.417-1.168 →		
Temperature, °F	491	491	491
Pressure, psia	465	370	265
Feed:	← Cyclohexane →		
Partial Pressure, psia	73	58	39
W/hr/W	6.97	6.97	6.97
Hydrogen:			
Partial Pressure, psia	392	311	225
Moles H_2/Mole Feed	5.37	5.32	5.74
Minutes on Feed	288	399	619
Product, moles per 100 moles feed			
Hydrogen	451.77	437.06	518.76
Methane	0.00	0.00	0.00
Ethane	0.34	0.26	0.00
Propane	0.17	0.21	0.17
I-Butane	0.79	1.24	2.45
N-Butane	0.00	0.00	0.00
I-Pentane	0.35	0.60	1.10
N-Pentane	0.00	0.00	0.00
I-Hexanes	0.49	0.54	0.52
N-Hexane	0.33	0.19	0.16
Methylcyclopentane	63.86	63.44	62.03
Cyclohexane	33.88	32.97	33.30
Cyclohexane +	0.36	1.16	1.17
Isomerization, %	63.86	63.44	62.03
Rate Constant, k_1, cc./grm. sec.	0.3168	0.4052	0.5805
Cracking, %	2.26	3.59	4.67
Rate Constant, k_2, cc./grm. sec.	0.0058	0.0106	0.0211
Hydrogen Balance, %	92.72	92.0	96.0

TABLE A

RUN DATA

Run Number	7G	8A	8B
Catalyst Type	← Pd-H-Faujasite →		
Size, mm	← 0.417-1.168 →		
Temperature, °F	490	522	520
Pressure, psia	465	660	565
Feed:	← Cyclohexane →		
Partial Pressure, psia	42	60	52
W/hr/W	6.97	6.97	6.97
Hydrogen:			
Partial Pressure, psia	423	600	512
Moles H_2/Mole Feed	10.15	10.00	9.76
Minutes on Feed	710	64	131
Product, moles per 100 moles feed			
Hydrogen	995.74	1005.44	933.17
Methane	0.00	0.00	0.00
Ethane	0.58	0.41	0.42
Propane	0.00	0.50	0.45
I-Butane	0.88	1.31	1.24
N-Butane	0.00	0.00	0.00
I-Pentane	0.33	0.91	0.51
N-Pentane	0.00	0.00	0.00
I-Hexanes	0.30	1.15	0.94
N-Hexane	0.23	0.55	0.47
Methylcyclopentane	55.09	69.11	69.50
Cyclohexane	42.59	25.33	26.74
Cyclohexane +	0.62	1.58	0.64
Isomerization, %	55.09	69.11	69.50
Rate Constant, k_1, cc./grm. sec.	0.3726	0.5792	0.6176
Cracking, %	2.32	5.56	3.76
Rate Constant, k_2, cc./grm. sec.	0.0104	0.0165	0.0135
Hydrogen Balance, %	99.0	100.7	97.6

TABLE A

RUN DATA

Run Number	8C	8D	8E
Catalyst Type	← Pd-H-Faujasite →		
Size, mm	← 0.417-1.168 →		
Temperature, °F	522	521	521
Pressure, psia	365	265	465
Feed:	← Cyclohexane →		
Partial Pressure, psia	33	24	45
W/hr/W	6.97	6.97	6.97
Hydrogen:			
Partial Pressure, psia	331	241	420
Moles H_2/Mole Feed	9.91	10.22	9.36
Minutes on Feed	219	316	449
Product, moles per 100 moles feed			
Hydrogen	958.00	1004.00	977.74
Methane	0.00	0.00	0.00
Ethane	0.49	0.85	0.78
Propane	0.62	0.81	0.42
I-Butane	2.68	4.07	2.11
N-Butane	0.97	1.43	0.69
I-Pentane	1.71	2.26	1.53
N-Pentane	0.59	0.00	0.00
I-Hexanes	1.26	0.96	1.27
N-Hexane	0.38	0.23	0.52
Methylcyclopentane	68.76	61.77	68.06
Cyclohexane	23.83	27.20	25.09
Cyclohexane +	0.80	3.10	1.24
Isomerization, %	68.76	61.77	68.06
Rate Constant, k_1, cc./grm. sec.	1.1513	1.1423	0.7700
Cracking, %	7.41	11.04	6.85
Rate Constant, k_2, cc./grm. sec.	0.0442	0.0916	0.0295
Hydrogen Balance, %	98.5	99.7	103.3

TABLE A

RUN DATA

Run Number	9A	9B	9C
Catalyst Type	← Pd-H-Faujasite →		
Size, mm	← 0.417-1.168 →		
Temperature, °F	519	520	520
Pressure, psia	665	565	465
Feed:	← Cyclohexane →		
Partial Pressure, psia	32	28	23
W/hr/W	6.97	6.97	6.97
Hydrogen:			
Partial Pressure, psia	633	537	442
Moles H_2/Mole Feed	19.69	19.30	19.10
Minutes on Feed	552	646	744
Product, moles per 100 moles feed			
Hydrogen	1941.43	1916.28	1893.95
Methane	0.00	0.00	0.00
Ethane	1.84	3.23	0.59
Propane	0.00	0.00	0.00
I-Butane	2.11	0.53	0.80
N-Butane	0.00	0.00	0.00
I-Pentane	0.70	0.24	0.34
N-Pentane	0.00	0.00	0.00
I-Hexanes	0.79	0.72	0.66
N-Hexane	0.33	0.30	0.26
Methylcyclopentane	63.45	67.27	66.63
Cyclohexane	32.37	29.81	31.10
Cyclohexane +	0.39	0.24	0.29
Isomerization, %	63.45	67.27	66.63
Rate Constant, k_1, cc./grm. sec.	0.7132	0.9641	1.0915
Cracking, %	4.17	2.92	2.28
Rate Constant, k_2, cc./grm. sec.	0.0291	0.0286	0.0193
Hydrogen Balance, %	99.2	99.7	99.5

TABLE A

RUN DATA

Run Number	9D	9E	10A
Catalyst Type	← Pd-H-Faujasite →		
Size, mm	← 0.417-1.168 →		
Temperature, ^{o}F	520	519	524
Pressure, psia	365	275	650
Feed:	← Cyclohexane →		
Partial Pressure, psia	18	13	102
W/hr/W	6.97	6.97	6.97
Hydrogen:			
Partial Pressure, psia	346	261	547
Moles H_2/Mole Feed	18.85	19.36	5.35
Minutes on Feed	1047	1139	1233
Product, moles per 100 moles feed			
Hydrogen	1873.24	1875.19	521.43
Methane	0.00	0.00	0.00
Ethane	0.77	1.13	0.20
Propane	0.00	1.05	0.51
I-Butane	3.08	3.01	4.68
N-Butane	0.00	0.00	0.00
I-Pentane	1.68	1.64	2.16
N-Pentane	0.00	0.00	0.42
I-Hexanes	0.64	0.85	2.71
N-Hexane	0.17	0.18	0.91
Methylcyclopentane	60.47	61.53	66.32
Cyclohexane	34.24	32.78	23.13
Cyclohexane +	0.66	0.33	1.15
Isomerization, %	60.47	61.53	66.32
Rate Constant, k_1, cc./grm. sec.	1.1190	1.6231	0.3668
Cracking, %	5.29	5.69	10.55
Rate Constant, k_2, cc./grm. sec.	0.0585	0.0930	0.0197
Hydrogen Balance, %	99.8	97.9	99.9

TABLE A

RUN DATA

Run Number	10B	10C	10D
Catalyst Type	← Pd-H-Faujasite →		
Size, mm	← 0.417-1.168 →		
Temperature, °F	520	521	520
Pressure, psia	565	365	465
Feed:	← Cyclohexane →		
Partial Pressure, psia	87	57	75
W/hr/W	6.97	6.97	6.97
Hydrogen:			
Partial Pressure, psia	478	307	390
Moles H_2/Mole Feed	5.51	5.36	5.23
Minutes on Feed	1418	1721	2185
Product, moles per 100 moles feed			
Hydrogen	494.37	445.95	512.76
Methane	0.00	0.00	0.00
Ethane	0.42	0.25	0.30
Propane	0.54	0.97	0.58
I-Butane	5.03	9.78	5.15
N-Butane	0.78	1.17	0.80
I-Pentane	2.72	5.02	2.51
N-Pentane	0.51	0.71	0.53
I-Hexanes	1.83	3.26	1.64
N-Hexane	0.50	0.79	0.40
Methylcyclopentane	65.94	59.91	66.19
Cyclohexane	23.02	20.40	23.41
Cyclohexane +	1.49	2.57	1.26
Isomerization, %	65.94	59.91	66.19
Rate Constant, k_1, cc./grm. sec.	0.4436	0.7022	0.5017
Cracking, %	11.05	19.69	10.40
Rate Constant, k_2, cc./grm. sec.	0.0251	0.0701	0.0277
Hydrogen Balance, %	96.3	94.3	100.3

TABLE A

RUN DATA

Run Number	10E	10F	11A
Catalyst Type	← Pd-H-Faujasite →		
Size, mm	← 0.417-1.168 →		
Temperature, °F	525	520	552
Pressure, psia	265	465	665
Feed:	← Cyclohexane →		
Partial Pressure, psia	43	42	59
W/hr/W	6.97	6.97	6.97
Hydrogen:			
Partial Pressure, psia	221	422	606
Moles H_2/Mole Feed	5.10	9.97	10.27
Minutes on Feed	2741	2814	3033
Product, moles per 100 moles feed			
Hydrogen	467.37	984.83	938.27
Methane	0.00	0.00	0.00
Ethane	0.92	0.30	0.58
Propane	1.64	0.53	1.22
I-Butane	15.53	3.22	8.33
N-Butane	1.42	0.00	1.71
I-Pentane	7.79	1.55	4.50
N-Pentane	0.67	0.00	0.87
I-Hexanes	3.49	0.91	5.35
N-Hexane	0.63	0.21	1.59
Methylcyclopentane	55.35	64.69	57.99
Cyclohexane	18.99	28.52	19.22
Cyclohexane +	1.77	1.60	3.34
Isomerization, %	55.35	64.69	57.99
Rate Constant, k_1, cc./grm. sec.	0.8875	0.6371	0.6054
Cracking, %	25.66	6.79	22.79
Rate Constant, k_2, cc./grm. sec.	0.1312	0.0305	0.0803
Hydrogen Balance, %	99.2	99.7	96.2

TABLE A

RUN DATA

Run Number	11B	11C	11D
Catalyst Type	← Pd-H-Faujasite →		
Size, mm	← 0.417-1.168 →		
Temperature, °F	551	552	550
Pressure, psia	565	465	365
Feed:	← Cyclohexane →		
Partial Pressure, psia	51	41	32
W/hr/W	6.97	6.97	6.97
Hydrogen:			
Partial Pressure, psia	514	424	332
Moles H_2/Mole Feed	10.15	10.31	10.25
Minutes on Feed	3391	3870	4732
Product, moles per 100 moles feed			
Hydrogen	981.08	984.29	992.42
Methane	0.00	0.00	0.00
Ethane	0.42	0.46	0.44
Propane	1.58	2.16	2.11
I-Butane	10.51	13.96	13.74
N-Butane	1.85	2.08	2.17
I-Pentane	5.54	6.95	6.89
N-Pentane	1.04	1.10	1.22
I-Hexanes	5.13	5.01	3.87
N-Hexane	1.50	1.15	0.88
Methylcyclopentane	56.88	52.48	52.95
Cyclohexane	19.53	18.44	19.84
Cyclohexane +	1.98	3.67	3.32
Isomerization, %	56.88	52.48	52.95
Rate Constant, k_1, cc./grm. sec.	0.6730	0.8026	0.9433
Cracking, %	23.59	29.07	27.21
Rate Constant, k_2, cc./grm. sec.	0.1004	0.1575	0.1867
Hydrogen Balance, %	99.75	99.3	100.1

TABLE A

RUN DATA

Run Number	11E	12A	12B
Catalyst Type	← Pd-H-Faujasite →		
Size, mm	← 0.417-1.168 →		
Temperature, °F	520	538	535
Pressure, psia	465	465	665
Feed:	← Cyclohexane →		
Partial Pressure, psia	40	41	59
W/hr/W	6.97	6.90	6.90
Hydrogen:			
Partial Pressure, psia	424	423	606
Moles H_2/Mole Feed	10.52	10.21	10.36
Minutes on Feed	4815	102	203
Product, moles per 100 moles feed			
Hydrogen	1019.77	988.41	1019.68
Methane	0.00	0.00	0.00
Ethane	0.29	0.29	0.25
Propane	0.69	0.82	0.81
I-Butane	4.86	6.29	7.58
N-Butane	1.10	1.32	0.00
I-Pentane	2.82	3.12	3.52
N-Pentane	0.73	0.99	0.81
I-Hexanes	0.96	3.59	3.08
N-Hexane	0.18	1.33	1.14
Methylcyclopentane	59.01	61.94	61.28
Cyclohexane	29.86	20.79	22.32
Cyclohexane +	2.25	2.86	2.61
Isomerization, %	59.01	61.94	61.28
Rate Constant, k_1, cc./grm. sec.	0.5720	0.8877	0.5614
Cracking, %	11.13	17.27	16.40
Rate Constant, k_2, cc./grm. sec.	0.0542	0.0816	0.0551
Hydrogen Balance, %	98.9	99.3	100.2

TABLE A

RUN DATA

Run Number	12C	12D	13A
Catalyst Type	← Pd-H-Faujasite →		
Size, mm	← 0.417-1.168 →		
Temperature, °F	535	537	535
Pressure, psia	565	365	665
Feed:	← Cyclohexane →		
Partial Pressure, psia	50	32	31
W/hr/W	6.90	6.90	6.90
Hydrogen:			
Partial Pressure, psia	515	333	634
Moles H_2/Mole Feed	10.33	10.39	20.67
Minutes on Feed	307	398	510
Product, moles per 100 moles feed			
Hydrogen	1019.19	988.49	2035.41
Methane	0.00	0.00	0.00
Ethane	0.34	0.77	0.81
Propane	0.95	2.51	0.73
I-Butane	6.99	15.52	1.79
N-Butane	1.44	3.13	0.00
I-Pentane	3.59	5.50	0.90
N-Pentane	1.03	2.35	0.00
I-Hexanes	1.59	1.57	1.03
N-Hexane	0.36	0.70	0.25
Methylcyclopentane	60.69	49.25	63.47
Cyclohexane	24.44	21.45	31.55
Cyclohexane +	2.45	5.61	0.94
Isomerization, %	60.69	49.25	63.47
Rate Constant, k_1, cc./grm. sec.	0.5772	0.8173	0.7444
Cracking, %	14.87	29.30	4.98
Rate Constant, k_2, cc./grm. sec.	0.0605	0.2026	0.0326
Hydrogen Balance, %	100.3	99.2	99.1

TABLE A

RUN DATA

Run Number	13B	13C	13D
Catalyst Type	← Pd-H-Faujasite →		
Size, mm	← 0.417-1.168 →		
Temperature, °F	533	535	535
Pressure, psia	565	465	365
Feed:	← Cyclohexane →		
Partial Pressure, psia	26	22	18
W/hr/W	6.90	6.90	6.90
Hydrogen:			
Partial Pressure, psia	538	443	347
Moles H_2/Mole Feed	20.36	20.10	19.46
Minutes on Feed	594	670	764
Product, moles per 100 moles feed			
Hydrogen	2051.46	1991.95	1931.41
Methane	0.00	0.00	0.00
Ethane	0.62	0.55	0.80
Propane	0.49	0.90	0.90
I-Butane	1.48	2.29	2.38
N-Butane	0.00	0.00	0.00
I-Pentane	0.55	1.38	1.12
N-Pentane	0.00	0.00	0.00
I-Hexanes	1.00	0.87	0.95
N-Hexane	0.19	0.20	0.16
Methylcyclopentane	62.41	62.08	63.77
Cyclohexane	33.67	32.40	30.24
Cyclohexane +	0.72	0.98	1.41
Isomerization, %	62.41	62.08	63.77
Rate Constant, k_1, cc./grm. sec.	0.7981	0.9874	1.3443
Cracking, %	3.92	5.53	5.99
Rate Constant, k_2, cc./grm. sec.	0.0293	0.0504	0.0671
Hydrogen Balance, %	100.8	99.6	99.7

TABLE A

RUN DATA

Run Number	13E	13F	14A
Catalyst Type	← Pd-H-Faujasite →		
Size, mm	← 0.417-1.168 →		
Temperature, °F	535	520	521
Pressure, psia	265	465	465
Feed:	← Cyclohexane →		
Partial Pressure, psia	13	42	44
W/hr/W	6.90	6.90	13.89
Hydrogen:			
Partial Pressure, psia	252	423	421
Moles H_2/Mole Feed	19.30	10.18	9.67
Minutes on Feed	870	942	130
Product, moles per 100 moles feed			
Hydrogen	1899.06	1010.44	956.91
Methane	0.00	0.00	0.00
Ethane	0.77	0.26	0.62
Propane	0.51	0.79	0.00
I-Butane	1.64	7.12	0.69
N-Butane	0.89	0.00	0.00
I-Pentane	1.44	3.19	0.31
N-Pentane	0.00	0.82	0.00
I-Hexanes	0.81	1.60	0.40
N-Hexane	0.15	0.43	0.22
Methylcyclopentane	63.04	56.89	63.69
Cyclohexane	31.59	27.92	34.34
Cyclohexane +	0.86	3.93	0.36
Isomerization, %	63.04	56.89	63.69
Rate Constant, k_1, cc./grm. sec.	1.7367	0.5686	0.9868
Cracking, %	5.37	15.18	1.98
Rate Constant, k_2, cc./grm. sec.	0.0840	0.0697	0.0181
Hydrogen Balance, %	99.1	100.6	99.5

TABLE A

RUN DATA

Run Number	14B	14C	14D
Catalyst Type	← Pd-H-Faujasite →		
Size, mm	← 0.417-1.168 →		
Temperature, °F	520	520	522
Pressure, psia	465	465	465
Feed:	← Cyclohexane →		
Partial Pressure, psia	40	42	43
W/hr/W	9.26	6.95	3.70
Hydrogen:			
Partial Pressure, psia	425	422	422
Moles H_2/Mole Feed	10.60	9.98	9.80
Minutes on Feed	236	360	610
Product, moles per 100 moles feed			
Hydrogen	1050.82	983.71	961.87
Methane	0.00	0.00	0.00
Ethane	0.83	0.65	1.12
Propane	0.00	0.00	0.58
I-Butane	0.60	1.43	5.97
N-Butane	0.00	0.00	0.90
I-Pentane	0.38	0.85	5.26
N-Pentane	0.00	0.00	0.63
I-Hexanes	0.60	0.84	5.89
N-Hexane	0.30	0.33	1.45
Methylcyclopentane	66.21	66.55	63.17
Cyclohexane	31.09	29.14	17.93
Cyclohexane +	0.69	1.08	1.20
Isomerization, %	66.21	66.55	63.17
Rate Constant, k_1, cc./grm. sec.	0.8317	0.6408	0.8213
Cracking, %	2.69	4.31	18.90
Rate Constant, k_2, cc./grm. sec.	0.0171	0.0187	0.0418
Hydrogen Balance, %	99.6	99.4	100.3

TABLE A

RUN DATA

Run Number	14E	14F
Catalyst Type	← Pd-H-Faujasite →	
Size, mm	← 0.417-1.168 →	
Temperature, °F	522	520
Pressure, psia	465	465
Feed:	← Cyclohexane →	
Partial Pressure, psia	34	41
W/hr/W	1.85	6.95
Hydrogen:		
Partial Pressure, psia	431	424
Moles H_2/Mole Feed	12.81	10.35
Minutes on Feed	788	883
Product, moles per 100 moles feed		
Hydrogen	1158.49	1007.03
Methane	0.00	0.00
Ethane	0.39	0.47
Propane	2.53	1.18
I-Butane	13.63	6.44
N-Butane	1.68	1.70
I-Pentane	11.79	2.87
N-Pentane	1.70	0.96
I-Hexanes	14.34	1.37
N-Hexane	4.35	0.34
Methylcyclopentane	39.16	54.68
Cyclohexane	14.86	26.60
Cyclohexane +	3.82	6.55
Isomerization, %	39.16	54.68
Rate Constant, k_1, cc./grm. sec.	0.8000	0.5861
Cracking, %	45.98	18.72
Rate Constant, k_2, cc./grm. sec.	0.0733	0.0875
Hydrogen Balance, %	96.4	99.6

TABLE A

RUN DATA

Run Number	15A	15B	15C
Catalyst Type	← Pd-H-Faujasite →		
Size, mm	← 0.417-1.168 →		
Temperature, °F	521	522	521
Pressure, psia	465	465	465
Feed:	← Methylcyclopentane →		
Partial Pressure, psia	40	38	40
W/hr/W	13.25	8.82	6.61
Hydrogen:			
Partial Pressure, psia	425	426	425
Moles H_2/Mole Feed	10.62	11.07	10.57
Minutes on Feed	109	202	325
Product, moles per 100 moles feed			
Hydrogen	1062.18	1121.18	1030.30
Methane	0.00	0.00	0.00
Ethane	0.44	0.32	0.30
Propane	0.44	0.59	1.05
I-Butane	1.38	3.47	8.36
N-Butane	0.55	0.00	1.38
I-Pentane	0.94	1.61	4.17
N-Pentane	0.00	0.00	1.00
I-Hexanes	1.01	1.78	2.35
N-Hexane	0.41	0.50	0.62
Methylcyclopentane	75.78	72.34	61.52
Cyclohexane	18.60	19.40	20.60
Cyclohexane +	1.51	2.65	2.99
Isomerization, %	18.60	19.40	20.60
Cracking, %	5.61	8.27	17.87
Hydrogen Balance, %	100.4	101.4	99.7

TABLE A

RUN DATA

Run Number	15D	15E	15F
Catalyst Type	← Pd-H-Faujasite →		
Size, mm	← 0.417-1.168 →		
Temperature, °F	522	523	520
Pressure, psia	465	465	465
Feed:	← Methylcyclopentane →		
Partial Pressure, psia	41	40	40
W/hr/W	4.41	3.52	13.25
Hydrogen:			
Partial Pressure, psia	424	425	424
Moles H_2/Mole Feed	10.38	10.64	10.52
Minutes on Feed	428	537	883
Product, moles per 100 moles feed			
Hydrogen	967.67	982.88	1031.30
Methane	0.00	0.00	0.00
Ethane	0.32	0.47	0.37
Propane	3.43	4.94	0.54
I-Butane	19.89	26.09	2.55
N-Butane	2.24	3.03	0.87
I-Pentane	6.31	6.70	1.68
N-Pentane	1.47	1.67	0.00
I-Hexanes	5.98	5.53	1.10
N-Hexane	1.61	1.64	0.29
Methylcyclopentane	42.55	37.10	75.02
Cyclohexane	18.80	18.38	17.83
Cyclohexane +	6.84	7.14	1.45
Isomerization, %	18.80	18.38	17.83
Cracking, %	38.65	44.52	7.15
Hydrogen Balance, %	98.6	98.5	99.3

TABLE A

RUN DATA

Run Number	16A	16B	16C
Catalyst Type	← Pd-H-Faujasite →		
Size, mm	← 0.417-1.168 →		
Temperature, °F	519	520	520
Pressure, psia	465	465	465
Feed: Cyclohexane + Methylcyclopentane (23/77 mole %)*			
Partial Pressure, psia	41	39	41
W/hr/W	13.40	8.94	6.70
Hydrogen:			
Partial Pressure, psia	424	426	423
Moles H_2/Mole Feed	10.37	11.01	10.23
Minutes on Feed	958	1068	1157
Product, moles per 100 moles feed			
Hydrogen	1023.82	1058.93	985.44
Methane	0.00	0.00	0.00
Ethane	0.41	2.09	0.32
Propane	0.45	0.42	1.11
I-Butane	1.84	3.00	8.64
N-Butane	0.00	0.78	1.60
I-Pentane	0.95	1.94	4.85
N-Pentane	0.00	0.15	1.13
I-Hexanes	0.86	1.45	2.66
N-Hexane	0.24	0.34	0.68
Methylcyclopentane	74.50	68.01	57.51
Cyclohexane	21.07	22.15	21.69
Cyclohexane +	0.80	2.46	4.27
Cracking, %	4.43	9.84	2.08
Hydrogen Balance, %	99.6	98.2	99.2

*Equilibrium composition at 520°F.

TABLE A

RUN DATA

Run Number	16D	16E	16F
Catalyst Type	← Pd-H-Faujasite →		
Size, mm	← 0.417-1.168 →		
Temperature, °F	521	522	520
Pressure, psia	465	465	465
Feed: Cyclohexane + Methylcyclopentane (23/77 mole %)*			
Partial Pressure, psia	38	39	42
W/hr/W	4.47	3.57	13.40
Hydrogen:			
Partial Pressure, psia	427	425	423
Moles H_2/Mole Feed	11.37	10.82	10.14
Minutes on Feed	1257	1360	1713
Product, moles per 100 moles feed			
Hydrogen	1045.42	964.56	1005.69
Methane	0.00	0.00	0.00
Ethane	0.29	0.77	0.34
Propane	1.63	4.09	0.56
I-Butane	14.54	40.12	2.58
N-Butane	1.89	4.29	0.94
I-Pentane	8.05	19.92	2.12
N-Pentane	1.25	1.45	0.53
I-Hexanes	6.10	6.34	1.23
N-Hexane	1.40	1.27	0.49
Methylcyclopentane	49.36	27.81	68.55
Cyclohexane	18.36	10.37	21.13
Cyclohexane +	4.21	3.85	3.15
Cracking, %	32.01	61.82	10.32
Hydrogen Balance, %	97.0	98.0	100.2

*Equilibrium composition at 520°F.

TABLE A

RUN DATA

Run Number	17A	17B
Catalyst Type	← Pd-H-Faujasite →	
Size, mm	← 0.417-1.168 →	
Temperature, °F	520	520
Pressure, psia	665	500
Feed:	← Cyclohexane →	
Partial Pressure, psia	43	78
W/hr/W	7.0	13.13
Hydrogen:		
Partial Pressure, psia	622	421
Moles H_2/Mole Feed	14.48	5.37
Minutes on Feed	111	201
Product, moles per 100 moles feed		
Hydrogen	1440.99	528.24
Methane	0.00	0.00
Ethane	0.69	0.36
Propane	0.00	0.34
I-Butane	1.11	1.02
N-Butane	0.00	0.54
I-Pentane	0.23	0.82
N-Pentane	0.00	0.05
I-Hexanes	0.81	0.70
N-Hexane	0.50	0.29
Methylcyclopentane	70.42	65.73
Cyclohexane	26.67	30.34
Cyclohexane +	0.37	0.77
Isomerization, %	70.42	65.73
Rate Constant, k_1, cc./grm. sec.	0.7763	0.6134
Cracking, %	2.91	3.93
Rate Constant, k_2, cc./grm. sec.	0.0132	0.0179
Hydrogen Balance, %	99.8	99.7

APPENDIX B

SAMPLE CALCULATIONS

APPENDIX B

SAMPLE CALCULATIONS

The calculations for this study were performed on the IBM-360 computer of the Louisiana State University Computing Center. The program employed in this work is a modification of the comprehensive data work-up program employed daily at the Esso Catalysis Project.

A. Experimental Conditions

Run number	4D
Feed	Cyclohexane
Catalyst	Pd-H-faujasite
Catalyst weight	1.8166 gm
Catalyst size	0.417-1.168 mm
Temperature	530°F
Pressure	465 psia
Minutes on balance	26
Hydrogen in	0.585 ft^3
Temperature of hydrogen in	92°F
Cyclohexane in	7.07 cc
Product gas out	0.638 ft^3
Temperature of gas out	94°F

B. Analytical Data

Component	GC Factor, gm-mole per unit area x10^3	Peak Area*
C_1	3.765	0.000
C_2	2.496	0.681
C_3	2.006	1.425
iC_4	1.707	5.807
C_4	1.685	2.655
iC_5	1.580	4.177
C_5	1.495	1.643
2-MP	1.308	3.691
3-MP	1.318	1.966
nC_6	1.278	1.273
MCP	1.411	212.041
CH	1.471	66.840
CH +	1.147	3.747

C. Material Balance Calculations

Basis: 26 min.

Weight of CH fed = $(16.33 \frac{cc}{hr})$ $(\frac{26}{60}$ hr) $(0.779 \frac{gm}{cc})$ = 5.5075 gm

Gram moles of CH fed = $\frac{5.5075}{84.16}$ = 0.0696

Grams of carbon in CH fed = (0.0696) (72 gm c/mole CH) = 5.0112 gm

Grams of H_2 in CH fed = (0.0696) (12.10 gm H_2/mole CH) = 0.8421 gm

Weight hourly space velocity = w/hr/w = (5.5075 gm/26 min)

(60 min/1 hr)/(1.8166 gm) = 6.9963

---

*As obtained from the Infotronics Digital Ingegrator Model CRS-110.

Volume of H_2 gas in @ $60^{\circ}F$ and 1 atm = (0.585 ft^3) (0.891) = 0.521 ft^3

Gram moles of H_2 gas in = (0.521 ft^3) (1.20 gm moles/ft^3) = 0.625 gm moles

Gram of H_2 as gas in = (0.625 gm moles) (2.016 $\frac{gm}{gm\text{-}mole}$) = 1.260 gm

Partial pressure of CH = (465 psia) (0.0696)/(0.0696 + 0.625) = 44 psia

Partial pressure of H_2 = 465-44 = 421 psia

H_2/CH molar ratio = (0.659)/(0.0696) = 9.5

Volume of product gas out @ $60^{\circ}F$ and 1 atm = (0.638) (0.885) = 0.564 ft^3

Gram moles of product gas out = (0.564 ft^3) (1.20 gm mole/ft^3) = 0.677 gm moles

Assume grams of carbon in cyclohexane feed = grams of carbon in product = 5.011 gm

Molar weighting factors for hydrocarbons in product gas = (peak area/100) (GC factor):

Component	(Peak Area/100) x (GC Factor)	Molar Weighting Factor
C_1	(0.000) (3.765)	0.0000
C_2	(0.007) (2.496)	0.0175
C_3	(0.014) (2.006)	0.0281
iC_4	(0.058) (1.707)	0.0990
C_4	(0.027) (1.685)	0.0455
iC_5	(0.042) (1.580)	0.0664
C_5	(0.016) (1.495)	0.0239
2-MP	(0.037) (1.308)	0.0484
3-MP	(0.020) (1.318)	0.0264
nC_6	(0.013) (1.278)	0.0166
MCP	(2.120) (1.411)	2.9913
CH	(0.668) (1.471)	0.9826
CH +	(0.037) (1.147)	0.0424
		Σ_{MWF} = 4.3881

Hydrogen-free mole fractions of hydrocarbon components in product gas = (molar weighting factor)/(Σ_{MWF}):

Component	(Molar Weighting Factor)/(Σ_{MWF})	Hydrogen Free Mole Fraction
C_1	(0.0000)/(4.3881)	0.0000
C_2	(0.0175)/(4.3881)	0.0040
C_3	(0.0281)/(4.3881)	0.0064
iC_4	(0.0990)/(4.3881)	0.0226
C_4	(0.0455)/(4.3881)	0.0104
iC_5	(0.0664)/(4.3881)	0.0151
C_5	(0.0239)/(4.3881)	0.0054
2-MP	(0.0484)/(4.3881)	0.0110
3-MP	(0.0264)/(4.3881)	0.0060
nC_6	(0.0166)/(4.3881)	0.0038
MCP	(2.9913)/(4.3881)	0.6816
CH	(0.9826)/(4.3881)	0.2239
CH +	(0.0424)/(4.3881)	0.0097

Grams of carbon per gram mole of product gas = (hydrogen-free mole fraction)(grams of carbon per gram mole of hydrocarbon):

Component	(Hydrogen-free mole fraction) x(grams of carbon per gram mole)	Gram carbon per gram mole gas out
C_1	(0.0000) (12.01)	0.0000
C_2	(0.0040) (24.02)	0.0961
C_3	(0.0064) (36.03)	0.2306
iC_4	(0.0226) (48.04)	1.0857
C_4	(0.0104) (48.04)	0.4996
iC_5	(0.0151) (60.05)	0.9067
C_5	(0.0054) (60.05)	0.3242
2-MP	(0.0110) (72.06)	0.7920
3-MP	(0.0060) (72.06)	0.4323
nC_6	(0.0038) (72.06)	0.2738
MCP	(0.6816) (72.06)	49.1160
CH	(0.2239) (72.06)	16.1342
CH +	(0.0097) (72.06)	0.6989
		Σ_{GC} = 70.5901

Actual gram moles of product gas out = (grams of carbon out)/(grams of carbon per gram mole of gas out) = (5.011)/(70.5901) = 0.0710

Gram moles of hydrocarbon components in product gas = (hydrogen-free mole fraction) (actual gram moles of product gas)

Component	(Hydrogen-free mole Fraction)x (actual gram moles of product gas)	Gram moles in Product gas
C_1	(0.0000) (0.0710)	0.00000
C_2	(0.0040) (0.0710)	0.00028
C_3	(0.0064) (0.0710)	0.00045
iC_4	(0.0226) (0.0710)	0.00160
C_4	(0.0104) (0.0710)	0.00074
iC_5	(0.0151) (0.0710)	0.00107
C_5	(0.0054) (0.0710)	0.00038
2-MP	(0.0110) (0.0710)	0.00078
3-MP	(0.0060) (0.0710)	0.00043
nC_6	(0.0038) (0.0710)	0.00027
MCP	(0.6816) (0.0710)	0.04839
CH	(0.2239) (0.0710)	0.01589
CH +	(0.0097) (0.0710)	0.00068
		0.0710

Gram moles of hydrocarbon components in product gas per 100 moles of CH fed:

Component	(Gram moles in product gas out) (100)/(gram mole of CH fed)	Gram moles per 100 moles of CH
C_1	(0.0000)/(0.0696)	0.00
C_2	(0.028)/(0.0696)	0.40
C_3	(0.045)/(0.0696)	0.65
iC_4	(0.160)/(0.0696)	2.30
C_4	(0.074)/(0.0696)	1.06
iC_5	(0.107)/(0.0696)	1.54
C_5	(0.038)/(0.0696)	0.55
2-MP	(0.078)/(0.0696)	1.12
3-MP	(0.043)/(0.0696)	0.62
nC_6	(0.027)/(0.0696)	0.39
MCP	(4.839)/(0.0696)	69.52
CH	(1.589)/(0.0696)	22.83
CH +	(0.068)/(0.0696)	0.98
		101.96

Isomerization, % = Mole % MCP = 69.52

Cracking, % = (Conversion of CH- Isomerization)

= [(100-22.83) - 69.52] = 7.65

Hydrogen free mole fraction of CH = Y_a = 22.83/101.96 = 0.2239

Hydrogen free mole fraction of MCP = Y_b = 69.52/101.96 = 0.6818

Grams of hydrogen in product gas = (grams of hydrogen per mole of hydrocarbon) (moles of hydrocarbon in product gas):

Component	(Grams of hydrogen per mole of hydrocarbon)x(moles of hydrocarbon)	Grams of hydrogen out
C_1	(4.032) (0.00000)	0.00000
C_2	(6.048) (0.00028)	0.00169
C_3	(8.064) (0.00045)	0.00363
iC_4	(10.080) (0.00160)	0.01613
C_4	(10.080) (0.00074)	0.00746
iC_5	(12.096) (0.00107)	0.01294
C_5	(12.096) (0.00038)	0.00459
2-MP	(14.112) (0.00078)	0.01101
3-MP	(14.112) (0.00043)	0.00607
nC_6	(14.112) (0.00027)	0.00381
MCP	(12.096) (0.04839)	0.58532
CH	(12.096) (0.01589)	0.19221
CH +	(16.128) (0.00068)	0.01097
		0.8413

$$\text{Hydrogen balance, \%} = 100 \times \frac{[H_2 \text{ out as gas} + H_2 \text{ out with hydrocarbons}]}{[H_2 \text{ in as gas} + H_2 \text{ in with hydrocarbons}]}$$

$$\text{Hydrogen balance, \%} = 100 \times \frac{[2.016\ (0.677-0.071) + 0.8413]}{[1.260 + 0.8421]} = 98.1$$

D. Computation of Rate Constants

1. Hydrocracking Rate Constant

$$k_2 = \frac{1}{t_s}\left\{\ln\left[\frac{1}{(1-Y_c)}\right]\right\}$$

k_1 = hydrocarcking rate constant

t_s = superficial contact time

$$t_s = M_w\left(\frac{P}{RT}\right)\left(\frac{3600}{W/hr/W}\right)\left(\frac{1}{1+R_H}\right)$$

M_w = molecular weight of CH feed = 84.16 $\frac{gm}{gm\ mole}$

P = pressure = 465 psia

T = temperature = 530°F = 990°R

R = gas law constant = 10.73 $\frac{ft^3\ psia}{{}^{o}R\ lb\text{-}mole}$

W/hr/W = weight hourly space velocity = 6.996 gm/hr/gm

R_H = H_2/CH molar ratio = 9.5

$$t_s = \left[\left(84.16\ \frac{gm}{gm\text{-}mole}\right)\right]\left[\frac{(465\ psia)\left(453.6\ \frac{gm\text{-}mole}{lb\text{-}mole}\right)}{\left(10.73\ \frac{ft^3\ psia}{{}^{o}R\ lb\text{-}mole}\right)}\right]\left[\frac{\left(\frac{1}{2.832\times10}\ \frac{ft^3}{cc}\right)}{(990^{o}R)}\right]\left[\frac{\left(3600\ \frac{sec}{hr}\right)}{6.996\ gm/hr/gm}\right]\left[\frac{1}{(1+9.5)}\right]$$

t_s = 2.889 $\frac{gm\text{-}sec}{cc}$

Y_c = hydrogen free mole fraction of cracked products =

$1-Y_a-Y_b$ = 0.0943

$$k_2 = \frac{1}{(2.889)}\left\{\ln\left[\frac{1}{(1-0.0943)}\right]\right\} = 0.034\ \frac{cc}{gm\text{-}sec}$$

2. Hydroisomerization Rate Constant

The hydroisomerization rate constant is calculated by trial and error as demonstrated in Chapter V. However, in order to set in

motion the Pattern search technique utilized in the present study, an initial approximation of the hydroisomerization rate constant must be supplied.

The initial estimate of the rate constant is obtained by considering only the first order reversible reaction of cyclohexane to methylcyclopentane. The rate constant for this simplified system is similar to that obtained for the hydrocracking reaction but it involves an equilibrium concentration term as follows:

$$k_1 = \frac{Y_b^E}{t_s} \left\{ \ln \left[\frac{1}{1 - \left(\frac{Y_b}{Y_a + Y_b} \right)} \right] \right\}$$

k_1 = hydroisomerization of CH rate constant.

Y_b^E = mole fraction of MCP in MCP + CH mixture at equilibrium.

$$Y_b^E = \frac{e^{(-4810/^{\circ}R + 6.114)}}{\left[1 + e^{(-4810/^{\circ}R + 6.114)}\right]} = \frac{e^{(-4810/990 + 6.114)}}{\left[1 + e^{(-4810/990 + 6.114)}\right]} =$$

$$0.778$$

$$\frac{Y_b}{Y_a + Y_b} = \frac{0.6818}{(0.6818 + 0.2239)} = 0.753$$

$$k_1 = \frac{(0.778)}{(2.889)} \left\{ \ln \left[\frac{1}{1 - \frac{0.753}{0.778}} \right] \right\} = 0.925$$

APPENDIX C

NOMENCLATURE

APPENDIX C

NOMENCLATURE

C	-	Objective function
C_i	-	Molar concentration of species i, i = a for cyclohexane, and i = b for methylcyclopentane
E_D	-	Axial dispersion coefficient
k_1	-	Rate constant for the cyclohexane to methylcyclopentane reaction
k_1'	-	Rate constant for the methylcyclopentane to cyclohexane reaction
k_2	-	Rate constant for the cyclohexane to cracked products reaction
k_3	-	Rate constant for the methylcyclopentane to cracked products reaction
K	-	Equilibrium constant for the cyclohexane - methylcyclopentane system
k_o^1, k_o^2	-	Frequency factors for the cyclohexane hydroisomerization and hydrocracking respectively
k_{o1}, k_{o2}	-	Constants dependent on catalyst and temperature for hydroisomerization and hydrocracking respectively
k_{o2}^1	-	Constant dependent on catalyst and temperature for hydrocracking

K_{CH}, K_{MCP}, K_C, K_H	-	Adsorption coefficients for cyclohexane, methylcyclopentane, cracked products, and hydrogen respectively
K_O	-	Adsorption coefficient for hydrocarbon components
K_π	-	Adsorption parameter associated with the total pressure formulation
M_W	-	Molecualr weight of cyclohexane feed
n	-	Adsorption model exponent, n = 1 for single site, and n = 2 for dual site.
N	-	Total gas molar flow rate
N_a, N_b	-	Molar flow rate of cyclohexane and methylcyclopentane respectively
N_{Di}	-	Axial dispersion rate of species i
P_{CH}, P_{MCP}, P_C, P_H	-	Partial pressures of cyclohexane, methylcyclopentane, cracked products, and hydrogen respectively.
P_O	-	Partial pressure of hydrocarbon components
P_i	-	Predicted hydrogen-free mole fraction of cyclohexane (i = 1) or methylcyclopentane (i = 2)
P	-	Total pressure
R	-	Gas law constant
r_A, r_B	-	Rate of appearance of cyclohexane and methylcyclopentane respectively
R_H	-	Molar hydrogen to hydrocarbon ratio
^oR	-	Absolute temperature, degrees Rankine
T	-	Temperature, degrees Fahrenheit
t_s	-	Superficial contact time based on catalyst wt.

V	-	Total gas volumetric flow rate
W_c	-	Catalyst weight
W/hr/W	-	Weight hourly space velocity
y_a, y_b	-	Mole fraction of cyclohexane and methylcyclopentane respectively
Y_a, Y_b, Y_c	-	Hydrogen-free mole fractions of cyclohexane methylcyclopentane and cracked products respectively
Y_a^o, Y_b^o	-	Hydrogen-free mole fraction of cyclohexane and methylcyclopentane respectively at a superficial contact time equal to zero.
Y_a^*, Y_b^*	-	Hydrogen-free mole fraction of cyclohexane and methylcyclopentane respectively at a superficial contact time equal to infinite.
z	-	Longitudinal reactor length
ΔE_1, ΔE_2	-	Activation energies for the cyclohexane hydroisomerization and hydrocracking respectively
π	-	Total pressure
σ	-	Standard deviation

VITA

Mamerto Goar Luzarraga was born in Sagua La Grande, Cuba, on July 6, 1944. He is the oldest of two sons of Jose Ramon and Irma Luisa Luzarraga. He attended Belen Jesuit High School in Havana, Cuba. Subsequently, he moved to Caracas, Venezuela, where he finished high school at Colegio San Ignacio on August of 1961. Later, he moved to the United States and received a Bachelor of Science Degree in Chemical Engineering from the University of Florida in 1967. In 1968, he received a Master of Science Degree in Chemical Engineering from the same university.

He was employed by the Esso Research Laboratories at Baton Rouge from 1968 to 1969. At that time, he took an educational leave to complete the requirements for a Ph.D. degree in Chemical Engineering at Louisiana State University.

In 1965, he married the former Vilma Rosa Vilaret and they have two sons, Mamerto Luis, and Jose Manuel.

EXAMINATION AND THESIS REPORT

Candidate: Mamerto Goar Luzarraga

Major Field: Chemical Engineering

Title of Thesis: Hydroisomerization and Hydrocracking of Cyclohexane Over a Faujasite Catalyst

Approved:

Major Professor and Chairman

Dean of the Graduate School

EXAMINING COMMITTEE:

Date of Examination:

April 21, 1971